AN ABSTRACT OF THE THESIS OF

Tengfei Fu for the degree of Master of Science in Civil Engineering presented on February 15, 2011

Title: Autogenous Deformation and Chemical Shrinkage of High Performance Cementitious Systems

Abstract approved:

_____

Dr. Jason H. Ideker

In the past ten years, renewed research interest has shown the benefits of internal curing by incorporating saturated lightweight fine aggregate (LWFA) in high performance concrete (HPC). As a result, the technology of internal curing has steadily progressed from laboratory studies to field applications. To determine the optimum LWFA content, information about the propensity for shrinkage in the cement paste, specifically the chemical shrinkage value, is needed. However, there is a lack of information on how to determine the ultimate chemical shrinkage value for HPC with supplementary cementitious materials (SCMs) and/or shrinkage reducing admixture (SRA). The purpose of this thesis was to identify a simple procedure to determine ultimate chemical shrinkage values for given concrete systems with SCMs and/or SRA. Modifications to the ASTM C1608 (Standard Test Method for Chemical Shrinkage of Hydraulic Cement Paste) were investigated up to a 14 day age. Neat paste (cement only), as well as binary and ternary systems, were measured to investigate the influence of SCMs and SRA on chemical shrinkage. Based on the observed data, an experimental prediction model was adopted and verified to estimate ultimate chemical shrinkage values for portland cement systems containing SCMs and/or SRA. The model agreed well with the obtained data and simplified the existing method of determining the ultimate chemical shrinkage value.

Another purpose of this research was to investigate the effect of SCMs and SRA on autogenous deformation of HPC for which a buoyancy method was used. The findings provided insight into the mechanisms behind autogenous shrinkage and effective strategies to reduce autogenous shrinkage.

Calcium aluminate cements (CACs) were also investigated as part of this research project as a rapid repair material for applications, such as high performance concrete bridge decks. Chemical shrinkage and autogenous deformation of CAC binders were tested in a similar manner to the OPC systems in this study. It was observed that GCX paste cured isothermally at 38 °C exhibited expansion with a particular shape of chemical shrinkage development curve. An X-ray diffraction suggested that the expansion might be related to the conversion process indicating that chemical shrinkage may be used as a predictor of conversion processes for CAC systems in isothermal condition.

© Copyright by Tengfei Fu
February 15, 2011
All Rights Reserved

Autogenous Deformation and Chemical Shrinkage of High Performance Cementitious Systems

by

Tengfei Fu

A THESIS

submitted to

Oregon State University

in partial fulfillment of
the requirements for the
degree of

Master of Science

Presented February 15, 2011

Commencement June 2011

Master of Science thesis of Tengfei Fu presented on February 15, 2011.

APPROVED:

Major Professor, representing Civil Engineering

Head of the School of Civil & Construction Engineering

Dean of the Graduate School

I understand that my thesis will become part of the permanent collection of Oregon State University libraries. My signature below authorizes release of my thesis to any reader upon request.

Tengfei Fu, Author

ACKNOWLEDGEMENTS

First and foremost, I would like to thank my advisor Dr. Jason H. Ideker. Without your sincere assistance, support and patience, none of this thesis would come into existence. I am truly appreciated for every effort you put in for me over the years. You are more than an advisor to me. You are also my mentor, my friend, and an example to follow.

I also would like to thank Dr. David Trejo, Dr. Michael H. Scott and Dr. Lech Muszyński for their service as my committee members. All your comments and questions are well appreciated.

I would like to thank all my colleagues and friends, Dr. Thomas Schumacher, Nicholas Tymvios, Tyler Deboodt, Kelsea Schwing, Shweta Keshari, Juan Zheng, Meng Li, Yisen Guo, Minjie Zhu, Wei Wang and Michael Johnson, for such a pleasant grad school experience.

And a special thanks to Oregon Department of Transportation for funding this project and providing further research opportunities.

Last, but far from least, I would like to thank my parents for the unconditional love and support all through the years. Thank you for always believing in me and encouraging me to chase my dreams. Also, I owe a great deal of gratitude to my fiancée, Miss Lu. Without your encouragement, patience and selfless sacrifices, I could never be the person I am.

CONTRIBUTION OF AUTHORS

Tyler Deboodt, fellow graduate student, was involved in the writing of Chapter 2.

TABLE OF CONTENTS

TABLE OF CONTENTS (CONTINUED)

LIST OF FIGURES

LIST OF FIGURES (CONTINUED)

LIST OF FIGURES (CONTINUED)

LIST OF TABLES

1 INTRODUCTION

1.1 INTERNAL CURING

Advances in concrete technology have led to the advent of high performance concrete (HPC) that typically has high cement content and low water to cementitious material ratio (w/cm) combined with supplementary cementing materials (SCMs) such as silica fume, fly ash and ground granulated blast furnace slag. High performance is achieved through high strength, low permeability, increased durability and/or higher abrasion resistance. However, these same parameters that improve many concrete properties may also adversely affect other properties, such as shrinkage strains and resulting increases in stress which can ultimately lead to cracking. In particular, a lower w/cm and the presence of certain SCMs such as silica fume can significantly increase the risk of early-age cracking due to the shrinkage in these systems, resulting in a decrease in durability and long-term performance.

Internal moisture loss due to the hydration process in the cement paste of HPC can increase autogenous shrinkage in the system. Autogenous shrinkage, also referred as self-desiccation, is a loss of water from the capillary void structure in a hydrating cement paste that may result in an overall net shrinkage of the concrete structure. In concrete with higher w/cm, water supplied by external curing is readily available and accessible by the hydrating paste. While in HPC with lower w/cm, the permeability of the concrete quickly becomes too low to allow the effective transfer of water from the external surface to the concrete interior. (*Bentz and Snyder 1999*) Under such situation, internal curing becomes especially beneficial.

To reduce shrinkage and ultimately cracking risk in HPC at early-ages, different curing methods have been utilized to maintain a high internal relative humidity (RH). Internal curing, by definition of ACI Committee 308 Curing Concrete, “refers to the process by

which the hydration of cement occurs because of the availability of additional internal water that is not part of the mixing water." (*Bentz et al. 2005*) The additional water is usually supplied by partial replacement of normal weight fine aggregate by saturated lightweight fine aggregates (LWFA) or superabsorbent polymer (SAP) particles. Benefits of internal curing include increased hydration and strength development, reduced autogenous shrinkage and cracking, reduced permeability and increased durability. (*Bentz et al. 2005*)

In recent years, numerous studies have been conducted in the laboratory showing the benefits of internal curing. As a result the technology of internal curing has steadily progressed from laboratory studies to field application. (*Henkensiefken et al. 2009*) The successful use of lightweight aggregate (LWA) has been reported in the north Texas area for concrete paving. As to the success and challenges in this field application, the most crucial step in the ready-mix concrete production cycle was identified as the adequate initial moisture conditioning of the LWA. (*Villarreal 2008*) Another field application success was the construction of a five-mile section of State Highway 121 north of Dallas, reported by Friggle and Reeves (*2008*). They purported that by using lightweight aggregate in concrete pavement, increased strength, reduced drying shrinkage cracking, and possibly less susceptibility to freeze thaw damage could be expected. (*Friggle and Reeves 2008*)

1.2 CHEMICAL SHRINKAGE AND INTERNAL CURING

A major task of this research effort was to determine the optimum replacement ratio of lightweight fine aggregate (LWFA) in the mixture. Bentz and co-workers developed an equation for determining the necessary replacement of the stardard fine aggregate with saturated LWFA. (*Bentz and Snyder 1999, Bentz et al. 2005*) This is shown in Equation 1.

$$M_{LWFA} = \frac{C_f \times CS \times \alpha_{max}}{S \times \Phi_{LWFA}} \; with \; \alpha_{max} = \frac{w/cm}{0.36} \leq 1 \qquad \text{Equation 1}$$

Where:

C_f = cementious content (kg/m^3) ;

CS = chemical shrinkage of the cement (ml water/g cement);

α_{max} = maximum expected degree of hydration;

S = maximum degree of expected saturation for LWFA;

Φ_{LWFA} = absorption of lightweight fine aggregate (kg water/kg dry LWFA).

Equation 1 is also referred as Bentz Equation. To use this predictive equation several variables will need to be determined including: C_f, CS, α_{max}, S and Φ_{LWFA}. Then the mass of the dry lightweight aggregate (ML_{WFA} in kg/m^3) needed can be calculated. The maximum degree of saturation (expected) for LWFA and absorption of lightweight fine aggregate were investigated as part of this project, but it was not in the scope of this thesis. According to Powers' model (*Powers 1935*), the maximum expected degree of hydration was determined by the w/cm and historical data from other authors for similar cementitious systems.

The chemical shrinkage value is important to optimize LWFA content in internal curing. Higher chemical shrinkage value might indicate more moisture is needed from LWFA. Therefore, a proper chemical shrinkage value is crucial when applying Equation 1. In previous research, chemical shrinkage value has been determined by the composition of cement. This method is not quite applicable to binary or ternary binder systems used in this research. Thus, a prediction model of chemical shrinkage value based on experimental data is adopted and verified in this thesis.

Testing in accordance with ASTM C 1608 was performed to determine the chemical shrinkage value (CS) in Equation 1 for the binder system for the standard Oregon Department of Transportation (ODOT) HPC bridge mixture. Modifications to this testing

method for this research project included automation of the method, testing materials including SCMs representative of the standard ODOT HPC bridge mixture (fly ash and silica fume).

Neat pastes were investigated as well as binary and ternary systems. The ternary systems incorporating fly ash and silica fume were representative of binder systems in HPC bridge decks in Oregon. Testing on neat pastes and binary systems allowed further quantification of the effects of SCMs on chemical shrinkage and will provide a contribution to existing literature as well as to furthering the goals of this research project.

Since the calcium aluminate cement (CAC) system has the potential to be the alternative choice for bridge deck, especially for emergency purpose, chemical shrinkage and autogenous deformation was also investigated for this binder system. More detail about the CAC system is presented in section 2.1.2.

1.3 RESEARCH SCOPE

The purpose of this thesis was to investigate early-age volume change, specifically chemical shrinkage and autogenous deformation, of high performance cementitious systems. The majority of testing was performed to capture chemical shrinkage values as one important factor needed for determining appropriate placement levels of saturated lightweight fine aggregate, as part of Oregon Department of Transportation (ODOT) Project SPR 711. This thesis is organized into 6 chapters. The following outline provides a brief description of the chapter contents.

A literature review is presented in Chapter 2. The literature review was conducted to highlight the current knowledge behind the primary early-age volume change mechanisms that can induce stresses and cause cracking in concrete, and to tie these to the benefits of internal curing. Measurement methods and shrinkage mitigation strategies

are the main focuses. The testing methods used in this project for chemical shrinkage and autogenous deformation are also indentified and described in this chapter.

Chapter 3 presents the properties of the materials used in this research, including ASTM C150 Type I/II cement (Lafarge), class F fly ash from Centralia Plant (Lafarge), silica fume (BASF) and a shrinkage reducing mixture (Tetraguard). The trade-name of these materials is given not in an effort to endorse any particular product but to provide useful knowledge to ODOT based on their typically HPC mixture designs and so that any researcher wishing to recreate or further investigate this work will have intimate knowledge of the products and testing procedures used.

Chapter 4 presents chemical shrinkage results across a wide range of different cementitious mixture designs based on a standard ODOT HPC bridge deck mixture (30% class F fly ash, 4% silica fume and 0.37 w/cm). A simple experimental prediction model was then adopted and verified. Chapter 4 also investigates several factors that affect chemical shrinkage, such as the addition of supplementary cementitious materials (SCMs), water to cementitious materials ratio and incorporation of shrinkage reducing admixture (SRA). In addition, the chemical shrinkage tests were also performed on calcium aluminate cement (CAC) as an alternative high performance binder system. X-ray diffraction (XRD) analysis was applied to further the application of chemical shrinkage test.

Chapter 5 details the evaluation of the autogenous deformation on OPC systems as well as CAC systems. The influences of SCMs and SRA on OPC systems are investigated. And the influence of temperature is studied on CAC system.

Chapter 6 summaries the major findings within this thesis and recommends several areas for future research and attention.

1.4 NOMENCLATURE

Although several SCMs and admixtures were used in this research, the replacement ratio of each “admixture” remained the same. For instance, the replacement ratio of fly ash, if there is any, remains 30% in all mixtures. In this sense, “FA” represents an OPC mixture with 30% replacement of fly ash and “SF” means OPC mixture with 4% replacement of silica fume. While “SRA” indicates 2% shrinkage reducing admixture by mass of cement is added to the mixture. Also “FA+SF” means a ternary blend including 30% fly ash and 4% silica fume. And “Neat” represents pure OPC paste without any SCMs or SRA.

2 LITERATURE REVIEW

Although HPCs generally possess certain highly favorable properties such as good workability, high strength and low permeability, field experience and laboratory experiments have shown that these types of concrete can be more sensitive to early-age cracking. (*Bentur 2003*) After introducing the HPC systems (OPC systems and CAC systems) tested in this research, this literature review identifies the main factors contributing to early-age volume change in HPC. These factors include: chemical shrinkage, autogenous deformation, plastic shrinkage and drying shrinkage. In addition, this review also identifies mitigation methods to reduce cracking potentials due to early-age volume change of HPC.

2.1 HIGH PERFORMANCE CONCRETE

In the last two decades, the terminology "High-Performance Concrete" has been introduced into the construction industry. Mehta and Aitcin suggested the term high-performance-concrete (HPC) in 1990, for concrete mixtures that possess high-workability, high-strength, and high durability. (*Mehta and Monteiro 2006*) However, the American Concrete Institute (ACI) developed a more comprehensive definition for high-performance concrete. In 1998, ACI Technical Activities Committee approved a definition and description of the performance characteristics of HPC as follows: (*Mehta and Monteiro 2006*)

> *"HPC is defined as a concrete meeting special combination of performance and uniformity requirements that cannot always be achieved routinely using conventional constituents and normal mixing, placing, and curing practices."*

To meet the performance requirement of particular application, a list of characteristics might be considered critical, these includes:

- Ease of placement;
- Compaction without segregation;
- Early-age strength;
- Long-term mechanical properties;
- Permeability;
- Density;
- Heat of hydration;
- Toughness;
- Volume stability, and;
- Long life in severe environments.

Nowadays, most high-performance concretes contain SCMs in addition to the typical portland cement binder. These materials include fly ash, silica fume, other natural pozzolans and ground-granulated blast furnace slag, utilized as binary or ternary blends. Additionally, admixtures are widely used to ensure workability and durability, such as high-range water-reducers (HRWR), air-entraining admixtures, corrosion inhibitors and shrinkage reducing mixtures (SRAs). All these SCMs complicate the mixture proportioning of HPC, and make HPC sensitive to changes in constituent materials properties. Variations in the chemical and physical properties of the cementitious materials and chemical admixtures require further investigation to ensure successful application in the field.

2.1.1 Ordinary Portland Cement with SCMs

Using SCMs in concrete manufacture has become increasingly more popular, both because of the beneficial qualities of the concrete as well as the positive environmental impact. Improved cohesiveness, enhanced workability, better strength control, reduction in permeability, increased resistance to sulfate and chloride attack, decrease in rate of embedded steel corrosion, and better resistance to alkali-aggregate reaction are all possible advantages to the use of SCMs. (*Kosmatka et al. 2002*)

Fly ash, the most widely used SCM, is comprised of the coal's uncombusted mineral impurities which fuse together and solidify as they are transported from the combustion chamber and cooled. This material is primarily silicate glass which contains silica, iron, calcium and alumina. It also contains minor amounts of potassium, carbon, sodium, sulfur and magnesium. These glassy particles are mainly solid spheres, though many hollow cenospheres are also present, which together form a finely divided powder resembling portland cement. (*Kosmatka et al. 2002*) This spherical shape generally ranges in size from less than 1μm to 100μm in diameter with the majority being under 20μm. (*Mehta and Monteiro 2006*) The size distribution, morphology, and surface characteristics of fly ash have a significant effect on the water demand, workability and rate of concrete strength development.

Fly ash is classified by its calcium oxide content which stems from the mineralogical composition of the coal. A fly ash containing less than or equal to 10% CaO, classified as Class F fly ash, is generally produced from the combustion of anthracite and bituminous coals. Fly ash with CaO contents greater than 10% are considered high calcium or Class C fly ashes which are products of the combustion of lignite and subbituminous coals. (*ASTM C618 2009*) Due to chemical composition, low calcium fly ashes typically provide better resistance against alkali-silica reaction (ASR) and sulfate attack; however, this variety provides slower early strength development than both Class C fly ash and conventional portland cement. The opposite is true for high calcium fly ash, which are less efficient in mitigating ASR expansion and sulfate attack, but have a less of a negative impact on the early strength of the concrete. (*Thomas et al. 1999*) Regardless of the chemical composition, the use of fly ash as a supplementary cementing material tends to reduce the water demand of fresh concrete while improving the impermeability of the material, thus increasing its resistance to fluid flow. This beneficial property increases as the concrete matures, particularly with the low CaO Class F fly ashes. (*Thomas et al. 1999*) When used as the sole SCM, fly ash is most commonly added in doses of 15% to

40% by mass of cementitious material, which greatly depends on the reactivity of the ash and the desired effects on the concrete. (*Mehta and Monteiro 2006*)

Silica fume, also known as microsilica, is a byproduct of the silicon metal and ferrosilicon alloy industries. Once condensed, silica fume primarily consists of amorphous silicon dioxide in the shape of small spheres, similar to fly ash particles. Unlike fly ash, however, silica fume particles have very small diameters, typically less than 1 μm, which makes them about 100 times smaller than the average cement particle. (*Kosmatka et al. 2002*) It is because of this small size that silica fume is particularly useful in ensuring a low degree of permeability and is therefore also utilized for high strength concrete. Due to much higher fineness of the material, typical doses of silica fume range between 5% and 10% of the total mass of the cementing material when used as an independent SCM source. (*Kosmatka et al. 2002*)

Using supplementary cementing materials individually can have potentially limiting effects on the properties of the concrete (e.g. high quantities of fly ash can impact early-age strength gain). Therefore, utilizing multiple SCMs can often enhance the concrete by independently adding beneficial qualities (e.g. synergistic effects). This is the theory behind ternary blends and quaternary blends. The use of both silica fume and low calcium fly ash has a number of synergistic effects: (*Thomas et al. 1999*)

- Silica fume compensates for low early strength of concrete with low CaO fly ash
- Fly ash increases long-term strength development of silica fume concrete
- Fly ash offsets increased water demand of silica fume
- Silica fume reduces the normally high levels of high CaO fly ash required for sulfate resistance and ASR prevention
- Very high resistance to chloride penetration can be obtained with ternary blends
- Low CaO fly ash compensates for higher heat release from cement with silica fume, and;
- The relatively low cost of fly ash offsets the increased cost of silica fume.

Use of fly ash, and particularly low CaO fly ash, as an SCM has been known to lower the early strength of the concrete, but enhances the workability for a given w/cm. Silica fume, however, results in a higher reactivity than fly ash due to its finer particle size. The downside to silica fume addition is the decreased workability resulting from the high surface area of the material. When used silica fume and fly ash are used together, both short term and long term benefits are enhanced. (*Khan et al. 2000*)

2.1.2 Calcium Aluminate Cements

CAC concrete has been successfully used in variety of applications for just over 100 years. (*Ideker 2008*) Due to its high alumina content (32-45% Al_2O_3), the term "high-alumina cement" (HAC) first came into use when this type of cement was used after World War I. (*Hewlett 1998*) CAC is different from OPC, in that the major reactive phases in these cements are calcium aluminates, compared to the calcium silicates which dominate OPC. These cements are therefore to be referred as calcium aluminate cements (CAC). As a result of different cement chemistry the hydration products of CAC are also different from OPC. Unlike portland cement where the same hydrates form at all reasonable temperature ranges (e.g. the concrete does not freeze or exceed 70 °C during curing), during CAC hydration several phase assemblages are possible: stable hydrates, metastable hydrates and more commonly mixtures of the two precipitates during the hydration process. The formation of these different phases is driven primarily by temperature at early-ages and by the presence of water at later ages. Inevitably, the lower density, yet space filling, metastable phases will transfer to stable phases with higher density, which leaves increased porosity in the matrix. The process is referred to as conversion. A more detailed description of this phenomenon and its consequences is presented in Chapter 4.

Since the annual production in tonnage of calcium aluminate cements is quite small compared to OPC, this results in a higher cost of 4 to 5 times that of OPC. (*Scrivener et al. 1999*) Therefore they do not compete directly with OPC in daily application where the

performance of OPC is satisfactory. However, several unique properties of CAC make them an ideal material of choice in special applications: (*Hewlett 1998, Scrivener et al. 1999*)

- Rapid strength development, even at low temperatures (emergency rehabilitation, cold weather casting);
- Rapid setting characteristics adjustable through proper admixture dosage;
- Resistance to a wide range of chemically aggressive conditions (sewage networks, industrial floor);
- Resistance to abrasion (hydraulic dams), and;
- High temperature resistance/refractory performance.

Among these characteristics, rapid strength development enables CAC concrete to stand out as an alternative binder system in transportation projects. Usually, CAC concrete can gain 25 MPa at the age of 6 hours. For either new construction or repairs, the maintenance turnaround time is measured by hours, which gives great advantage to CAC concrete in the following applications:

- Night-time repair work on highway slabs with maintenance turnaround times of only 3 hours following the application of concrete;
- Repairs on airport runways and docking bays;
- Industrial infrastructure repairs with minimum impact on operations;
- Repairs of bridge joint closures, and;
- Ultra-rapid turnaround time for tunnels and mines.

Therefore, CAC binder system was identified as a preferable material for further consideration in this research. Chemical shrinkage and autogenous deformation were investigated and compared to the OPC binder systems for ODOT bridge decks.

2.2 CHEMICAL SHRINKAGE

2.2.1 Introduction

The absolute volume of cement and water is greater than the eventual hydration products due to chemical reactions forming new products of higher density than original reactants.

This reduction in volume is commonly referred to as chemical shrinkage. Chemical shrinkage was first investigated as a measurement of the degree of chemical reaction that had occurred in a hydrating cement paste. (*La Chatelier 1900*) Since then, chemical shrinkage has been frequently used as an indicator of the progression of hydration reactions.

2.2.2 Test Method

There are three principal measurement methods of chemical shrinkage: dilatometry, pycnometry and gravimetry. (*Justnes et al. 2000*) The principles of the three methods are shown in Figure 2.1 adapted from Bouasker and co-workers (*2008*).

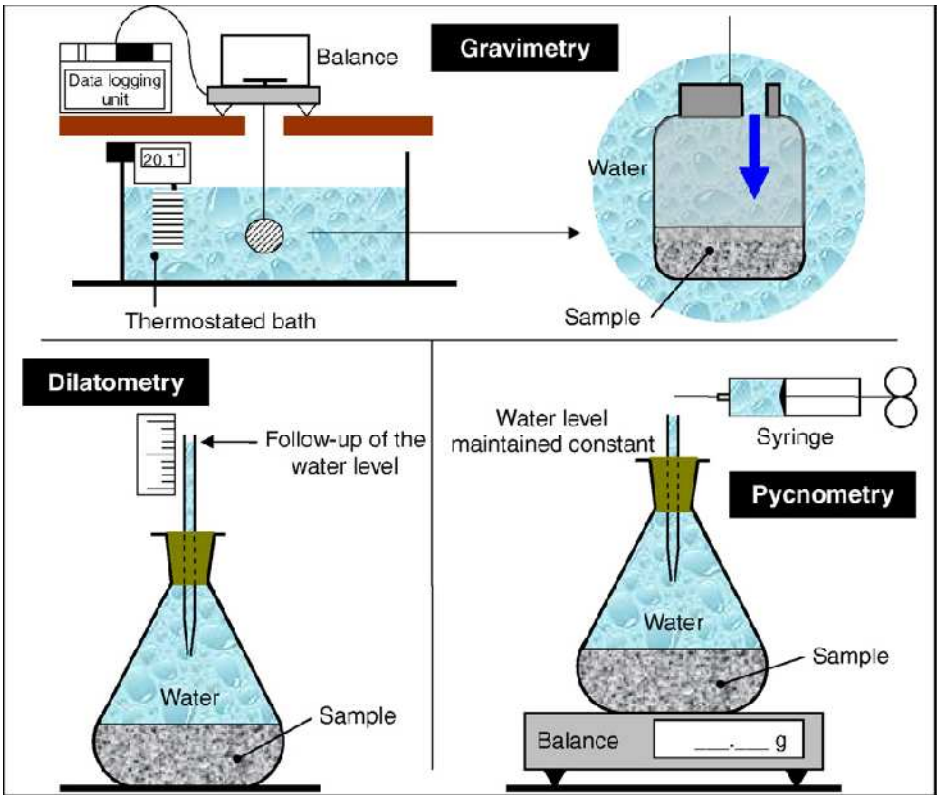

Figure 2.1: Chemical shrinkage measurement methods (*Bouasker et al. 2008*)

Among these test methods, the most widely used is dilatometry which has been adapted as standard test method ASTM C1608. In short, the standard way to measure this

reduction in volume involves casting a small volume of cement paste in a rigid vial. Water is carefully placed above the sample almost immediately after mixing the paste. A pipette fitted through a rubber stopper is fitted into the top of the vial so that water rises into the pipette to an initial level. The quantity of water "absorbed" by the paste is monitored over the course of time by monitoring the decrease in height of the water in the pipette. Samples are placed in a water bath to maintain isothermal conditions, typically at 20 °C, although other researchers have investigated the influence of temperature as well. (*ASTM C1608 2005, Costoya 2008, Ideker 2008, Peethamparan et al. 2010*)

The chemical shrinkage is computed as the measured absorbed water per gram of cement in the paste specimen. The mass of cement powder (M_{cement}) in the vial is given by:

$$\boldsymbol{M_{cement} = \frac{(M_{vial+paste} - M_{vialempty})}{(1.0 + \frac{w}{cm})}} \qquad \text{Equation 2}$$

Where:

$M_{vial+paste}$ = mass of the glass vial with the added cement paste (g);

$M_{vialempty}$ = mass of the empty vial (g);

w/cm = water to cement ratio by mass of the prepared paste.

At time *t*, the chemical shrinkage per unit mass of cement $CS(t)$ is computed as:

$$\boldsymbol{CS(t) = \frac{[h(t) - h(60min)]}{M_{cement}}} \qquad \text{Equation 3}$$

Where:

h(t) = water level(ml) in capillary tube at time t;

h(60) = water level in (ml) capillary tube at 60 minutes.

To monitor chemical shrinkage for a longer period of time (e.g. up to 14 days) than recommended by ASTM C1608 (currently 24 hours), an automated test set-up was developed. The test set-up is shown in Figure 2.2. It usually took 30 to 40 minutes after

initial contact to get samples ready for measurements. After all samples were set up, an additional 10 to 20 minutes were needed to bring all samples to the desired temperature. Therefore, the data point of 60 minutes after initial water contact was selected for all samples as starting reference for chemical shrinkage measurement.

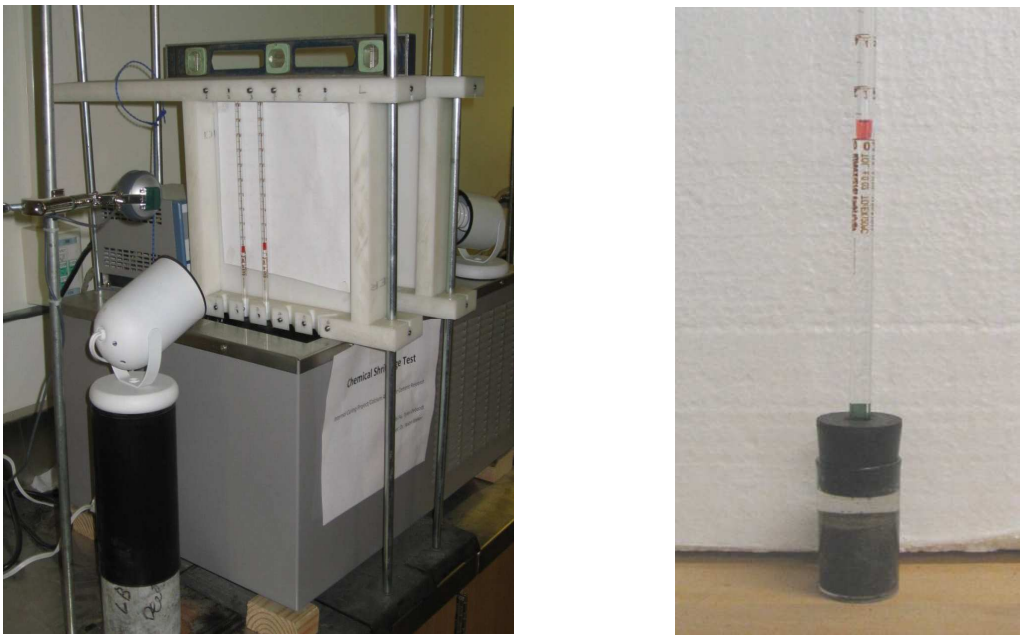

a) Test set up b) Specimen

Figure 2.2: Automated chemical shrinkage test set-up

A webcam with high resolution of 1.3 megapixels was placed in front of the pipettes to allow for automated image acquisition. Images were taken approximately every 5 minutes resulting in over 4000 images. Then they were analyzed using a computer software program developed in the Laboratory of Materials of Construction (LMC) at EPFL in Lausanne, Switzerland to determine the total water uptake by the hydrating cement paste. (*Bishnoi 2009*) This image analysis provided significant enhancement to the accuracy of chemical shrinkage results. (*Costoya 2008, Ideker 2008*)

Figure 2.3 shows typical chemical shrinkage results for OPC and CAC systems recorded and processed by the automated image analysis system. And a measurement taken by hand is also shown in Figure 2.4.

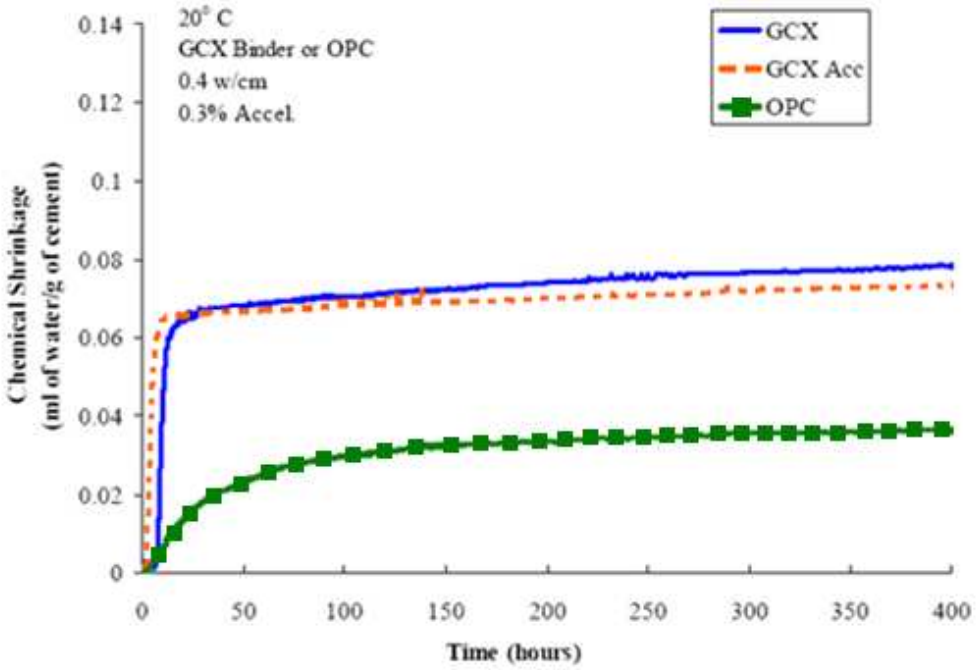

Figure 2.3: Typical automated chemical shrinkage results (*Ideker 2008*)

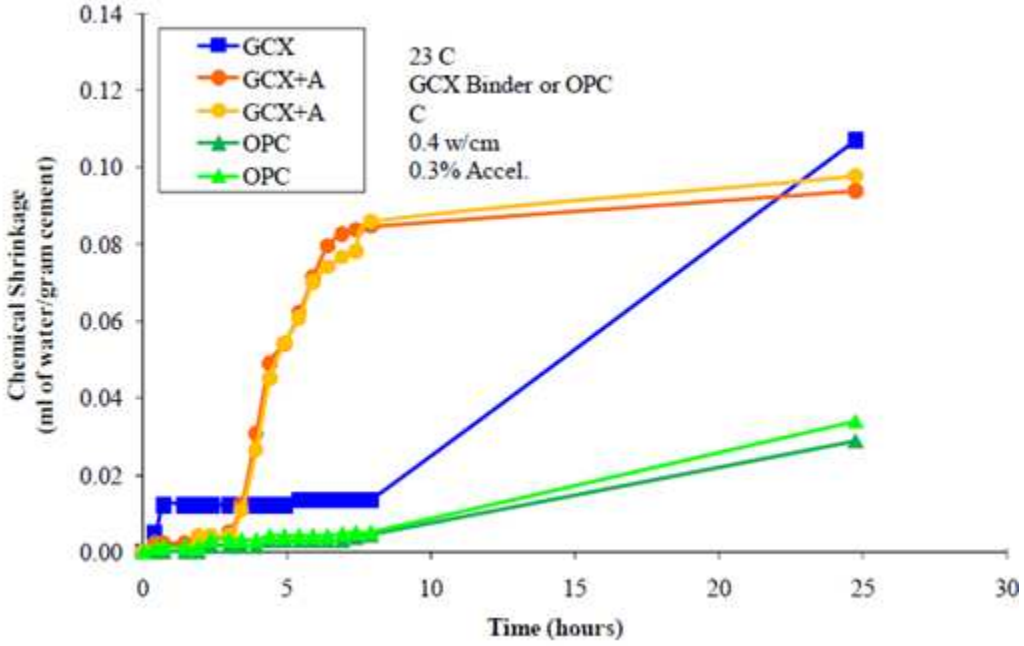

Figure 2.4: Chemical shrinkage results by hand (*Ideker 2008*)

From the comparison, it can be seen that that the automated procudure can obatin much more discrete and smother measurements to a long time with less effort. More detail about this automated test set is presented in Chapter 4..

Another frequently used method is gravimery method, shown in Figure 2.5.

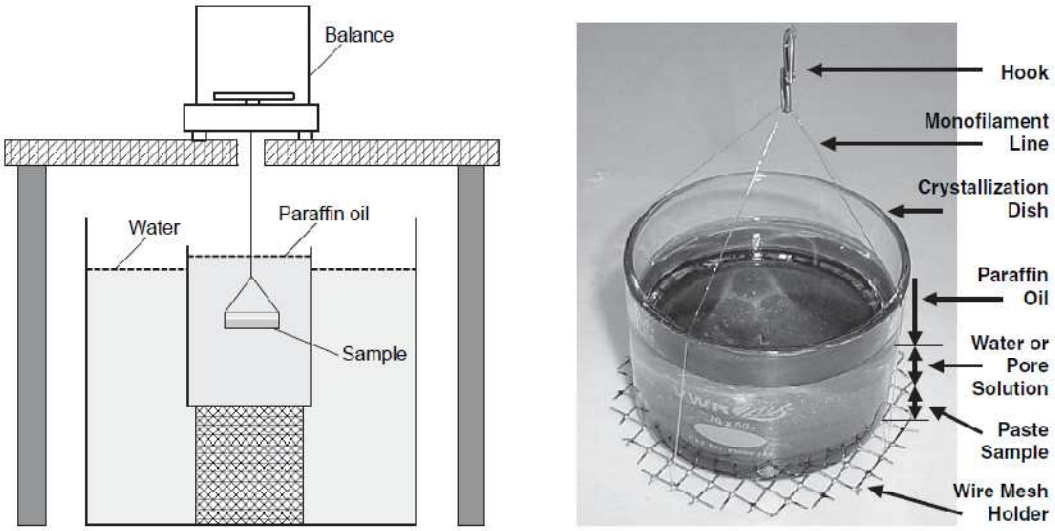

a) an illustration of the buoyancy method b) a photo of chemical shrinkage specimen

Figure 2.5: An illustration of the experimental chemical shrinkage set-up (*Sant et al. 2006*)

Due to its automated data logging ability, similar set-ups have been used in many recent investigations. (*Bouasker et al. 2008, Castro 2010, Sant et al. 2006*) Usually the measurement is performed by monitoring the change in buoyancy that occurs for a sample suspended in paraffin oil. By connecting the balance and a computer, the weight change of the sample can be continuously logged, and it corresponds to the consumption of the water in the chemical reaction. The time-variant chemical shrinkage, V_{CS}, which stars at 30 minutes after the initial contact of water and cement, can be determined as follows: (*Sant et al. 2006*)

$$V_{CS} = \frac{\Delta V_{paste}(t)}{g_{cement}} = \frac{W_{sub}(t) - W_{sub}(30)}{\rho_{oil} \cdot g_{cement}} \qquad \text{Equation 4}$$

Where:

$\Delta V_{paste}(t)$ = the volume change (ml) of the paste;

g_{cement} = the mass of the cement content (g) in the paste;

$W_{sub}(t)$ = the submerged weight (g) of the paste at time t;

$W_{sub}(30)$ = the initial submerged weight (g) of the paste 30 minutes after water addition, and;

ρ_{oil} (g/ml) = the density of the paraffin oil in the bath.

2.3 AUTOGENOUS DEFORMATION

2.3.1 Introduction

Autogenous deformation is defined as "the bulk deformation of a closed, isothermal, cementitious material system not subjected to external forces" (*Jensen and Hansen 2001*). The word "closed" signifies that no exchange of matter (in particular moisture) takes place between the cementitious material and the surroundings. The word "isothermal" signifies that the temperature is kept constant. Autogenous deformation should be divided further into autogenous shrinkage and autogenous expansion. The Japanese Concrete Institute defines autogenous shrinkage as:

> *"Autogenous shrinkage is the macroscopic volume reduction of cementitious materials when cement hydrates after initial setting. Autogenous shrinkage does not include volume change due to loss or ingress of substances, temperature variation, application of an external force and restraint (Tazawa 1999)."*

Similarly, the autogenous expansion is defined as:

> *"Autogenous expansion is the macroscopic volume increase of cementitious materials when cement hydrates after initial setting. Autogenous expansion does not include volume change due to loss or ingress of substances, temperature variation, application of an external force and restraint (Tazawa 1999)."*

Autogenous shrinkage is a phenomenon closely related to changes in internal relative humidity (RH). In OPC concretes without SCMs, autogenous shrinkage is negligible when compared to drying shrinkage. (*Davis 1940*) However, in HPC with low w/cm and

the addition of silica fume, autogenous shrinkage can be significant enough to induce micro- or macro-cracking and may impact the concrete quality and ultimately its durability. (*Lura 2003*)

While the mechanisms leading to autogenous shrinkage are not yet fully understood, it is generally agreed upon that a relationship exists between autogenous shrinkage and changes in relative humidity of capillary pores in the cement paste. (*Grasley and Lange 2007, Jensen and Hansen 2001*) This relationship can be explained by the difference in chemical shrinkage between cementitious materials in HPC. For instance, the chemical shrinkage of OPC is typically around 0.07, which means a 7% mass of water per mass of cement is needed to complete the hydration process. While in an HPC system, the same coefficients for silica fume, slag and fly ash are respectively 0.22, 0.18 and 0.10 to 0.16 (range for fly ash). (*Bentz 2007*) This implies that for complete hydration in HPC, more water is required. In HPC as the internal RH decreases due to increasing water demand the resulting capillary pressure arising from water leaving small capillaries (Φ<50 nm) can be great enough to cause these pores to collapse and as a result a macroscopic shrinkage occurs – termed autogenous shrinkage. (*Mehta and Monteiro 2006*)

Figure 2.6 shows an illustration of this process, and the grey area represents paste and white area represents the void left by hydration.

a) a small pore within cement matrix

b) when water is consumed by hydration, the pore may collapse

c) the pore almost closed

Figure 2.6: Illustration of the collapse of a small capillary (Φ<50 nm)

Based on this collapse of small capillary mechanism, the critical factor controlling autogenous shrinkage is the supply of water. However, simply increasing the w/cm is not an option as that low w/cm ensures high strength, low permeability and increased durability in HPC. Furthermore, increasing an external water supply (such as wet curing) is also of little effect in HPC as the refinement of the pore structure and decrease in permeability even at early-age is significant enough to limit the transport of water to reacting cementitious phases. (Durán-Herrera et al. 2007)

Several innovative shrinkage mitigation strategies, such as internal water curing by LWFA/SAP and incorporation of SRAs, have been developed. (*Kovler and Jensen 2005*) Internal water curing using saturated LWFA or SAP, which has become increasingly popular options in the last 10 years (*Roberts 2004*), is capable of providing internal sources of water that could replace the water consumed by the hydration process. Several field applications have shown that autogenous shrinkage in HPC can be significantly mitigated using this type of internal curing approach. (*Cusson 2008, Villarreal 2008*) Shrinkage reducing admixtures are effective in reducing the surface tension of the pore solution inside the concrete. As a result when water leaves these pores to participate in hydration reactions a lower initial pressure exists which significantly reduces the potential for capillary pores to collapse as water leaves them. (*Bentz 2005*) The application of materials that allow internal curing can mitigate autogenous shrinkage as well as drying shrinkage (also discussed in section 2.5.3).

It was observed more than a century ago by Le Chatelier that if a cement paste hydrates in saturated conditions, it will expand. Recently, Le Chatelier's experiment was reproduced with modern cements at the University of Sherbrooke. Cracks were observed on the surface of the flasks containing cement paste as a result of autogenous expansion. (*Durán-Herrera et al. 2008*) One possible explanation is that no capillary pressure in a hardening paste cured in saturated conditions develops to oppose the expansion of the solid phases. (*Powers 1935*)

To capture the autogenous deformation or to assess the effectiveness of shrinkage mitigation strategies, many measurements techniques for autogenous deformation have been developed. These measurement techniques have been debated as to their accuracy and ease of use. However, until 2009 no standard test method had been adopted by major standards organizations (ACI, ASTM, AASHTO and RILEM). The recent adoption of ASTM C 1698-09 for assessing autogenous deformation has pushed one method into the forefront for standard testing purposes. Fundamentally, all proposed measurements of autogenous deformation (strain) can be characterized into two different categories: measurement of volumetric strain and measurement of linear strain. ASTM C 1698-09 is a linear deformation testing method which is further described in 2.3.2.1. The remainder of this section provides a detailed summary of test methods for assessing autogenous deformation.

2.3.1.1 Volumetric Measurements of Autogenous Deformation

Volumetric measurements of autogenous strain are frequently performed by placing the fresh cement paste in an elastic rubber membrane immersed in a liquid. The fundamental elements of the volumetric method as it is used today were initiated in 1940's (*Yates 1941*): a rubber membrane containing cement paste submerged in water. The change in volume of the cement paste is measured by the amount of liquid displaced by the immersed sample, typically by measuring its weight change. This method is also referred to as the buoyancy method. The membrane method was developed to test autogenous deformation of cement paste. A typical membrane sample filled with cement paste is shown in Figure 2.7.

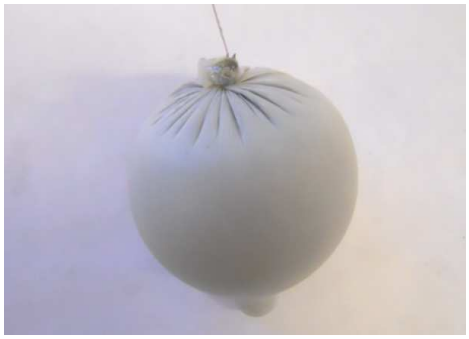

Figure 2.7: Polyurethane membrane filled with cement paste

A typical testing setup involves casting a total of 100 g to 150 g of fresh cement into a membrane. Caution is taken to avoid entrapping air bubbles that may reduce the accuracy of the buoyancy method. The membrane is then tightly closed with a knot and the desired length of 0.12 mm polyethylene line is affixed to the sample by means of a plastic strap. The line is tied to a stainless steel hook to suspend the sample beneath a weigh below scale. The sample is then submerged in a container containing a liquid which is placed in a water bath. The test is carried out under constant temperature (typically 20 ± 0.2°C). A representative experimental set-up is shown in Figure 2.8.

Figure 2.8: Experimental set-up for membrane method to test autogenous strain for cement paste

Recent research has elucidated some of the challenges with this testing method. A thorough investigation on issues related to osmosis was conducted by Lura and Jenson (*2005*). They proved that the water uptake of the samples is a significant artifact of membrane method. Therefore, proper considerations should be given to: (*Lura and Jensen 2005*)

- Types of membrane used;
- Buoyancy liquid used, and;
- Temperature control.

2.3.1.2 Discussion of Results

The results of volumetric and linear measurements of autogenous strain should be identical. However, the test results of the membrane method are usually three times, or sometimes one magnitude, higher than the linear measurement. (*Lura and Jensen 2005*) The reason for this inconsistency is transport of buoyancy liquid through the rubber membrane, especially when water is used as the buoyancy liquid. From the point that the sample is submerged under water, osmosis through the membrane will initiate. The self-desiccation due to the process of hydration and the salts dissolved in the water inside will provide a driving force (osmosis) to draw more water through the membrane, which in turn causes a mass gain which can significantly alter the testing results. It has been shown that if the buoyancy liquid is changed from water to paraffin oil, the water absorption though the membrane can be eliminated. The results using this modification show strong agreement with the linear measurement. (*Lura and Jensen 2005, Sant et al. 2006*) Another challenge in this testing method is the selection of the membrane material. Because latex membranes can dissolve in paraffin oil, polyurethane membranes are recommended for testing autogenous strain for cement pastes.

Although the most significant artifacts can be eliminated by using polyurethane membranes immerged in paraffin oil, special attention should be given to other artifacts which might cause inaccuracies. The pressure of the membrane and the buoyancy liquid

could cause greater deformation on the weak interface layer between membrane and pastes compared to the bulk paste. (*Lura and Jensen 2005*) And the entrapped air can be avoided by mixing under vacuum and using deaired and deionized water. (*Lura et al. 2009*) In addition, the reabsorption of bleed water might cause inaccuracies. The bleed water might be drawn back into the cement paste as a consequence of internal volume reduction caused by chemical reactions. (*Jensen 1996*) However, if the paste contains silica fume, this effect may be insignificant. (*Lura and Jensen 2005*)

Another issue associated with autogenous deformation is the interpretation of the test results. The first several hours of autogenous deformation results are recorded when the cement pastes are in the plastic state before setting. During this state, the internal volume reduction completely changed into a bulk deformation of the system. In this sense, the chemical shrinkage and autogenous shrinkage are the same during this state. And the shrinkage during this period of time is referred as setting shrinkage (see Figure 2.9). (*Jensen and Hansen 2001*) The time where the autogenous deformation curve diverges from the chemicals shrinkage curve is usually similar to the final set as determined by the Vicat test. (*Sant et al. 2006*)

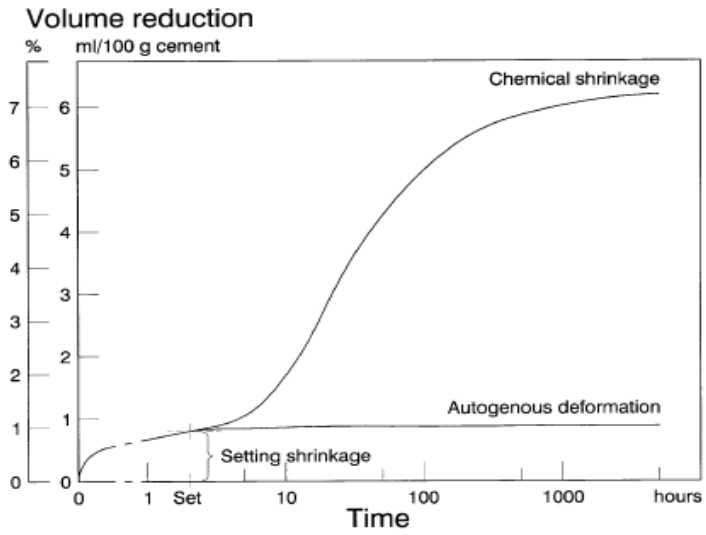

Figure 2.9: Typical results of autogenous deformation and chemical shrinkage tests (*Jensen and Hansen 2001*)

Figure 2.9 demonstrates the deviation of autogenous shrinkage from chemical shrinkage due to the formation of a rigid microstructure that can resist macroscopic volume change. However, it is important to note that in a hardened microstructure even relative small changes in strain can result in significant stress build-up which may result in cracking, especially at early-ages.

2.3.2 Linear Measurements of Autogenous Deformation

Linear measurement of autogenous strain is usually performed by placing the cement paste in a rigid mold with low friction between the interface of the paste and the mold wall. (*Lura and Jensen 2007*) The change in length can be recorded using a linear variable differential transformer (LVDT) at the end of a specimen. Several methods existing measuring methods are discussed in detail in this section:

- Corrugated tube method;
- Modified ASTM C157 method;
- Free deformation frame method, and;
- Shrinkage drain method.

2.3.2.1 Corrugated Tube Method

A specially designed plastic tube is used in the corrugated tube method. This method has recently been adopted as ASTM C1698-09. The cement paste is cast under vibration into tight corrugated plastic molds (low density polyethylene plastic, LDPE). For a deformation of 10,000 µm, the restraint force on the paste is less than 0.5 N (corresponding to a stress of 0.001 MPa). (*Jensen 1996*) A cross section of this mold is shown in Figure 2.10.

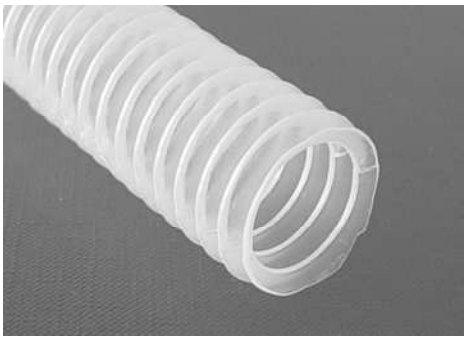

Figure 2.10: Special corrugated plastic mold (Φ=30 mm) for autogenous deformation measurements. (*Lura 2003*)

The sample typically has approximately a length of 300 mm and 30 mm in diameter. The specimens are placed in a dilatometer, and to maintain isothermal temperature should be immersed into a glycol bath. The test is typically run at an isothermal temperature of 20 ± 0.1 °C. A schematic at the top view of the dilatometer is shown in Figure 2.11a and an actual set-up is shown in Figure 2.11b. The dilatometer frame consists of two steel plates joined rigidly by four solid invar steel rods. Each specimen is supported longitudinally by two smaller parallel rods attached to the steel plates. The specimens are typically fixed at one end, and the sample can thus move freely on the support rods. The entire set-up is immersed into a glycol bath (to prevent any water transport through the sealed end caps should a leak occur), which can also function as lubricant to reduce frictional forces. The longitudinal deformation is measured at the free end by an LVDT, and the results are recorded automatically through appropriate data acquisition devices. (*Lura 2003*)

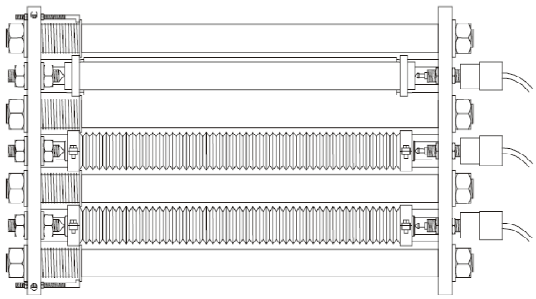

a) Schematic(*Jensen 1996*) b) Representative picture (*Lura and Jensen 2007*)

Figure 2.11: Dilatometer with corrugated moulds for measurements of linear autogenous strain

Although the corrugated tube method is easy to perform and is repeatable, some care should be taken during testing. Air entrapped within the tube might cause inaccuracies, which can be insignificant when special attention is given when preparing the specimen. Because the test runs under glycol bath, proper sealing is very important and should be checked by monitoring the weight of each sample before and after the test. (*Lura and Jensen 2005*)

The larger corrugated tube (as shown in Figure 2.12) may be used to test autogenous strain of concrete. In this case, temperature control becomes more critical due to the larger size making active temperature control a necessity. Friction and locking in the mold could also affect the accuracy of the results.

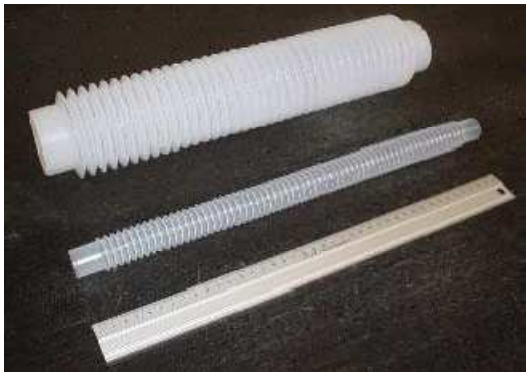

Figure 2.12: Larger corrugated tubes for testing autogenous strain of concrete (*Bentz et al. 2009*)

2.3.2.2 Modified ASTM C157

The standard ASTM C 157 unrestrained length change procedure is performed to evaluate drying shrinkage. By completely sealing these standard specimens, autogenous shrinkage may also be measured. This method usually starts at an age of 24 h after casting. As a result a majority of characteristics of the early-age behavior are not captured. Several modified methods have been proposed to test autogenous shrinkage of concrete by using these concrete prism specimens. (*ASTM C157 2006*)

Figure 2.13 shows the standard experiment set-up for testing autogenous strain by the JCI. (*Tazawa 1999*) Similar equipments (see Figure 2.14) have been evaluated at the Virginia Polytechnic Institute and State University by the Virginia Transportation Research Council (*Ramniceanu et al. 2010*), and also in Ottawa by the National Research Council Canada's Institute for Research in Construction. (*Cusson 2008*)

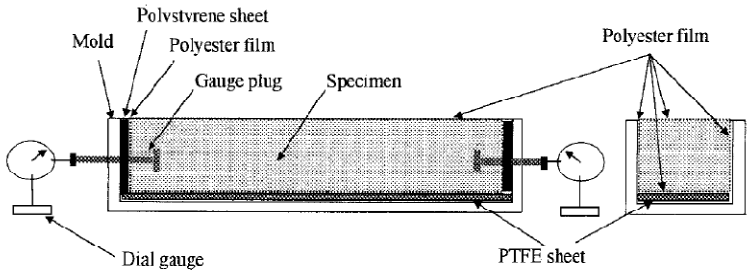

Figure 2.13: JCI standard test set-up for evaluating autogenous strain, 40×40×160 mm (mortar) and 40×40×400 mm (concrete) (*Tazawa 1999*)

Figure 2.14: Modified ASTM C157 Prism Mold (*Ramniceanu et al. 2010*)

The basic concept behind the modified method is to monitor the concrete prisms shortly after casting under constant room temperature. A petroleum gel and thin plastic film are applied to reduce friction between the specimen and the steel walls of the molds. The longitudinal length changes are recorded using LVDTs at both ends, which are fixed to the steel base of the equipment. At early-ages, temperature variations within the specimen may result in inaccurate readings due to thermal deformations. However, temperature control may be possible by applying a circulating water system to the specimen. Restraint caused by the steel forms is still of significant concern with this testing method, as well

as the challenges arising through modifications made to the system to include active temperature control. Recent research done by Virginia Transportation Research Council (VTRC) used a modified ASTM C157 method to investigate the volume change of typical bridge deck concrete mixtures. Teflon tape along with lithium grease was applied to prevent adherence to the mold wall. Dimensional changes were recorded by two LVDTs. The final report of this research indicates that this modified ASTM C157 method gave the most consistent results and also recommends Virginia Department of Transportation implement this method to control the shrinkage of field concrete mixtures. (*Ramniceanu et al. 2010*)

2.3.2.3 Free Deformation Frame Method

A free deformation frame (see Figure 2.15) was developed in mid 1990s to measure autogenous deformation of a concrete mixture as a companion test with rigid cracking frame. (*Springenschmid 1998*) Later, the free deformation frame was used successfully by some other researchers. (*Ideker 2008, Lura 2003, Slatnick et al. 2011*)

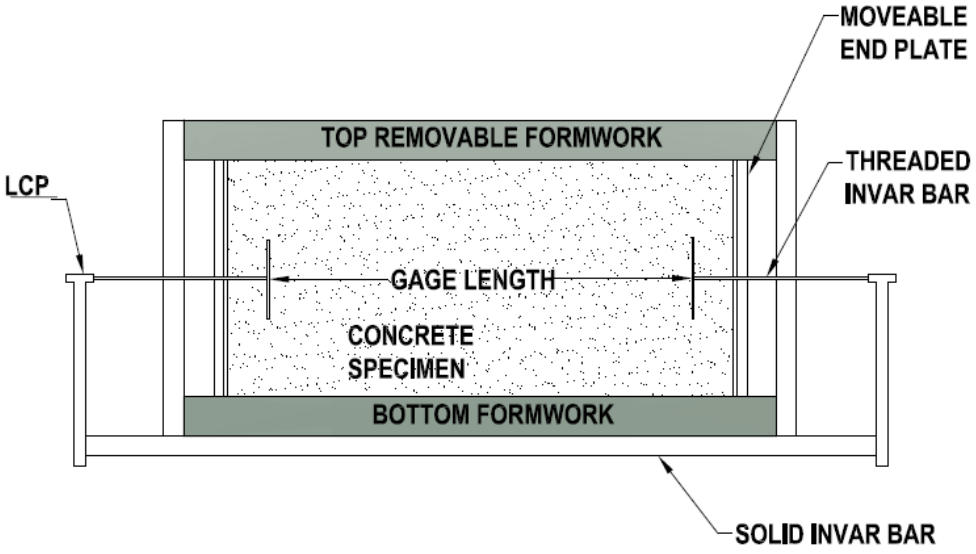

Figure 2.15: Typical free deformation frame (*Ideker 2008*)

In a recent research in University of Texas, Austin, a free deformation frame with dimensions of 150×150×520 mm was used as shown in Figure 2.16. Concrete specimens were cast in the frame. Two threaded invar bars were screwed into the specimens at both end. Two LVDTs were applied at each end to collect strain data at 5 minutes interval. Grease was applied to the threaded bars to recover and reused after the test. The specimen was completely sealed from the outer environment by plastic sheet and water-resistant aluminum tape. Lubricant was applied between the plastic sheet and frame walls. The temperature was monitored by thermocouples embedded in the specimen. Temperature control was achieved by a circulator that circulates a 50/50 mixture of water and antifreeze through copper pipes that are placed in the frame. (*Slatnick et al. 2011*)

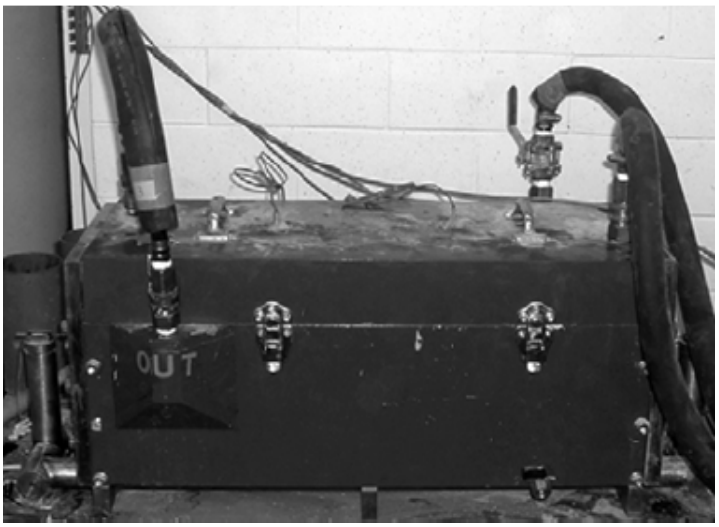

Figure 2.16: Free deformation frame at the University of Texas, Austin (*Slatnick et al. 2011*)

Compare to other linear testing methods, due to the larger specimen cross section, actual concrete can be tested. However, the larger dimensions make keeping isothermal conditions difficult, especially when CAC or rapid portland cement is used. For better temperature control purpose, a 1/3 scaled versions of the free deformation frame with a programmable heating and cooling circulation systems was used by Ideker (2008). The scaled frame with dimensions of 51×51×175 mm and a 135 mm effective gage length were successfully maintained temperature within ±2 ° C of desired temperature. (*Ideker 2008*)

2.3.2.4 Schleibinger Shrinkage Drain

The Schleibinger Shrinkage Drain, a commercially available apparatus, was evaluated at the University of Michigan (*Riding et al. 2008*). The shrinkage drain is made of a one meter long U-shape stainless steel channel, with cross sections of 60 mm by 100 mm and length of 1000 mm for concrete. The specimen is anchored at one end, and the length change is registered at the other end by LVDT.

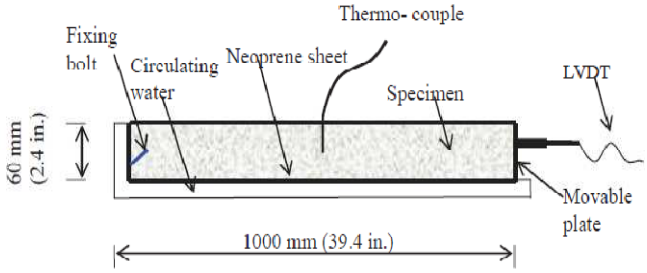

a) Schematic illustration (*Wei and Hansen 2008*)

b) Representative picture (*Bentz et al. 2009*)

c) Specimens in testing (*Bentz et al. 2009, Wei 2009*)

Figure 2.17: Linear measurement of autogenous shrinkage (Schleibinger Shrinkage Drain)

To accurately test the free deformation, minimizing friction between the specimen and the testing rig, preventing moisture loss to the external environment and keeping isothermal curing conditions are major concerns. The specimen is sealed on the top with polystyrene film after casting, and a soft, flexible, 2 mm-thick foam rubber is placed alongside the wall to minimize friction. Isothermal temperature (23±1 ºC) is maintained

by circulating constant-temperature water through the channels built-into the sides and bottom of the mold.(*Wei 2009*) A thermocouple is embedded in the specimen to monitor the temperature history. To further reduce the effect of friction between specimen and walls, a V-shape channel may also be used to minimize the surface area of the fresh concrete and also to reduce the potential for eccentricity within the longitudinal specimen. A single operator repeatability study showed the method might be used as reliable measuring tool for early-age shrinkage. (*Newlands et al. 2008*)

2.3.3 Other Measurement Methods of Autogenous Strain

Numerous other measurements have been proposed to evaluate autogenous deformation of cementitious systems. Some of these are identified in this study, with particular advantages highlighted for inclusion in this research project.

2.3.3.1 Non-corrugated Cylindrical Molds Method

In this method concrete is cast in sealed plastic concrete cylinder molds and shrinkage is monitored with a simple dial gauge (see

Figure 2.18).

Figure 2.18: Cylindrical mold method (*Bentz et al. 2009*)

The simplicity of this test set-up makes this method good for on-site testing, with the possibility of multiple tests possible of being conducted at the same time. If the material of the cylinder is properly selected, the inaccuracy caused by friction can be minor.

(*Bentz et al. 2009*) However, it is difficult to achieve active temperature control in this set-up to maintain isothermal temperature. Furthermore, with a limited length to diameter ratio, the measured longitudinal length change is inaccurate when correlated to realistic strain. Due to the ease in set-up and the capability to test many samples at the same time, this method still might provide useful reference for on-site applications and rough estimation of concrete performance.

2.3.3.2 Vibrating Wire Method

The basic idea behind this technique is to detect resonant frequency of a length of steel wire, which when embedded in fresh concrete, can be altered by deformation of the concrete specimen throughout curing. The wire is protected by a thin-wall steel tube on the outside and embedded in the concrete specimen. A certain length of steel wire is stretched between two brackets which are in direct contact with the concrete specimen. As the concrete deforms the length of the wire will also deform and as a result the resonant frequency of the wire will be altered. A pickup coil can be used to detect the vibration frequency in the form of an alternating current and will then provide output signals. A thermocouple can also be incorporated into the gauge to simultaneously detect temperature and then temperature variations can be accounted by using the coefficient of thermal expansion of the concrete. (*Durán-Herrera et al. 2007*) Figure 2.19 shows a typical test set-up using a vibrating wire gage.

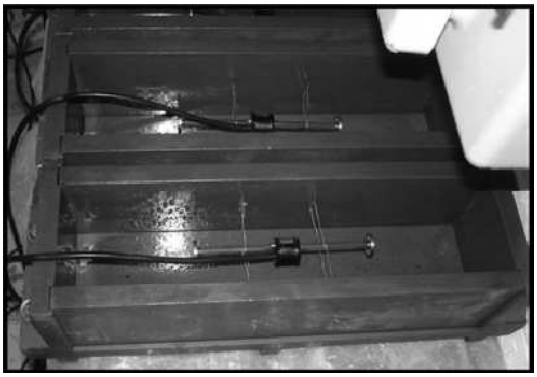

Figure 2.19: Vibrating wire method (*Durán-Herrera et al. 2007*)

2.3.4 Comparison and Summary

A thorough review of testing protocols and interpretation of results in terms of measurement of early-age volume change in cement pastes was provided by Sant et al (*2006*). They summarized the membrane method, linear method and modified ASTM C157 method as follows: (*Sant et al. 2006*)

- The "blind application" of ASTM C157 cannot capture a significant amount of shrinkage before the beginning of the test (standard 24 hours after casting) and the setting time should be included in interpreting the results (see Figure 2.20), and;
- The volumetric method (membrane method) and linear method (corrugated tube) show very similar results provided that the osmosis is prevented by choosing a proper membrane and buoyancy liquid.

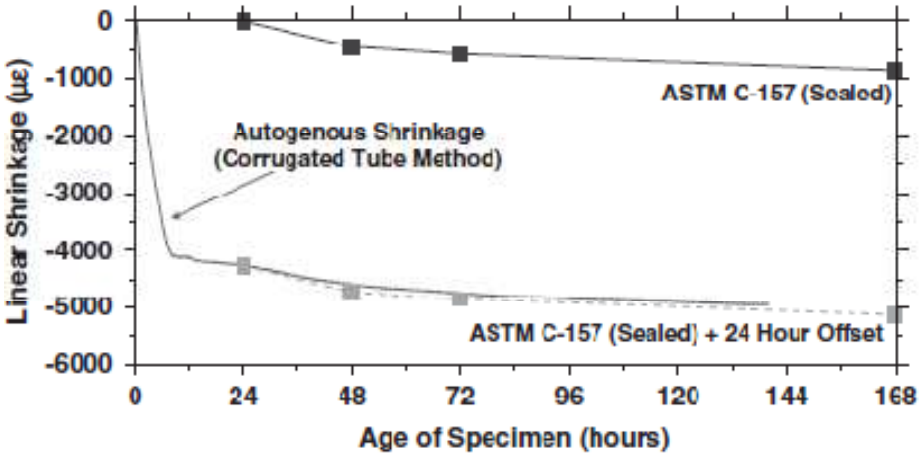

Figure 2.20: Comparison of autogenous shrinkage measured in sealed specimens using ASTM C 157 procedure (beginning at 24 h) and corrugated mold procedure (beginning immediately after mixing) for a w/c=0.30 mixture (*Sant et al. 2006*)

Provided the precautions outlined in this section are accounted for, most test methods show a reasonable correlation after setting, as shown in Figure 2.21 (*Sant et al. 2006*).

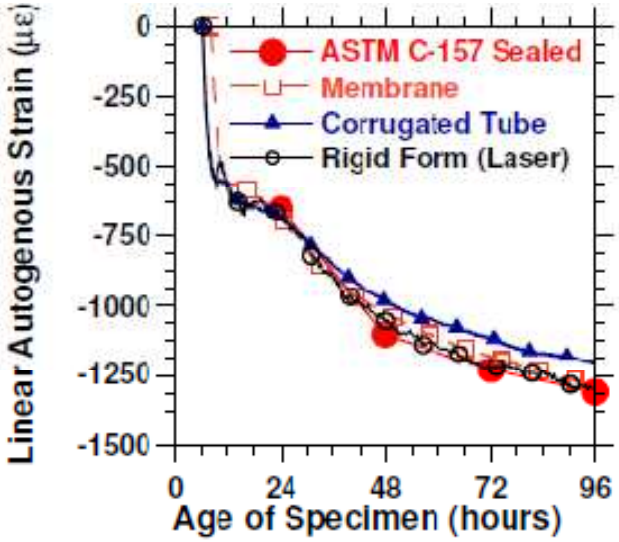

Figure 2.21: Comparison of different autogenous deformation testing methods (*Sant et al. 2006*)

Within this literature review, a variety of methods to test autogenous deformation of cementitious systems were identified. While a detailed summary of all available test methods is beyond the scope of this literature review, those methodologies with the most promise for successful identification of autogenous deformation characteristics were given. Through highlighting the methodologies which are most feasible and reliable, a sufficient reference is provided for the current research project in order to properly select or modify existing methods to test autogenous deformation. All methods identified within this study are summarized in Table 2.1 with remarks provided as to the efficacy of each testing methodology.

Table 2.1: Comparison of unrestrained autogenous deformation test methods

Test Method	Material	Advantages	Disadvantages
Membrane Method	Paste	Good temperature control Captures expansion	Challenging for initial setup Issues with bleeding Selection of testing procedures critical
Corrugated Tube Method	Paste Mortar Concrete	Temperature control Captures expansion Equipment commercially available(*Bentz 2008*) Easy to perform and repeat **Method adopted as ASTM C 1698-09 (*ASTM C1698 2009*)**	Length undefined before setting Friction/locking of sample in mold, especially when testing concrete using large corrugated tube Difficult sealing Issues with bleeding at early-ages
Modified ASTM C157	Concrete	Possible temperature control Easy to perform and repeat	Temperature variation/control Friction of sample in mold Questionable expansion measurement in some versions Does not capture early-age behavior
Free Deformation Frame Method	Mortar Concrete	Active temperature control Captures expansion Easy to interprets results	Friction of sample in mold Complicated and expensive equipment
Shrinkage Drain	Mortar Concrete	Temperature control Equipment commercially available Able to simultaneously register temperature and relative humidity	Friction of sample in mold Difficult sealing
Cylindrical Molds Method	Concrete	Very simple set-up Able to do multiple tests at the same time Good for on-site testing Might be used to test settlement (subsidence shrinkage)	Difficult temperature control Inaccuracies when interpreting test results Possible differential settlement Lack of agreement between vertical displacement and strain
Vibrating Wire Method	Concrete	Temperature control Directly record strain	Size of gage may influence results Difficult sealing

2.3.5 Mitigation Strategies

Research since the early 1990s has shown that LWA saturated with water could provide internal curing to mitigate autogenous shrinkage in concretes incorporating silica fume, thereby reducing shrinkage related stresses and the potential for early-age cracking. (*Hammer 1992*) Momentum in the area of internal curing using saturated LWAs has increased since the year 2000 with increasing evidence of application of internal curing in field concretes. (*Roberts 2004*)

Research has led to the development of an equation (Bentz Equation) for predicting the amount of saturated LWFA needed to protect HPC from deleterious autogenous shrinkage. (*Bentz and Snyder 1999, Bentz et al. 2005*) This equation takes into account several important variables including the chemical shrinkage of the cement, degree of saturation and the absorption capacity of LWFA. However, there is still a need to verify and extend this equation to HPC incorporating SCMs such as fly ash and silica fume (and in particular ternary blends).

Recent research investigating free and restrained shrinkage of HPC test samples incorporating internal curing (LWA or SAP) showed that the reduction in autogenous shrinkage (and in fact an autogenous expansion was observed) corresponded to a reduction in the generation of tensile stresses. (*Cusson and Hoogeveen 2008, Slatnick et al. 2011*) These researchers also showed that for optimum partial replacements of fine aggregate with saturated LWFA that the early-age strength and modulus, desirable in HPC mixtures could be retained. Cusson and Hoogeveen (*2008*) also showed that the risk of concrete cracking could be conservatively estimated using free shrinkage strain data. They also demonstrated that the early-age autogenous expansion which pushed elastic and creep strains into a zone of compression allowed for tensile strength development in the concrete to occur ahead of the development of tensile stresses due to shrinkage which also reduced the risk of early-age cracking. However, the concrete mixtures investigated by both of these researchers did not incorporate SCMs such as fly ash or silica fume, and

as a result it will be necessary to further this work by demonstrating the efficacy of internal curing applied to systems capable of generating higher autogenous shrinkage strains. (*Cusson and Hoogeveen 2008, Slatnick et al. 2011*)

2.4 PLASTIC SHRINKAGE

2.4.1 Introduction

Plastic shrinkage refers to volume change occurring while the concrete is still fresh, before hardening. It is usually observed in the form of cracks occurring before or during finishing. The American Concrete Institute (ACI) committee 116 defines plastic shrinkage cracking as "cracking that occurs in the surface of fresh concrete soon after it is placed and while it is still plastic" (*ACI Committee 116 2000*). Plastic shrinkage in concrete is a combination of chemical and autogenous shrinkage and is mainly governed by the loss of water due to rapid evaporation of moisture from the surface that exceeds the bleeding rate. (*Kosmatka et al. 2002, Mora-Ruacho et al. 2009*) Plastic shrinkage cracks rarely impair the strength of concrete floors and pavements. Nevertheless, in addition to being unsightly, the existence of cracks might potentially reduce the long term durability due to the accelerated ingress of aggressive agents. (*Lura et al. 2007*) Therefore, appropriate measures should be taken prior to and during construction by minimizing surface evaporation through use of fogging, wind breaks, shading, plastic sheet covers, wet burlap, spray-on finishing aids (evaporation retarders), SRAs and plastic fibers. (*Kosmatka et al. 2002*) More recent research has been focused on the applications of SRAs and saturated LWFA to combat many types of shrinkage including plastic shrinkage cracking. (*Henkensiefken et al. 2009, Lura et al. 2007, Mora-Ruacho et al. 2009*)

2.4.2 Mechanisms of Plastic Shrinkage

According to Lura et al. (*2007*), plastic shrinkage cracks are generally attributed to four driving forces. The first driving force is the rapid evaporation of water, which creates

menisci and high tensile stresses in the capillary water near the surface. This is the reason that finer cements and mixtures containing silica fume are usually more susceptible to plastic shrinkage cracking where these systems have smaller pores, refined porosity and permeability, and higher capillary tension exists to drive shrinkage. The second driving force leading to plastic shrinkage cracking is differential settlement. Plastic shrinkage cracking is more likely to happened and frequently observed above reinforcing steel or at locations where there is a sudden change in cross sectional thickness. The third driving force is differential thermal dilation in which a temperature gradient develops inside fresh concrete due to evaporation of water from the surface. The forth driving force is frequently attributed to autogenous shrinkage in the plastic phase. This indicates that even if evaporation of water is prevented, there is still potential for plastic shrinkage cracking. While these four factors are often addressed independently, they act simultaneously in practical applications and contribute to the potential for cracking. (*Lura et al. 2007*)

2.4.3 Predicting Evaporation

Because the rapid evaporation of surface water is one of the major driving forces, estimating the evaporation rate can alert end-users to the potential risk of plastic shrinkage cracking. When the concrete temperature and ambient conditions create high evaporation rates, the chance for plastic shrinkage cracking increases substantially. When the evaporation rates exceed 1.0 $kg/m^2/h$, plastic shrinkage cracks are expected. Precautionary measures should be taken when evaporation rates exceed this value. When the rate is between 0.5 and 1.0 $kg/m^2/h$, plastic shrinkage cracking may occur. The nomograph shown in Figure 2.22 is commonly used to estimate evaporation rates. (*Concrete Q&A 2007*) In addition, Snell and Munir developed a computer program which is available free-of-charge in an online system http://construction.asu.edu/cim/curing/curingfirstpage.htm (*Snell and Munir*).

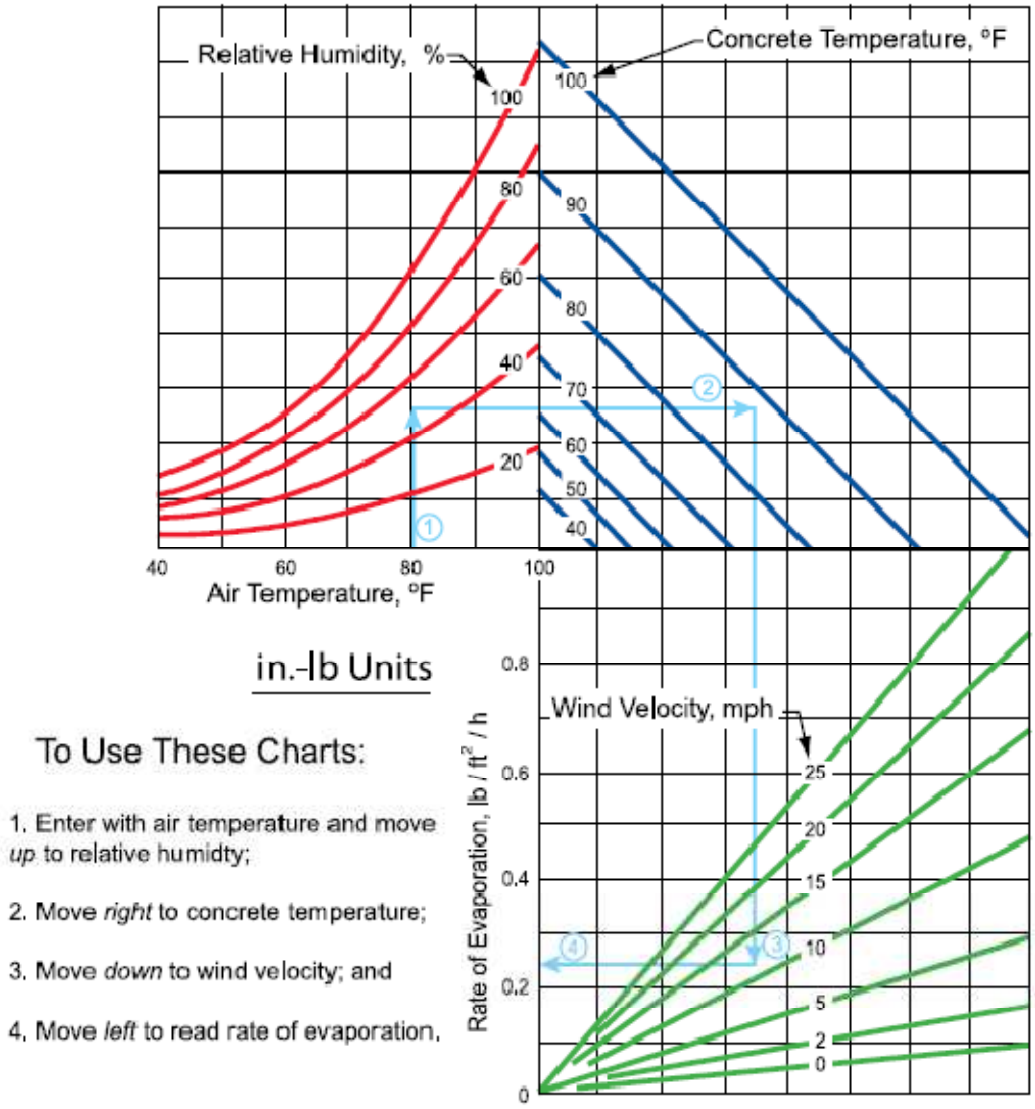

Figure 2.22: Effect of concrete and air temperature, relative humidity, and wind velocity on rate of evaporation of surface moisture from concrete (*Kosmatka et al. 2002*)

One important factor, the concrete bleeding rate, is not included either in the nomograph or in the computer program. The bleeding rate of different concrete mixtures can vary significantly. Therefore, the evaporation rate is better to be viewed as an indicator of how quickly initial curing procedures will have to be started, rather than a set limit for initiation of plastic shrinkage cracking. (*Concrete Q&A 2007*)

2.4.4 Test Methods

To study the development of plastic shrinkage cracking and efficacy of mitigation techniques the most commonly utilized test is ASTM C1579 - Standard Test Method for Evaluating Plastic Shrinkage Cracking of Restrained Fiber Reinforced Concrete (Using a Steel Form Insert). (*ASTM C1579 2006*) Figure 2.23 shows the geometry of the test setup.

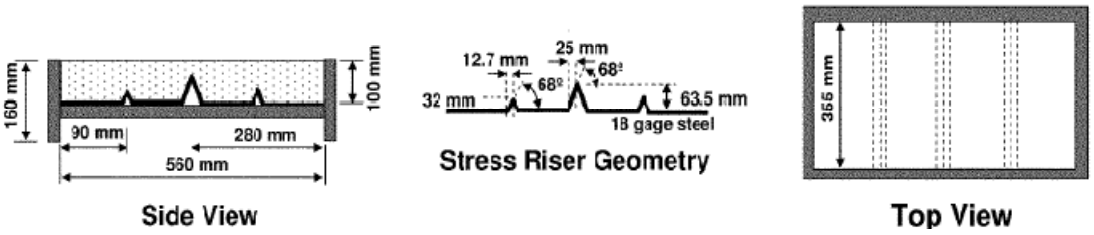

Figure 2.23: Geometry of slab forms for plastic shrinkage cracking test (*Lura et al. 2007*)

The samples are placed into an environmental chamber 25 min after the initial contact of water and cement. The conditions in the chamber specified in the standard are: temperature of 36 ± 3°C, relative humidity (RH) of 30 ± 10% and wind velocity of 24 ± 2km/h. (*Henkensiefken et al. 2009*) After 6 hours, the fans are turned off, and the specimen remains in the chamber for another 18 hours.

After 24 hours, image analyses are performed on pictures of the specimen to analyze cracks and crack widths, providing statistically valid information about crack widths and their variability. (*Henkensiefken et al. 2009*) Figure 2.24 shows the procedure of image analysis. A detailed description can be found in literature. (*Qi et al. 2003*)

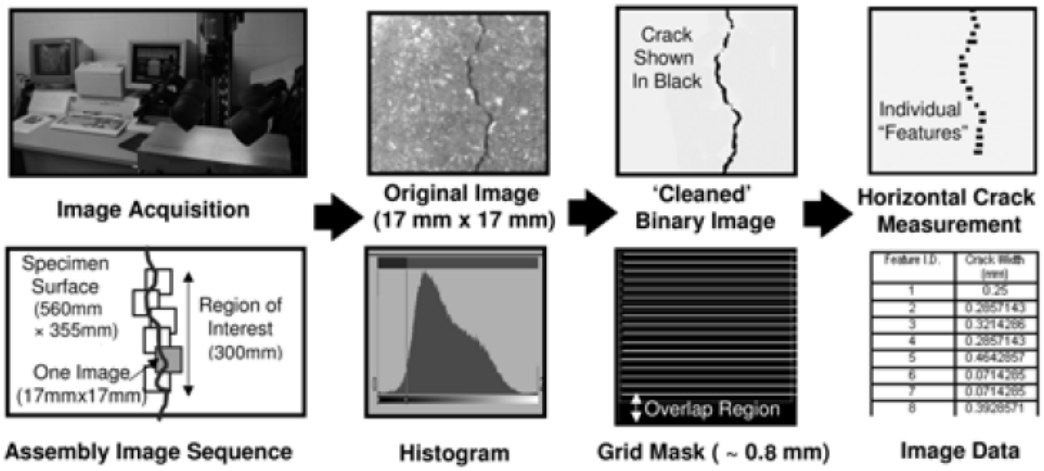

Figure 2.24: Illustration of plastic cracking image analysis procedure (*Henkensiefken et al. 2009*)

In addition to the cracking test/assessment, mass loss, settlement and temperature variation are usually measured to provide further insight of plastic shrinkage. (*Lura et al. 2007*)

2.4.5 Mitigation Strategies

To mitigate plastic shrinkage and the potential of cracking, several measures were mentioned in the introduction including fogging, wind breaks, shading, plastic sheeting, wet burlap, spray-on finishing aids (evaporation retarders), shrinkage-reducing admixtures (SRAs) and plastic fibers. However, experiments have shown that fresh concrete may undergo severe shrinkage which might lead to cracking even if evaporation is physically prevented. (*Lura et al. 2007*) Therefore, some innovative shrinkage mitigation strategies such as application of SRAs and saturated LWFA have become the focus of recent research. (*Cusson 2008, Mora-Ruacho et al. 2009, Radlinska et al. 2008, Villarreal 2008*)

2.4.5.1 Application of SRAs

Although significant research has examined the use of SRAs in concrete, the majority of studies have focused on long-term shrinkage and cracking in hardened concrete, in particular by reducing autogenous shrinkage. Generally, concrete containing SRAs exhibits less cracking. Far fewer studies have been conducted on the role of SRAs in fresh concrete. Lura et al. (*2007*) investigated mortar dosed with 1, 2 and 5% SRAs to improve the understanding of the influence of SRAs on the development of plastic shrinkage cracking. The researchers also provided a clear explanation of the mechanisms governing plastic shrinkage cracking in concrete. The experimental results showed that the addition of SRAs reduced the width of plastic cracks in mortars exposed to evaporation immediately after casting. (*Lura et al. 2007*)

Similar conclusions have been found by Mora-Ruacho et al. (*2009*). The application of SRAs, super-plasticizers and combinations thereof were investigated in this research. They concluded that the incorporation of an SRA or a suitable super-plasticizer reduced plastic shrinkage cracking substantially by lowering the evaporation rate thereby delaying the peak capillary pressure and reducing the risk of plastic shrinkage related cracking. (*Mora-Ruacho et al. 2009*)

2.4.5.2 Application of saturated LWFA

The incorporation of saturated LWFA has been used to reduce shrinkage cracking associated with self-desiccation (autogenous shrinkage) in the hardened state. However, little research has been conducted to investigate the impact of internal curing on plastic shrinkage cracking. Henkensiefken et al. (*2009*) recently examined mortar and concrete systems cast with saturated LWFA. An expanded shale LWFA was used and studied at different replacement levels for the fine aggregate. The results showed that a significant reduction in settlement and plastic shrinkage cracking of mortars and concretes can be achieved by the replacement of normal weight sand with saturated LWFA. Provided that sufficient replacement of saturated LWFA is incorporated into the fresh mortar it was

demonstrated that plastic shrinkage cracking could be reduced or eliminated under the investigated exposure conditions. (*Henkensiefken et al. 2009*)

2.5 DRYING SHRINKAGE

2.5.1 Introduction

Drying shrinkage is the "shrinkage that is caused by the loss of water to the surrounding environment (i.e. external drying)" (*Radlinska et al. 2008*). This type of shrinkage occurs when hardened concrete is exposed to air that has less that 100% relative humidity. (*Al-Manaseer and Ristanovic 2004*) Drying shrinkage will occur until the internal relative humidity of the cement paste reaches equilibrium with the atmospheric relative humidity. (*Radlinska et al. 2008*) Many factors affect drying shrinkage of concrete. These factors include the type and fineness of cement, type of aggregate, w/cm, relative humidity, admixtures used, duration of curing and the size of the concrete specimen. (*Huo and Wong 2000*)

Unsealed concrete specimens experience various types of shrinkage including chemical shrinkage, autogenous deformation, and drying shrinkage (loss of moisture to the environment). These phenomena occur in the cement paste and are due to a loss of water from capillary voids typically less than 50 nm. (*Mehta and Monteiro 2006*) Liquid-vapor interfaces (menisci) develop in the pores of the cement paste. The formation of the menisci occurs due to a reduction of the internal relative humidity of the cement paste. As fresh concrete is exposed to a dry environment, these menisci develop on the surface due to the loss of moisture to the environment, as well as within the cement paste matrix due to autogenous shrinkage. This results in capillary tension that can lead to shrinkage throughout the entire paste matrix. Factors leading to this loss of moisture do not act independently, but rather the aggregation of their effects is what ultimately results in shrinkage and subsequent stress generation in concrete. (*Radlinska et al. 2008*)

Drying shrinkage may continue for many years depending on the mass and shape of the concrete. The rate and ultimate amount of shrinkage are usually higher for small masses of concrete, such as slabs and walls, making shrinkage more detrimental (usually resulted in cracking) in such elements. (*Kosmatka et al. 2002*, *Nilson et al. 2004*) On the other hand, for larger masses of concrete, shrinkage continues longer. Tests performed by Bissonnette and coworkers have shown that the rate of drying is much slower for a larger specimen (50×50×400 mm) compared to a smaller specimen (4×8×32 mm). Hygrometric equilibrium had not been reached on some of the larger specimens even after 500 days. (*Bissonnette et al. 1999*)

2.5.2 Drying Shrinkage Test Methods

2.5.2.1 ASTM C 157

The ASTM C157 test is the most commonly accepted method to determine the change in length of hardened concrete specimens prepared in the laboratory due to drying shrinkage. These specimens are exposed to controlled temperature and moisture. The length change is caused by forces other than externally applied forces or temperature changes. Measuring the change in length allows for the assessment of expansion or contraction of different concrete or mortar mixtures. This test method may be useful for testing samples that require nonstandard mixing or curing conditions.

To perform this test concrete specimens measuring 100×100×285 mm if the all the aggregate passes a 50mm sieve are cast. However, if all the aggregate passes a 25 mm sieve, a specimen of 75×75×285 mm may be used. After mixing and placing concrete in the molds, the specimens are to be placed in a moist room in accordance to ASTM C 511. The specimens should be removed from the molds at an age of 23½ ± ½ hours after mixing. Upon demolding, the specimens are placed in a lime-saturated solution maintained at 23±0.5 °C for a minimum of 30 minutes. The specimens are removed from the solution at 24±½ hour after water-cement contact and an initial comparator reading is taken. After taking the initial reading, specimens are placed in a lime-saturated solution

and cured for 28 days at 23±1 °C. When this curing period has commenced, the specimens are placed in a drying room that is maintained at 23±1 °C and at a relative humidity of 50±4%. It is important to provide adequate spacing between prisms to allow for even drying. The spacing requirement recommended by the ASTM standard is a minimum of 25 mm on all sides of the specimen. Comparator readings should take place at 4, 7, 14, and 28 days, and after 8, 16, 32, and 64 weeks. The length change of the specimen ΔLx can be determined by the following equation:

$$\Delta L_x = \frac{CRD - CRD_{Initial}}{G} \times 100 \qquad \text{Equation 5}$$

Where:

CRD = difference between the comparator reading of the specimen and the reference bar at any age;

G = gage length (250 mm).

This test is effective for evaluating drying shrinkage of concretes with a high w/cm, but problems may arise when testing concrete with a w/cm of < 0.42. (*Aitcin 1988*) The problems can be attributed to the self-desiccation of the cement paste. In return, the self-desiccation leads to autogenous shrinkage that develops in the first 24 hours before the specimen has been demolded. (*Sant et al. 2006*) Since autogenous deformation is a cement paste phenomena, different studies need to be performed to quantify the amount of deformation that occurs in early-ages in HPC. The amount of autogenous shrinkage needs to be accounted for when using the ASTM C 157 on HPCs. This may be done on companion sealed specimens that are stored under the same conditions. In essence the difference in shrinkage between the two methods is the drying component of shrinkage. Knowing the main mechanisms responsible for shrinkage can help to make a determination of the best approach for mitigation methods to reduce the risk of drying shrinkage. Other methods to determine autogenous deformation are outlined in section 2.3.

2.5.2.2 ASTM C 1581

Over the last few decades, the shrinkage ring test has gained popularity as a testing technique to compare the time to cracking for different concrete mixtures. The ring test, due to its simplicity and economy, has been developed into both AASHTO PP34 (*2004*) and ASTM C1581. (*ACI Committee 231 2010*)

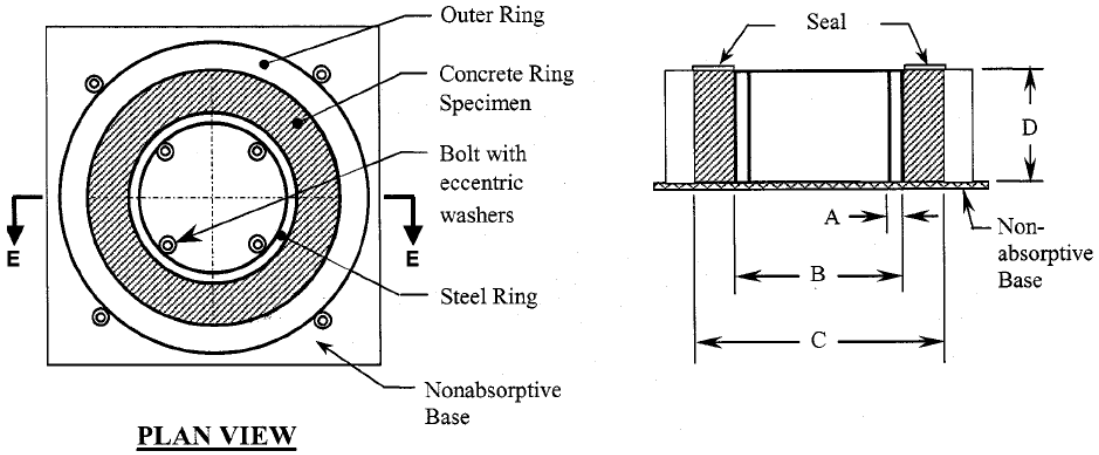

Figure Dimensions	Inch-Pound Units	SI Units
A	0.50 ± 0.12 in.	12.5 ± 0.13 mm
B	13.0 ± 0.12 in.	330 ± 3 mm
C	16.0 ± 0.12 in.	406 ± 3 mm
D	6.0 ± 0.25 in.	150 ± 6 mm

Figure 2.25: Restrained ring mold (*ASTM C1581 2004*)

A sample of freshly mixed mortar or concrete is compacted in a circular mold around an instrumented steel ring as shown in Figure 2.25. The compressive strain developed in the steel ring caused by the restrained shrinkage of the specimen is measured from the time of casting (see Figure 2.26). The curing environment allows the specimens to be moist cured using wet burlap covered with a polyethylene film for at least 24 h at 23.0 ±2.0 °C. If curing is to last more than 24 h, the outer ring is removed at 24 h and the curing process continues. After curing, the outer ring is removed. If it is still in place, the burlap

and polyethylene film should be removed as well. Then the top surface of the specimen is sealed with either molten paraffin wax or adhesive aluminum-foil tape.

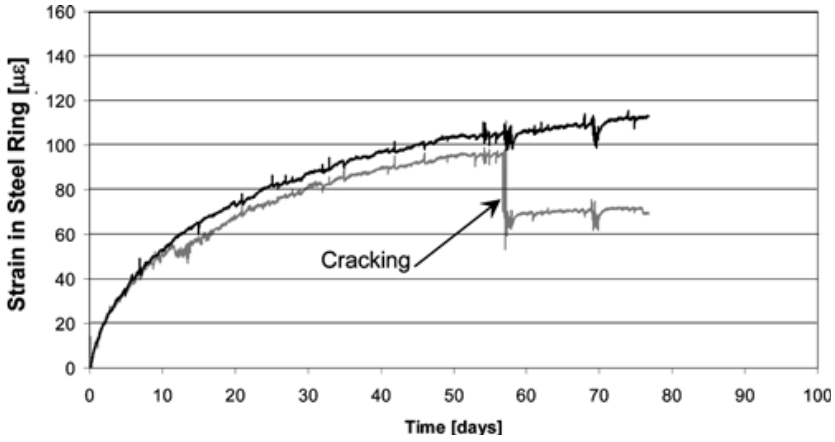

Figure 2.26: Typical restrained shrinkage ring test strain output(*Brown et al. 2007*)

The time after terminating the curing process is recorded. The strain on intervals of 30 minutes or less is continuously monitored. Additionally, the temperature and relative humidity of the testing environment are recorded. The strain in the steel ring for each strain gage against the specimen age is then plotted versus time. A sudden decrease in strain (Figure 2.26) indicates the concrete has cracked.

The time to cracking and induced tensile stress characteristics of concrete can be determined in accordance with the ASTM C 1581 test method. This method has the potential to analyze variations in proportions and material properties of concrete due to drying shrinkage and deformations caused by autogenous shrinkage and heat of hydration. Effects on induced tensile stresses caused by variations in concrete composition can be easily studied using this method. Results from this test are useful for determining the likelihood of early-age cracking of concrete that is subjected to restrained shrinkage. Although this method can determine this likelihood, it should be noted the actual cracking tendency depends on many factors. These factors include effect of stress relaxation (creep), degree of restraint, rate of property development, construction and curing methods, specimen geometry and bond between the concrete and steel, and

environmental conditions. The ACI Committee 231 report on early-age cracking provides an overview of the qualitative use of the restrained ring test. (*ACI Committee 231 2010*)

2.5.3 Mitigation Strategies

A variety of mitigation strategies have been identified, developed and investigated by many researchers to mitigate the deleterious effects of drying shrinkage. The major factors that affect the potential for drying shrinkage potential are listed below.

2.5.3.1 Mixing and Curing Conditions

Water to Cementitious Material Ratio

"The most important controllable factor affecting drying shrinkage is the amount of water per unit volume of concrete (*Kosmatka et al. 2002*)." A denser cement paste matrix resulting from a lower w/cm, contributes to decreased permeability. Therefore, less drying shrinkage is expected due to less evaporation after curing. It is estimated that the drying shrinkage is reduced by up to 30 microstrain per 5.9 kg/m^3 of water removed from the mix design (*Babaei and Fouladgar 1997*).

Curing

Due to the low w/cm in HPC, a combination of drying shrinkage, autogenous shrinkage and plastic shrinkage could greatly increase the cracking potential of these concretes. There are various methods to provide external curing for the concrete. Some methods trap the moisture, e.g. curing compounds, sealers, and coatings, and delay the shrinkage. Fogging or wet burlap holds off shrinkage until the concrete has hardened. After hardening and the external curing source has been removed, the concrete will shrink when exposed to a relative humidity of less than 100 % and have the potential for cracking caused by stress generation during shrinkage (*Kosmatka et al. 2002*). Therefore, the external curing should be prolonged long enough to eliminate drying shrinkage during the curing process (*Nilson et al. 2004*). However, because the permeability of HPC drops

so quickly in the first few days, external curing might not be sufficient to eliminate drying shrinkage.

Internal curing could also help reduce drying shrinkage. Research on replacement of LWFA and the addition of SAPs has been primarily focused on autogenous deformation. However, the principle of either strategy is to provide bulk internal water during curing to compensate self-desiccation. Meanwhile, the bulk water could also compensate moisture loss to the external environment, in such a way the drying shrinkage could be reduced. One study indicated that concrete with saturated LWFA resulted in a slightly higher tensile strength, but lower modulus of elasticity(*Zhang et al. 2005*). In this study, the shrinkage was less than half at 28 days and 40% lower at 91 days for the saturated LWFA concrete compared to conventional concrete.

Reinforcement

Reinforcement in concrete restricts drying shrinkage, but does not prevent it. Shrinkage in reinforced concrete may be less than shrinkage in unreinforced concrete. However, the restraint provided by reinforcement might increase stress due to shrinkage and result in cracking. The amount of shrinkage depends on the quantity of steel placed in the concrete (*Kosmatka et al. 2002*). If the concrete does crack, reinforcement is beneficial for reducing the size of the cracks. By placing smaller bars in the concrete to achieve the needed requirement of steel will perform better at controlling crack width than utilizing larger bars (*Babaei and Fouladgar 1997*). Fibers can also be used in concrete to help minimize drying shrinkage. From previous research, drying shrinkage strains were 35% lower in cement paste containing at least 1% fibers by volume when compared to cement paste without fibers (*Chen and Chung 1996*).

2.5.3.2 Cementitious Materials and Admixtures

Cement Type

Different cements have varying chemical compositions, which influence the drying shrinkage of the constructed concrete (*Babaei and Fouladgar 1997*). The use of Type K

cement can be used to reduce drying shrinkage cracking. As Type K cement hydrates, it forms an expansive material called ettringite. The ettringite forms and expands during the first several days of curing. After the maximum amount of expansion has occurred, the Type K cement concrete will shrink at a rate similar to that of portland cement concrete. However, due to the additional time spent in a state of expansion, the concrete will typically gain additional beneficial strength to resist shrinkage forces. If the specimen is reinforced, the expansion of Type K cement may cause compressive stresses in the concrete due to the restraint of the reinforcement. When the concrete shrinks the internal compressive stresses decrease. Since the concrete is already in an expanded state the shrinkage may not be enough to induce tensile stresses that are greater than the tensile capacity of the concrete. Figure 2.27 displays the length change characteristics of Type K cement concrete compared to OPC concrete (*Gruner and Plain 1993*).

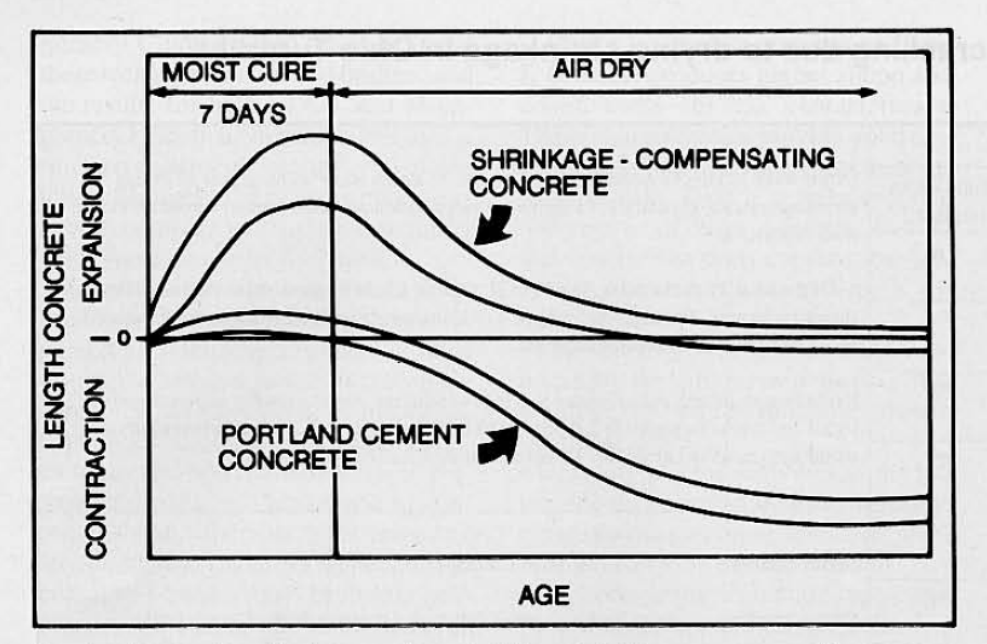

Figure 2.27: Typical length change characteristics of shrinkage compensating and portland cement concretes (*Gruner and Plain 1993*)

Fly Ash

Increasing the amount of fly ash as a supplementary cementing material in a concrete mixture has been observed to decrease the amount of drying shrinkage. The drying shrinkage decreases with the addition of fly ash because there is an overall reduction in the amount of portland cement, thereby lowering the reaction rate which may lead to a slower development of very fine pores that could lead to early-age autogenous shrinkage. Incorporating fly ash with a lower w/cm reduces the amount of cement paste. Figure 2.28 demonstrates the positive effects of fly ash on reducing drying shrinkage (*Kumar et al. 2007*). Research performed further showed that shrinkage in concrete containing a high volume (between 50 % and 70 % replacement of cement) was 30 % lower than OPC concrete (*Atiş 2003*).

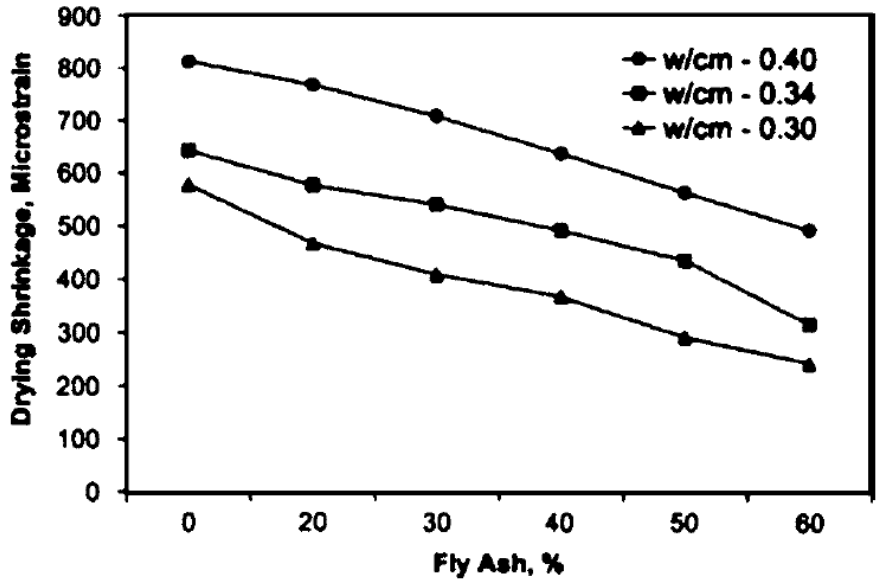

Figure 2.28: Variation of drying shrinkage of concrete with fly-ash content (*Kumar et al. 2007*)

Admixtures

SRAs have been shown to be successful in reducing drying shrinkage and cracking related due to the corresponding shrinkage. Due to the reduction in capillary tension by as much as 50%, the addition of SRAs is successful in reducing drying shrinkage as well as plastic shrinkage and autogenous shrinkage (*Bentz 2006*). Some chemical admixtures

do not have this same profound effect on shrinkage and using an accelerator can actually increase drying shrinkage. This is caused by a rapid increase in the heat of hydration which will promote drying shrinkage. Air entrainment typically has little or no effects on drying shrinkage (*Kosmatka et al. 2002*). However, the addition of superplasticizer in concrete mixture can increase shrinkage even though the water content is less. Research showed that concrete with superplasticizer could increase the shrinkage by up to 50% (*Atiş 2003*).

2.5.3.3 Aggregates

Aggregate Selection

Generally, most aggregates do not change volumetrically, and shrinkage is mainly considered a paste property. (*Radlinska et al. 2008*) As a result, increasing the aggregate content with competent aggregates in a mixture design can significantly decrease shrinkage as aggregates generally resist shrinkage forces from the paste. (*Nilson et al. 2004*) However, the shape of the aggregate is an important factor when determining drying shrinkage. Crushed aggregates provide better restraint to shrinkage because of an angular and rough surface. The rough surface provides an increased surface area, which results in higher restraint against the shrinkage of the cement paste. (*RILEM Committee 119 1998*) Moreover, the porosity of the aggregate can affect the shrinkage by making it become more compressible.

A concise summary about aggregate effect on shrinkage was given by Troxell and Davis (*1956*):

> "In general, concretes low in shrinkage often contain quartz, limestone, dolomite, granite, or feldspar, whereas those high in shrinkage often contain sandstone, slate, basalt, trap rock, or other aggregates which shrink considerably of themselves or have low rigidity to the compressive stresses developed by the shrinkage of paste." (*Troxell and Davis 1956*)

2.6 SUMMARY

HPC has been used successfully in modern concrete. However, due to its special properties, such as low w/cm, low permeability and addition of SCMs, HPC is more prone to cracking than conventional concrete. Several volume changes such as chemical shrinkage, autogenous deformation, plastic shrinkage and drying shrinkage were identified in this chapter. Measurement methods and mitigation strategies were also introduced for each volume change. Evidence in the literature shows the potential beneficial effects of internal curing with LWFA and the incorporation of SRA to minimize early-age volume change for HPC. The aim of this literature review was to identify measurement methods which could be applied in the support of the research goals for this thesis.

3 MATERIALS AND METHODS

3.1 MATERIALS

The standard ODOT HPC bridge deck mixture typically contains 30% class F fly ash and 4% silica fume replacement by weight of cement. The ASTM C150 Type I/II cement and ASTM C618 class F fly ash were provided by Lafarge North America. The silica fume and shrinkage reducing mixture (Tetraguard AS20) were provided by BASF. Two calcium aluminate cements provided by Kerneos Aluminate Technologies were also investigated, Ciment Fondu and GCX Binder.

3.1.1 Cements

The OPC used in this research is standard Type I/II cement (as per ASTM C150), provided by Lafarge North America. The cement was obtained from the Lafarge Eugene (Oregon) terminal in 200 L plastic drums, sealed and stored indoors. Two CACs from Kerneos Aluminate Technologies were used in this research: Ciment Fondu and GCX Binder. Ciment Fondu came in 43 kg bags and kept indoors, in 200 L plastic drums and 20 L bucket for user convenience. The GCX binder was shipped from The University of Texas at Austin, originally manufactured in 2007 and used for a fundamental study of CAC early-age behavior project to compare to previous research results. The GCX binder is kept in 200 L plastic drum and double lined with plastic bags. Due to sourcing issues of bauxite (main mineral which goes into the manufacture of CAC), GCX binder was suspended from manufacture. To allow for comparison and bench-marking to previous studies limited work in this thesis was conducted using this binder. Furthermore, previous research has shown strong similarities in early-age volume change between different CACs. The chemical composition of the all cement used is shown in Table 3.1.

Table 3.1: Cement and fly ash oxide analysis*(wt %)

Oxide	OPC Type I/II	Class F Fly Ash	GCX Binder	Ciment Fondu
CaO	64.21	10.20	35.99	35.54
SiO_2	20.51	55.24	5.24	4.62
Al_2O_3	4.72	15.77	52.61	40.25
Fe_2O_3	3.23	6.27	2.10	15.15
MgO	0.80	3.64	0.45	0.76
Na_2O	0.30	3.64	0.06	0.14
K_2O	0.29	2.08	0.38	0.14
TiO_2	0.23	0.94	2.18	1.71
MnO_2	0.08	0.12	0.05	0.31
P_2O_5	0.07	0.23	0.16	0.15
SrO	0.17	0.32	0.06	0.03
BaO	0.07	0.62	0.04	0.01
SO_3	2.70	0.70	0.04	0.16
Total Alkalies as Na_2O	0.49	-	-	-
Loss on Ignition	2.63	0.23	0.66	1.03
Insoluble Residue	0.21	-	-	-

*All analysis was based on samples taken in fall 2010 by an independent testing laboratory. Certificates can be found in Appendix A.

3.1.2 SCMs

As mentioned above, two different supplementary cementitious materials (SCMs) were used in this research. A class F fly ash from Lafarge North America, Centralia Plant (Washington), was used as it was a locally available fly ash for ODOT. A silica fume (Rheomac® SF 100) from BASF was used, containing nearly pure silica dioxide in noncrystalline form with approximately 1% crystalline silica. The composition of class F fly ash is shown in Table 3.1.

3.1.3 SRA

One SRA (Tetraguard A20), provided by BASF, was investigated for its potential application for ODOT. The chemical contain in this SRA is polyoxyalkylene alkylether. The recommended dosage from the manufacturer was 2% by mass of all cementitious materials in the mixture. It is compatible with the high-range water reducer and silica fume selected for this project.

3.2 TESTING METHODS

3.2.1 Paste Mixing Procedure

A mixing procedure was adopted from the ASTM standard paste mixing procedures (*ASTM C305 2006*) with some specific modification to meet the needs of this research program. The cement paste mixtures were prepared with deionized (DI) water stored in room temperature around 20 ºC along with all other cementitious materials. The mixing procedures were as follow:

- First all the water (and SRA if used) was placed in the mixing bowl;
- Then cement, fly ash and silica fume (in such sequence) were added to the mixing bowl, and allowed 30 seconds for all cementitious materials to absorb water;
- The mixer was started at low speed (140±5 r/min) for 30 seconds;
- The mixer was stopped for 15 seconds and in this time the sides of the bowl were scrapped to ensure uniform mixing;
- The mixer was restarted at medium speed (285±10 r/min) and mixed for another 60 seconds.

In sum, 30 mixtures and about 200 samples were prepared and tested in this research.

3.2.2 Chemical Shrinkage Testing Procedure

ASTM C1608 was used as the standard testing procedure to investigate chemical shrinkage. To prepare the paste sample, the standard procedure outlined in ASTM C305 was applied. Cement paste (with or without SCMs) was mixed with deionized water at room temperature, and was carefully placed in a vial (25 ml) with dimension of 50mm in height and 25mm in diameter. A paste sample of 10g to 15g was carefully placed in the vial, and a discussion of effect of sample thickness is presented in section 4.1.3.1. Deionized water was filled the vial to the top. A one-hole robber stopper with an inverted glass pipette (1 ml) passing through it, was placed slowly on top of the vial to make sure no air bubbles were trapped. For CAC systems 2 ml glass pipettes were used. Additional water is filled from the top of the pipette close to the largest reading in the pipette. Next, a few drops of transmission fluid (red in color) were added by a syringe in order to prevent evaporation and also to provide the reference for the automated photo-data

acquisition system. Then, all the vial/pipette combinations were placed in the specifically designed rack, which allow all samples submerged completely in the water bath for temperature control.

To monitor chemical shrinkage for a longer period of time (e.g. up to 14 days) than recommended by ASTM C1608 (currently no less than 24 hours), an automated test set-up was developed. A functioning set-up was shown in Figure 2.2 in section 2.2.2. In front of the pipettes, there is a webcam with a resolution higher than 1.3 megapixels for image acquisition. Images are taken approximately every 5 minutes resulting in over 4000 images (for a 14 day test) which were then analyzed using a computer software program developed in the Laboratory of Materials of Construction (LMC) at EPFL in Lausanne, Switzerland to determine the total water uptake by the hydrating cement paste. (Bishnoi 2009)

Figure 3.1 shows typical pictures recorded at the beginning of the test and at the 14 days respectively. The zero point of chemical shrinkage was set to 60 minutes after initial contact of water and cement to allow for proper isothermal conditions to be reached while still being well ahead of the setting point of the cement specimen. The 14 days values were read out from the digital images as close to 336 hours as possible.

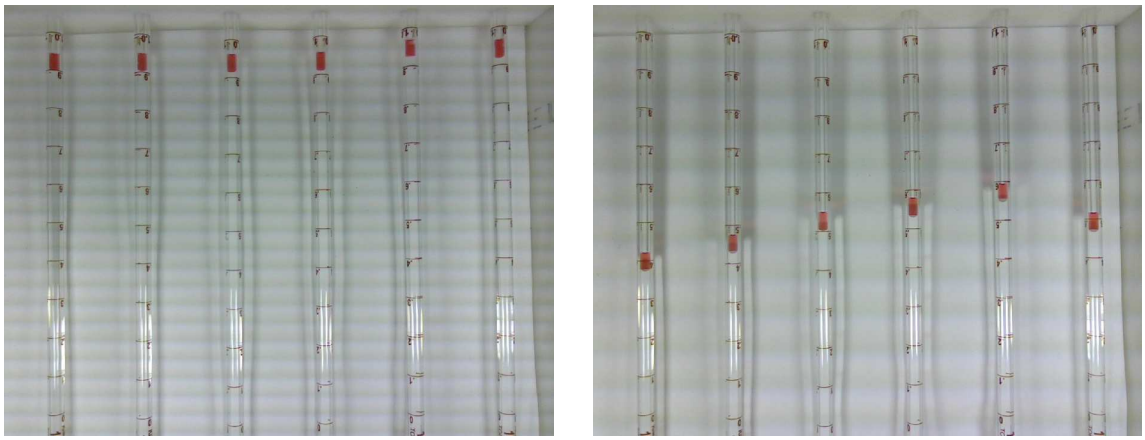

a) at 60 minutes b) at 14 days (336 hours)

Figure 3.1: Typical chemical shrinkage image a) at the beginning and b) at 14 days.

3.2.3 Autogenous Deformation Testing Procedure

As mentioned in section 2.3.1.2, proper consideration should be given when conducting the membrane method. To avoid significant artifacts related to osmosis, a polyurethane condom (Durex Avanti Brand) was selected as the membrane and paraffin oil was selected to be the buoyancy liquid.

About 100g cement was poured into a condom through a wide mouthed funnel. Then the sample was agitated to remove air bubbles, and tightly closed by a zip tie. Attention was paid to avoid any entrapment of air bubble. The excess part of the condom was then cut off and several drops of super glue were applied to the exposed cut. Then quick set epoxy was applied around the knot of zip tie to ensure a good seal. Typical samples used are shown in Figure 2.7 in section 2.3.1.1.

To start test, the sample was submerged in the beaker filled with paraffin oil, and hung from a hook beneath the balance with sensitivity of 0.01g. The beaker was placed in the water bath under desired temperature. A 50 kg steel plate was place on top of the testing rack to minimize vibrations. The weigh change of submerged sample was recorded by automatically at 5 minutes intervals by controlling software (Hyperlink) up to 50 hours. A complete set-up is shown in Figure 2.8 in section 2.3.1.1.

Volumetric strain of the specimen can be calculated from the submerged weight change according to Equation 6:

$$\varepsilon_{vol} = \frac{\Delta V_{paste}(t)}{V_{paste(t_0)}} = \frac{W_{sub}(t) - W_{sub}(t_0)}{\rho_{oil} \cdot V_{paste}(t_0)} = \frac{W_{sub}(t) - W_{sub}(t_0)}{W_{initial} - W_{sub}(t_0)} \qquad \text{Equation 6}$$

Where:

$\Delta V_{paste}(t)$ = the volume change (ml) of the specimen at time t;

$V_{paste}(t_0)$ = the initial volume (ml)of the specimen at the time t_0 which is the time the sample initially submerged in paraffin oil;

$W_{sub}(t)$ = the submerged weight (g) of the specimen at time t;

$W_{sub}(t_0)$ = the initial submerged weight (g) of the specimen, and;

ρ_{oil} = the density (g/ml) of paraffin oil.

$\rho_{oil} \cdot V_{paste}(t_0)$ is the initial buoyancy force of the sample which equals to the difference between initial weigh of the sample before submerged ($W_{initial}$) and the initial submerged weight ($W_{sub}(t_0)$). Usually it took 15 to 20 minutes to set up the sample submerged in paraffin oil (t_0=15 to 20 mins).

Then volumetric strain is converted to linear strain (ε_{lin}) by assuming isotropic deformations: (*Sant et al. 2006*)

$$\varepsilon_{lin} = \frac{\varepsilon_{vol}}{3} \qquad \text{Equation 7}$$

3.3 PASTE TESTING MATRIX

To investigate the influence on chemical shrinkage and autogenous deformation, different w/cm, and SCMs replacements were used. In addition, the effect of SRA was also studied. The paste test matrix is shown in Table 3.2 and. All tests were performed at 20 ºC isothermal condition controlled by water bath.

Table 3.2: Chemical shrinkage test matrix for OPC at 20 ºC isothermal

20 ºC	Neat	FA	SF	FA+SF	SRA	FA+SRA	SF+SRA	FA+SF +SRA
w/cm=0.32	3	3	3	3	3	3	3	3
w/cm=0.37	3	3	3	3	3	3	3	3
w/cm=0.42	3	3	3	3	3	3	3	3

Table 3.3: Autogenous deformation test matrix for OPC

20 ºC	Neat	FA	SF	FA+ SF	FA+SF+SRA
w/cm=0.32	2	-	-	-	-
w/cm=0.37	2	2	2	2	2
w/cm=0.42	2	-	-	-	-

Table 3.4 shows the test matrix for the CAC systems. For each combination of w/cm and curing temperature, three chemical shrinkage samples and two autogenous deformation samples were tested. In addition, the vicat setting test was tested for each mixture.

Table 3.4: Test matrix for CAC

	GCX	Fondu
w/cm=0.35	20 °C	20 °C
w/cm=0.40	38 °C	38 °C

4 CHEMICAL SHRINKAGE

As mentioned in Chapter 2, the volume of cement and water when separate is greater than when they are combined, and this reduction in volume is commonly referred to as chemical shrinkage. Testing in accordance with ASTM C1608 was performed to determine the chemical shrinkage value (CS) in the Bentz Equation for the binder system used in the standard ODOT HPC bridge mixture.

Over 100 chemical shrinkage samples were tested to characterize the chemical shrinkage of cementitious systems under 20 º C isothermal conditions. Neat pastes (portland cement only) were investigated as well as binary and ternary systems. The ternary systems (incorporating fly ash and silica fume) were representative of binder systems in HPC bridge decks in Oregon. Testing on neat pastes and binary and ternary systems will allow further quantification of the effects of SCMs on chemical shrinkage and ultimately will provide a clearer picture of the role that such materials play in shrinkage of HPC. This work will provide a contribution to existing literature, as very little information on chemical shrinkage of ternary systems exists. It will also further the goals of this research project. In addition, the effect of SRA was also investigated due to its potential application in ODOT bridge decks to ultimately reduce the risk of shrinkage induced cracking. Applied separately or together with replacement of LWFA, SRA has a potential in ODOT bridge deck applications to reduce shrinkage

Twelve calcium aluminate cement samples were tested for chemical shrinkage to compare with OPC system. The tests suggest that the chemical shrinkage characteristics of metastable phases versus stable hydrates have certain relation with conversion phenomenon under isothermal conditions. Qualitative X-ray diffraction (XRD) analysis was used to verify conversion.

4.1 OPC RESUTLS AND ANALYSIS

As mentioned in Chapter 2, Figure 2.3 and Figure 2.4 show that the automated image analysis was successfully applied in research in EPFL, Switzerland and the University of Texas, Austin. This method provides significant enhancement to the accuracy of chemical shrinkage results. (*Costoya 2008, Ideker 2008*) The computer program is capable of analyzing the pictures by referencing red transmission fluid as an index. At the same time, measurements were also taken by hand. A t-test (paired two sample for means, Table 4.1) for the standard deviation of hand measurements and automated measurements gave a p-value of 0.038, which means the automated measurements were consistently of less variance. And for all 24 different OPC mixtures, the standard deviations of 21 mixtures are less than 0.0014ml/g, determined by ASTM C1608. All the results presented in this chapter are from measurements obtained by automated computer program.

Table 4.1: T-test: paired two sample for means

	SD of Program Value	SD of Hand value
Mean	0.00078867	0.00090834
Variance	6.0687E-07	6.2273E-07
Observations	24	24
Hypothesized Mean Difference	0	
df	23	
t Stat	-1.8553	
P(T<=t) one-tail	0.038209	

Tests were performed on OPC neat paste, binary and ternary systems, as well as systems with SRA under 20 ºC isothermal conditions. A brief summary of the 14 day chemical shrinkage value is listed in Table 4.2.

Table 4.2: Chemical shrinkage the 14 day value (ml/g), OPC 20 ºC isothermal

	Neat	SF	FA	SF+FA	SRA	SF+SRA	FA+SRA	SF+FA+SRA
w/cm=0.32	0.0443	0.0435	0.0411	0.0407	0.0479	0.0448	0.0434	0.0414
w/cm=0.37	0.0448	0.0451	0.0426	0.0413	0.0485	0.0449	0.0429	0.0424
w/cm=0.42	0.0451	0.0444	0.0444	0.0426	0.0534	0.0522	0.0487	0.0464

Each value in Table 4.2 is the average of three samples, measured by the automated computer program. The standard deviations were also calculated and presented in Table B.1, Table B.2 and Table B.3, Appendix B.2. To better present the results, a clustered column chart is shown in Figure 4.1.

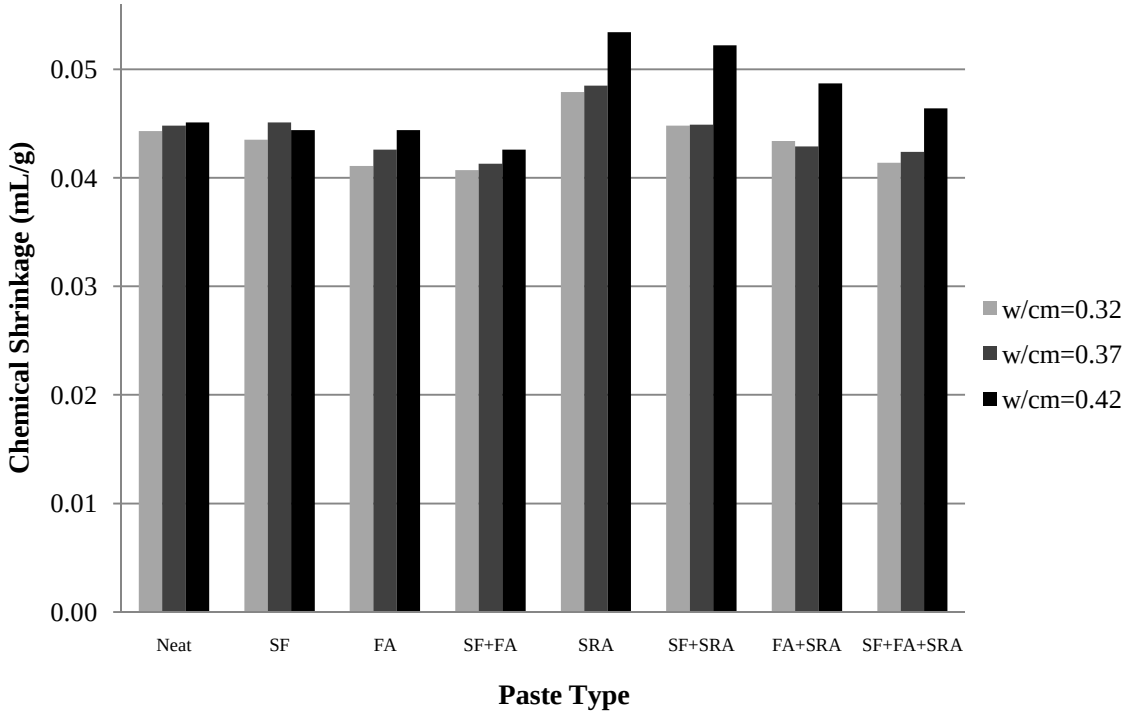

Figure 4.1: Chemical shrinkage 14 days value, OPC 20 ºC isothermal

It can be seen in Figure 4.1 that the CS values of most mixtures fall in the range of 0.04 and 0.05 ml/g, and increase with the w/cm. Also, the presence of SRA increases the CS value especially for mixtures with a 0.42 w/cm. In addition, a trend shows that the CS values decrease with an increase of the SCMs content in the mixture.

By applying automated logging system, the shape of the chemical shrinkage curve can also be precisely illustrated, representing the reaction rate of each mixture. The shape of the curve is affected by influential factors such as type of cement, curing temperature, w/cm, fineness of cement, and SCMs or SRA addition in mixture. (*Xiao et al. 2009*) More discussion is presented in section 4.4. Figure 4.2 shows all the chemical shrinkage development curves of samples with a 0.32 w/cm. Chemical shrinkage curves for 0.37 and 0.42 w/cm pastes can be found in Appendix B.1, Figure B.1 and Figure B.2.

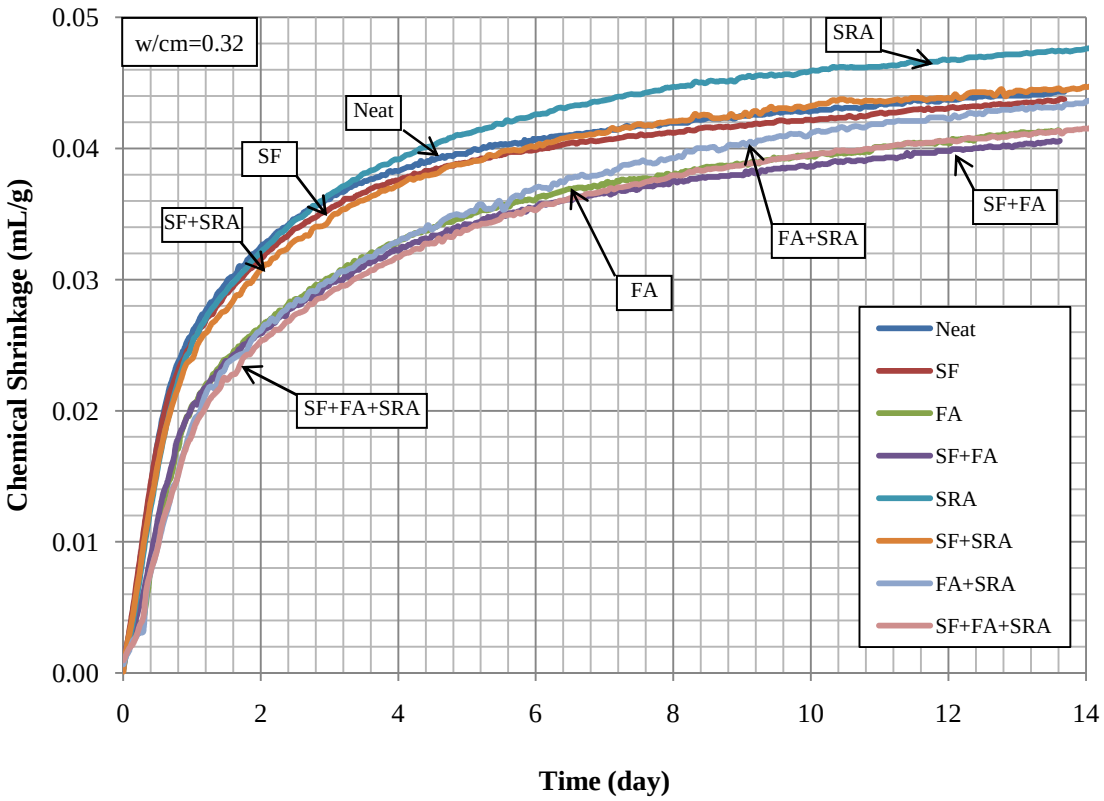

Figure 4.2: Chemical shrinkage development curve, OPC w/cm=0.32 at 20 ºC isothermal

Each curve in Figure 4.2 represents the average of three samples for one particular mixture. It can be seen that all curves have similar shapes, while the ones with FA have lower reaction rates and end up lower in 14 day CS values. The effect of SRA is not significant for 0.32 w/cm, but the CS values increase in mixtures with SRA still can be noticed.

To better compare the development of chemical shrinkage, lists of chemical shrinkage values at increasing age from 1 hour up to 14 days are presented in Table 4.3.

Table 4.3: Chemical shrinkage value at different age (ml/g), OPC 20 ºC isothermal

	Neat	**SF**	**FA**	**SF +FA**	**SRA**	**SF+ SRA**	**FA+SRA**	**SF+ FA+ SRA**
				w/cm=0.32				
1h	0.002	0.002	0.001	0.002	0.002	0.002	0.002	0.002
4h	0.005	0.006	0.003	0.004	0.008	0.009	0.003	0.004
12h	0.017	0.017	0.016	0.016	0.023	0.022	0.019	0.018
1d	0.026	0.025	0.022	0.022	0.030	0.029	0.026	0.025
3d	0.036	0.035	0.031	0.030	0.041	0.039	0.035	0.034
5d	0.040	0.039	0.035	0.034	0.045	0.042	0.040	0.038
7d	0.041	0.041	0.037	0.037	0.046	0.044	0.042	0.040
10d	0.043	0.042	0.039	0.038	0.048	0.045	0.044	0.041
14d	0.044	0.044	0.041	0.041	0.048	0.045	0.043	0.041
				w/cm=0.37				
1h	0.001	0.001	0.001	0.001	0.001	0.001	0.001	0.001
4h	0.004	0.004	0.002	0.002	0.004	0.004	0.002	0.002
12h	0.015	0.012	0.010	0.010	0.014	0.010	0.010	0.009
1d	0.025	0.023	0.019	0.019	0.024	0.020	0.020	0.019
3d	0.037	0.035	0.031	0.029	0.037	0.035	-*	-*
5d	0.041	0.040	0.036	0.034	0.042	0.040	0.036	0.036
7d	0.043	0.042	0.038	0.037	0.045	0.043	0.039	0.038
10d	0.044	0.044	0.040	0.039	0.047	0.044	0.041	0.041
14d	0.045	0.045	0.043	0.041	0.049	0.045	0.043	0.042
				w/cm=0.42				
1h	0.001	0.0003	0.001	0.001	0.001	0.001	0.001	0.001
4h	0.004	0.003	0.003	0.003	0.003	0.004	0.003	0.003
12h	0.015	0.015	0.011	0.012	0.014	0.014	0.008	0.007
1d	0.025	0.023	0.021	0.021	0.025	0.025	0.017	0.017
3d	0.035	0.033	0.032	0.031	0.038	0.038	0.033	0.031
5d	0.039	0.037	0.036	0.036	0.044	0.043	0.039	0.036
7d	0.041	0.040	0.039	0.038	-*	-*	0.042	0.039
10d	0.043	0.042	0.043	0.041	-*	-*	-*	-*
14d	0.045	0.044	0.044	0.043	0.053	0.052	0.049	0.046

*Due to technical problem, several data points were missing during the tests.

The rest of this chapter presents an approach for predicting the ultimate chemical shrinkage value and justification for why this value is more appropriate for use in the Bentz Equation. Analysis and discussion of the chemical shrinkage results in terms of effect of sample thickness, w/cm, SCMs, and SRA follows.

4.1.1 Prediction Model

ASTM C1608 recommends the minimum testing time to be at least 24 hours. From the test results showed in Table 4.3, the 1 day CS value represents only approximately 40% to 60% of the 14 day value. While the ultimate CS value, which is the value at the age of infinite time and curing, is even higher due to the continuous hydration process. In Cusson's research, a 7 day value was used in the Bentz Equation to calculate the replacement ratio of lightweight fine aggregate. (*Cusson 2008*) Nevertheless, the water demand due to hydration might be underestimated.

The previous research showed that the chemical shrinkage of cement paste was decided by its chemical composition. The most important four minerals in cement clinker were C_3S, C_2S, C_3A and C_4AF (in cement chemistry, C represents CaO, S represents SiO_2, A represents Al_2O_3 and F represents Fe_2O_3). With different composition proportions, the reaction rate and ultimate chemical shrinkage value varies. A semiempirical model was proposed to predict the evolution of chemical shrinkage of cement and Equation 8 shows the calculation of the ultimate chemical shrinkage value based on cement composition: (*Bentz et al. 2005, Mounanga et al. 2004*)

$$CS_{Ultimate} = 0.0704\,[C_3S] + 0.0724\,[C_2S] + 0.117[C_4AF] + 0.171[C_3A] \qquad \text{Equation 8}$$

Values in the brackets percentage of the composition of certain mineral and the coefficient in front have a unit of ml/g. The coefficients are very sensitive to values chosen for the densities of the different composition phases, which resulted in a difference between researchers. (*Justnes et al. 1998, Mounanga et al. 2004, Paulini 1992*) However, there are several complications behind this equation:

- The coefficients change if assuming different hydration condition, which could be confusing. For example, if assuming sufficient sulfate to convert all of the aluminate phases to ettringite, 0.115 instead of 0.171 should be used. And 0.086 instead of 0.117 should be used if assuming total conversion of the aluminate phases to monosulfate; (*Bentz et al. 2005*)

- The coefficients were developed for one particular type of cement tested only up to 24 hours. Influence from composition other than the four major minerals was omitted, such as MgO and sulfate content, which might have an impact on the reaction rate and/or ultimate chemical shrinkage value; *(Bentz et al. 2005, Liu and Fang 2006)*
- The equation can only consider the incorporation of silica fume. With the presence of other SCMs such as fly ash and slag, the equation cannot be applied. This is due to different composition and hydration properties of these admixtures, and;
- To use the equation, oxide analysis is required to estimate the mineral composition by Bogue calculation which is flawed in and of itself. This requires extra time and effort. Nevertheless, this calculation is not valid when SCMs, such as fly ash and silica fume, are involved. Scanning electronic microscope (SEM) can be used to directly obtain composition information, but requires even more time and effort, which may be avoided, impractical to use or not available for the large number of users interested in internal curing using LWFA.(*Bentz et al. 2005*)

Based on the above mentioned reasons, a simple empirical prediction model for ultimate chemical shrinkage value proposed by Xiao and coworkers was applied in this study. A hyperbolic function converging at a certain point could be the best to describe and predict the tested chemical shrinkage shape: (*Xiao et al. 2009*)

$$CS(t) = \frac{CS_u \times t^a}{t^a + b} \qquad \text{Equation 9}$$

Where:

$CS(t)$ = chemical shrinkage value at age of t (day);

CS_u = ultimate chemical shrinkage value;

a = hydration constant related to cementitious materials properties, and;

b = hydration constant related to time point to reach the 50% ultimate CS.

To determine a particular shape of a CS curve, three perimeters are needed. CS_u represents the ultimate chemical shrinkage value which the curve converges. And a is hydration constant which depends on cement composition, curing temperature, w/cm, fineness of the cement and addition of SCMs or SRA. Another hydration constant b is

determined by the time needed to reach half of the ultimate CS value. If $t_{50\%}$ the time when CS ($t_{50\%}$) = $CS_u/2$, $b = t^a_{50\%}$. A nonlinear curve fit was performed to find each set of parameters for one particular mixture. The results are shown in Table 4.4.

Table 4.4: Curve fit and predicted ultimate chemical shrinkage values

	Parameters			Correlation Coefficient R^2	Predicted 14 days CS (ml/g)			
	Predicted Ultimate CS (ml/g)	a	b		Measured	Predicted	Diff%	Degree of Hydration α
w/cm=0.32 at 20°C isothermal								
Neat	0.0463	1.024	0.847	0.998	0.0443	0.0438	1.0%	0.96
SF	0.0462	0.980	0.883	0.998	0.0435	0.0433	0.5%	0.94
FA	0.0457	0.963	1.442	0.996	0.0411	0.0410	0.1%	0.90
SF+FA	0.0458	0.895	1.418	0.997	0.0407	0.0404	0.8%	0.89
SRA	0.0520	0.949	1.187	0.998	0.0479	0.0474	1.0%	0.92
SF+SRA	0.0490	0.924	1.114	0.998	0.0448	0.0446	0.4%	0.92
FA+SRA	0.0502	0.924	1.848	0.996	0.0434	0.0432	0.4%	0.86
SF+FA+SRA	0.0476	0.928	1.765	0.997	0.0414	0.0414	0.1%	0.87
w/cm=0.37 at 20°C isothermal								
Neat	0.0469	1.153	0.948	0.998	0.0448	0.0448	0.1%	0.96
SF	0.0482	1.122	1.254	0.999	0.0451	0.0453	0.4%	0.94
FA	0.0451	1.089	1.461	0.995	0.0426	0.0416	2.3%	0.95
SF+FA	0.0440	1.078	1.500	0.994	0.0413	0.0404	2.2%	0.94
SRA	0.0532	1.020	1.346	0.998	0.0485	0.0487	0.4%	0.91
SF+SRA	0.0484	1.213	1.460	0.999	0.0449	0.0457	1.8%	0.93
FA+SRA	0.0469	1.053	1.570	0.997	0.0429	0.0428	0.3%	0.91
SF+FA+SRA	0.0461	1.074	1.629	0.996	0.0424	0.0420	0.8%	0.92
w/cm=0.42 at 20°C isothermal								
Neat	0.0469	1.018	1.043	0.996	0.0451	0.0437	3.0%*	0.96
SF	0.0454	1.019	1.082	0.998	0.0444	0.0423	4.8%*	0.98
FA	0.0489	0.938	1.497	0.996	0.0444	0.0435	2.1%	0.91
SF+FA	0.0475	0.910	1.397	0.995	0.0426	0.0422	0.9%	0.90
SRA	0.0606	0.914	1.617	0.995	0.0534	0.0529	0.9%	0.88
SF+SRA	0.0596	0.912	1.540	0.996	0.0522	0.0523	0.3%	0.88
FA+SRA	0.0560	0.980	1.999	0.992	0.0487	0.0487	0.1%	0.87
SF+FA+SRA	0.0534	0.946	2.053	0.994	0.0464	0.0457	1.5%	0.87

*Mixtures encountered technical problem during data logging, the measured values interpreted by computer program were susceptible.

The fitted curves show good consistency with the tested curves, with correlation coefficient over 0.99. At the age of 14 days, the difference between the predicted value and the measured value is less than 2.4%. The degree of hydration at the age of 14 days is

also calculated based on predicted ultimate CS value. Figure 4.3 shows a typical comparison between fitted curve and measured curve.

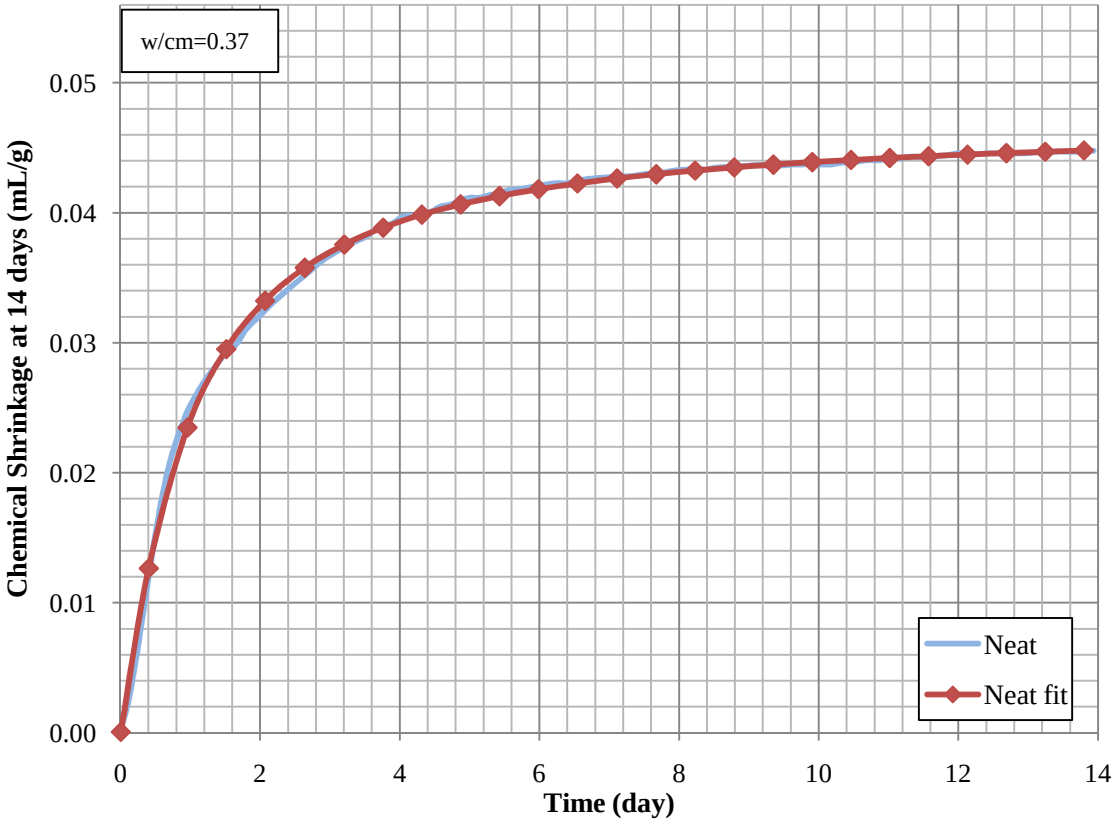

Figure 4.3: Prediction of neat paste of 0.37 w/cm at 20 ºC isothermal

It shows that the predicted CS curve agrees with the test curve well. At later age (after 7 days), the fitted curve very well captured the shape of the chemical shrinkage curve. Other comments on the prediction model are presented in section 4.1.3.

4.1.2 Recommended Modification on Procedure for Determining Chemical Shrinkage Value

As discussed previously, the presence of SCMs and SRA does not allow calculation of ultimate chemical shrinkage value (Equation 8) of the cement paste from composition analysis. The selection of a CS value for use in the Bentz Equation therefore needs further refinement including such parameters. To further investigate the impact of

selected CS values at different ages, the data set of mixtures with 0.37 w/cm was selected. An influence factor was defined to be the percentage difference of needed LWFA between selected CS value and predicted ultimate CS value. The values of 1 day, 7 day and 14 day were selected, and also the FA+SF mixture and SF+FA+SRA are of particular interest. All the other parameters remain unchanged in the equation. Table 4.5 shows the results of such analysis.

Table 4.5: Influence factor analysis for needed LWFA amount

w/cm=0.37 20°C isothermal		Neat	FA+SF	SF+FA +SRA
Predicted CS_u		0.047	0.044	0.046
CS at	1 day	0.025	0.019	0.019
	7 day	0.043	0.037	0.038
	14 day	0.045	0.041	0.042
Influence Factor at	1 day	-46.6%	-56.8%	-58.8%
	7 day	-8.2%	-15.8%	-17.5%
	14 day	-4.4%	-6.0%	-8.0%

The analysis shows that if a 1 day CS value was used, the influence factors were unacceptable (over 46%). For the specific concrete mixture design (FA+SF) for the ODOT HPC, if a 7 day CS value was used, the amount of LWFA needed in internal curing was about 16% less than required theoretically. And if a 14 day CS value was used, it would result in 6% less LWFA than required, which would be acceptable from an engineering perspective. Reasonably, the influence factor would be even smaller if a 28 day or older CS value was used. Therefore, the 14 day or 28 day CS value is acceptable to determine the LWFA content. Nevertheless, the predicted ultimate chemical shrinkage using Equation 9 is recommended.

Another study on the stability of predicted ultimate chemical shrinkage values is presented in Table 4.6 using Xiao and coworkers' data. The selected data set was from type II OPC paste with 30% class F fly ash up to age of 60 days. The predicted CS_u was calculated using the data set up to designated age.

Table 4.6: Predicted CS_u using CS data up to different ages

	14d	17d	21d	24d	28d	40d	50d	60d
Predicted CS_u	0.0617	0.0645	0.0649	0.0641	0.0645	0.0647	0.0648	0.0641

It is noted that after the age of 14 days, the predicted ultimate chemical shrinkage values are stable, in the range of 0.064 to 0.065 ml/g. It also shows that the data set up to 14 day age resulted in about 3% different from values calculated from longer age data, which is acceptable and well within coefficient of variation for other testing parameters, such as absorption capacity and saturation degree of LWFA. Moreover, the ultimate chemical shrinkage values predicted using data of 17 day or older age show no particular trend.

Based on all aforementioned discussion, ultimate chemical shrinkage value based on a prediction model is recommended. A procedure to obtain predicted CS_u is summarized as follow:

- Step 1: Perform ASTM C1608 test on the sample cement paste, SCMs and SRA can be included;
- Step 2: Record the chemical shrinkage development curve up to 14 or 28 days;
- Step 3: Use Equation 9 to fit the curve, find CS_u;

The proposed procedure simplified the chemical shrinkage determination by chemical composition analysis, regardless of the SCMs and other admixtures applied in the mixture. This enables the application of Equation 9 to more complicated mixtures with SCMs or other chemical admixtures like SRA. Table 4.5 shows that it is important to incorporate an appropriate chemical shrinkage value in determining LWFA content. Nevertheless, the optimum LWFA content is not solely decided by the chemical shrinkage value. Factors such as absorption/desorption properties of LWA, change in strength and durability parameters are also of great consideration in terms of optimizing LWFA content. Research has been shown that a 20% partial replacement of natural sand by saturated LWFA of a 0.35 w/cm concrete would insignificantly decrease the strength and increase permeability. (*Durán-Herrera et al. 2007*) While other research has showed

that due to the internal curing process, the concrete show higher strength and less permeability. (*Cusson 2008, Henkensiefken et al. 2009*) To verify the proposed procedure, further experimentation is needed to comprehensively investigate all influential factors to optimize LWFA content. Several of these factors will be investigated in the next steps of the current ODOT internal curing project.

4.1.3 Factors Influence Chemical Shrinkage

4.1.3.1 Effect of Sample Thickness

At the beginning of the chemical shrinkage test, several quick tests were performed to check the sensibility of sample thickness. Three series were tested under 20 ºC isothermal condition up to 14 days: 1) neat paste with 0.37 w/cm; 2) binary paste (30% fly ash) with 0.32, 0.37 and 0.42 w/cm; 3) ternary paste (30% fly ash and 4% silica fume) with 0.32, 0.37 and 0.42 w/cm. The results are shown in Figure 4.4.

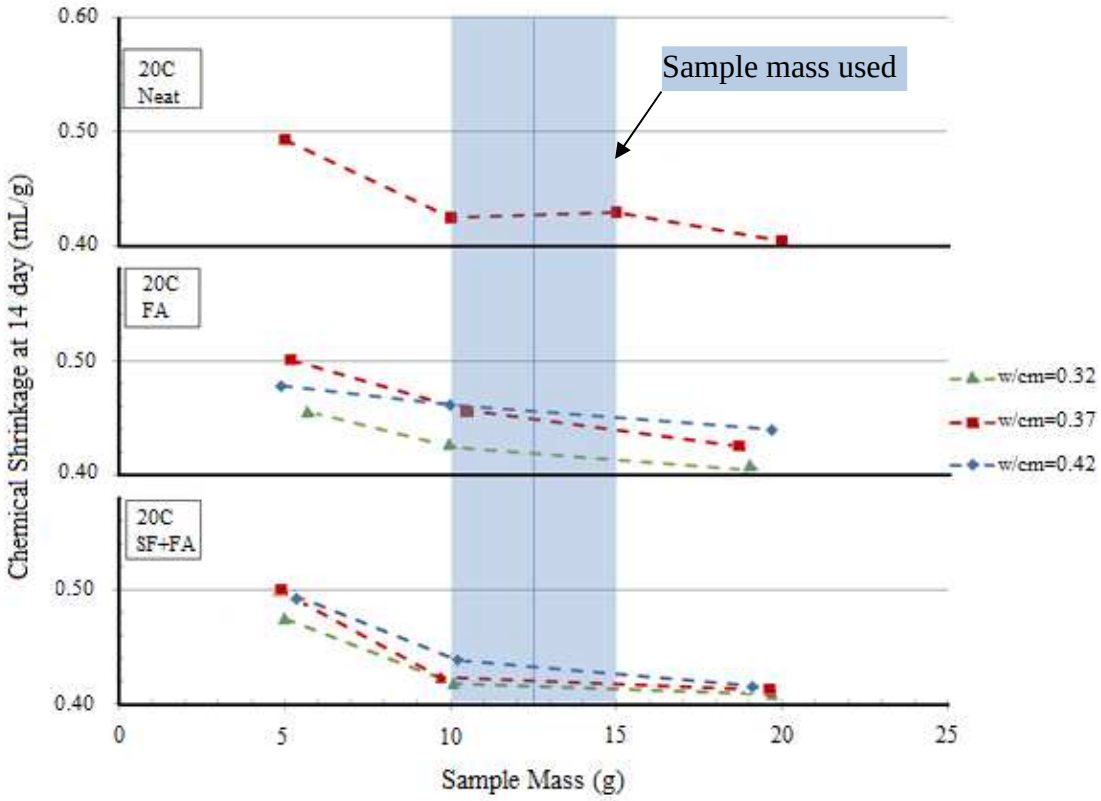

Figure 4.4: Sensitivity of sample size

From the results, the chemical shrinkage is shown to increase with a decrease of sample thickness. Although the sample in the test has infinite water supply, the water is not readily available to travel through the pores in paste matrix. In other words, the further the paste is from the surface of the sample, the more limited the water accessibility there is. Moreover, due to the addition of SCMs, the paste is more densely packed with even lower water accessibility which is exactly the case for HPC with low w/cm (less than 0.35) containing SCMs. Comparison between FA results and FA+SF results shows that the presence of silica fume lowered the tested chemical shrinkage values.

As per ASTM C1608, the thickness should be 5mm to 10mm, which is approximately 5g to 10g paste in the vial used in this testing. Boivin et al. have shown that for low w/cm samples with thickness less than 10mm, the influence was insignificant. (*Boivin et al. 1998*) Nonetheless, one test result shows that the CS values of 0.37 w/cm is higher than CS values of 0.42 w/cm. This is contradictory to the general conclusion. Furthermore, the results are more stable when the sample size is between the range of 10g to 15g than the range of 5g to 10g. Therefore, a sample size between 10g and 15g is selected in this research (shaded area in Figure 4.4).

4.1.3.2 Effect of Water to Cement Ratio

Figure 4.1 shows a trend that chemical shrinkage increases with w/cm. One explanation would be as the w/cm decreases, the water accessibility will decrease due to more densely packed paste matrix. The trend is also shown in Figure 4.5.

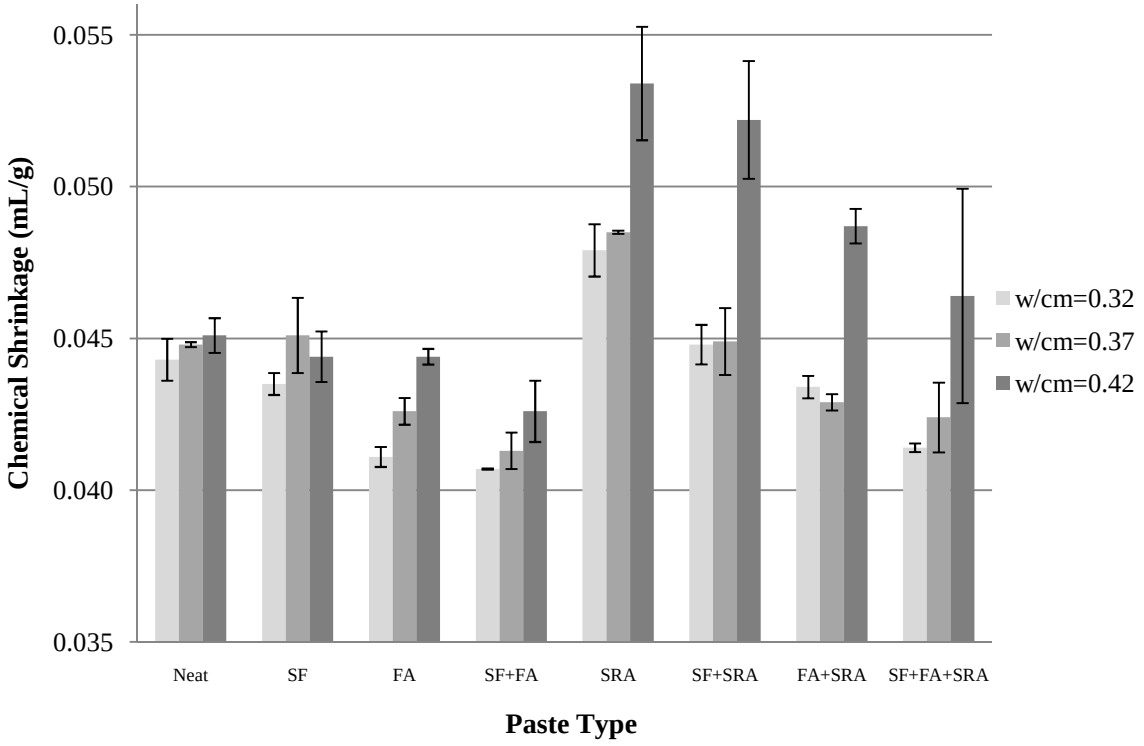

Figure 4.5: Chemical shrinkage 14 days value with error bars, OPC at 20 ºC isothermal

However, results with error bars shown in Figure 4.5 indicate that the difference due to w/cm is of no statistical significance. Only the 0.42 w/cm pastes with the presence of SRA show a significant increase in chemical shrinkage to pastes with lower w/cm. A possible explanation on the effect of SRA is given in section 2.3.1. If only looking at the influence of w/cm in neat paste, the trend shows an increase of CS value with the increase of w/cm in the range tested here, although this increase is not statistically significant:

- Tested 14 day chemical shrinkage values are very similar (0.044ml/g for 0.32 w/cm, 0.045ml/g for 0.37 w/cm and 0.045ml/g for 0.42 w/cm);
- Table 4.3 shows that the development of chemical shrinkage for a neat paste, and;
- The predicated ultimate chemical shrinkage values are almost the same (0.046ml/g for 0.32 w/cm, 0.047ml/g for 0.37 w/cm and 0.047ml/g for 0.42 w/cm) based on Equation 9.

From Equation 9, $\sqrt[a]{b}$ represents the time needed to reach 50% $CS_{u.}$ Table 4.7 shows a summary of time needed to reach 50% CS_u for all mixtures. From this table it is quite clear that for mixtures without SRA, the w/cm has very little effect on chemical shrinkage development.

Table 4.7: Time needed to reach 50% CS_u (day)

w/cm	Neat	SF	FA	SF+FA	SRA	SF+SRA	FA+SRA	SF+FA+SRA
0.32	0.9	0.9	1.5	1.5	1.2	1.1	1.9	1.8
0.37	1.0	1.2	1.4	1.5	1.3	1.4	1.5	1.6
0.42	1.0	1.1	1.5	1.4	1.7	1.6	2.0	2.1

The conclusion would be under the given testing conditions (infinite water supply) with similar sample size, the effect of w/cm is insignificant on a neat paste mixture with varying w/cm. This is not necessarily true in the field when the sample dimensions are different and combined with limited water supply. Therefore the maximum hydration degree is incorporated in the Bentz Equation states that when w/cm is below 0.36, 100% hydration degree is not possible therefore less water would be needed for hydration from external sources or saturated LWFA.

4.1.3.3 Effect of SCMs

According to Bentz, the typical chemical shrinkage value for silica fume is 0.20 to 0.22 ml/g, and 0.10 to 0.16 ml/g for Type F fly ash. (*Bentz 2007*) Compared to OPC, those values are much higher in magnitude. However, these data are only partially based on experimental results combined with a set of hypothesized reactions. (*Bentz and Remond Aug. 1997, Feng et al. 2000*) Several other researchers showed that usually the reaction degree of SCMs is quite low in blended cement and it is almost impossible to reach 100% reaction rate. (*Termkhajornkit et al. 2005, Xiao et al. 2009, Yajun and Cahyadi 2004*) In another words, the SCMs works as fillers at early-age in blended cement mixture to quite a high degree since the reaction degree is low. Figure 4.6 shows the experimental data of pozzolanic reaction degree.

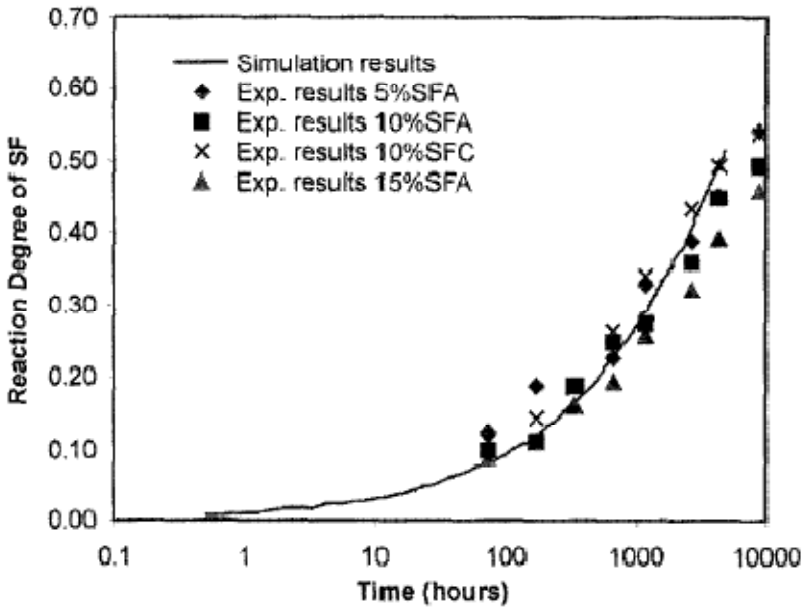

Figure 4.6: Pozzolanic reaction degree data(*Yajun and Cahyadi 2004*)

Figure 4.6 shows that about 10% reaction degree can be achieved at age of 100 days for 5% silica fume blended cement. It has been observed that the microstructure of silica fume blended cement paste is improved compared with OPC due to much smaller particle size and additional C-S-H gel formation from pozzolanic reaction.

From Table 4.2, it shows that the presence of fly ash significantly decreases the chemical shrinkage values at 14 days. And the combination of fly ash and silica fume further decreases the chemical shrinkage value. Figure 4.7 better demonstrates this effect.

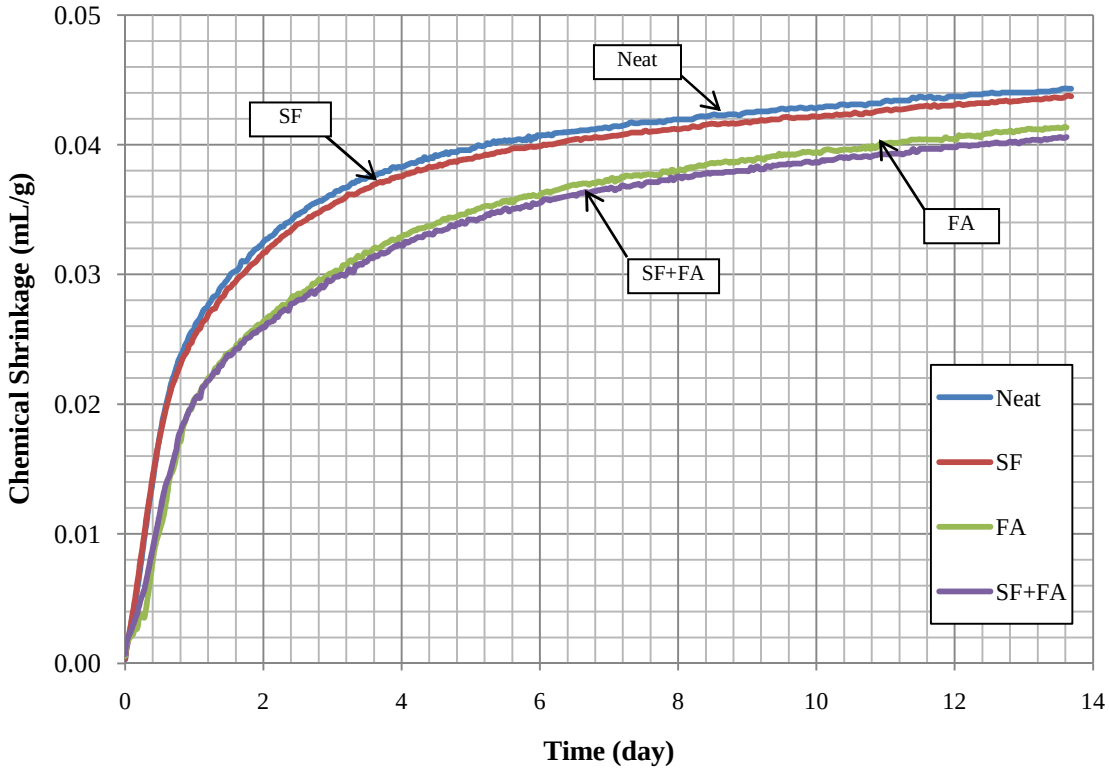

Figure 4.7: CS development curve, OPC w/cm=0.32 at 20 ºC isothermal (without SRA)

Figure 4.7 indicates that with the presence of fly ash (30% replacement of cement by mass), the chemical shrinkage curve development was delayed. One possible explanation would be the glass content (silicate) in fly ash cement paste did not react in the early-age due to lack of calcium hydroxide (CH) from cement hydration. Sakai and coworkers found that regardless of glass content and composition, the fly ash in fly ash cement paste cured at 20 ºC did not react until 7 days. (*Sakai et al. 2005*) It also shown in Figure 4.7 that the presences of silica fume in conjunction with fly ash replacement further lowered the chemical shrinkage value. However with a low replacement ratio (4%) the impact is insignificant. Comparison between neat paste and blended paste is shown in Table 4.8.

Table 4.8: Chemical shrinkage value compared to Neat paste

w/cm		Neat/Neat	SF/Neat	FA/Neat	SF+FA/Neat
0.32	14 days	1.00	0.98	0.93	0.92
	CS_u	1.00	1.00	0.99	0.99
0.37	14 days	1.00	1.01	0.95	0.92
	CS_u	1.00	1.03	0.96	0.94
0.42	14 days	1.00	0.98	0.98	0.95
	CS_u	1.00	0.97	1.04	1.02

Although the early-age chemical shrinkage values decreased with incorporation of SCMs, Table 4.8 shows the difference for predicted ultimate chemical shrinkage values are more closely decided by the trend of the chemical shrinkage development curve. In 0.42 w/cm mixtures, the CS_u ended up higher in blended paste. Therefore the model indicated although the chemical shrinkage in the early-age may be reduced by SCMs, the long term values could come back up due to higher degree of hydration of SCMs compared to neat cement pastes.

In terms of chemical shrinkage development without SRA, Table 4.7 shows the presence of fly ash delayed the hydration by 0.5 days. And silica fume had similar effect but due to small amount of replacement in this study this delay was insignificant.

4.1.3.4 Effect of SRA

Many researchers have shown that by incorporating shrinkage reducing mixture, the drying shrinkage and plastic shrinkage could be significantly reduced due to the effect that SRA reduces the surface tension of the mixing water and subsequently the pore solution inside the concrete. (*Bentz et al. 2001, Bentz 2006, Folliard and Berke 1997, Lin and Huang 2010, Saliba et al. 2011*) However, few reports have been performed on the effect of SRA on chemical shrinkage. This research revealed certain information about the effect of SRA on chemical shrinkage which might be helpful when SRA and LWFA are used in conjunction.

Figure 4.5 shows that chemical shrinkage value of almost every mixture increases with the incorporation of SRA, and it is statistically significant. A summary of increasing chemical shrinkage values are shown in Table 4.9.

Table 4.9: Chemical shrinkage change with SRA*

w/cm		SRA	SF+SRA	FA+SRA	SF+FA+SRA
0.32	14 days	8.1%	3.0%	5.6%	1.7%
	CS_u	12.2%	6.0%	9.8%	4.1%
0.37	14 days	8.3%	-0.4%	0.7%	2.7%
	CS_u	13.4%	0.4%	4.2%	4.8%
0.42	14 days	18.4%	17.6%	9.7%	8.9%
	CS_u	29.3%	31.3%	14.4%	12.4%

*Percentage change to the same mixture without SRA.

The data shows that the presence of SRA increases the chemical shrinkage value significantly. One possible explanation would be that due to the reduction of surface tension, many of small capillary pores which would collapse without SRA present would not collapse, leaving a more open pore structure to accommodate more water ingress in the chemical shrinkage testing performed here. Therefore, with infinite water supply in the chemical shrinkage test, ample water was able to fill these voids , resulting in high chemical shrinkage value. For lower w/cm (0.32 and 0.37), an 8% increase of CS value was observed for neat paste while less than 3% increase in CS were observed for ternary blended paste. Due to the presence of SCMs with much smaller particle size, the porosity was reduced in these mixtures. As a result fewer voids were left in the paste matrix resulting in less water back fill. And for higher water cement ratio (0.42), due to higher porosity the increases are as high as 18% for neat paste and 9% for ternary blended mixture. However, it is quite interesting to point out that this effect was diminished when w/cm increases up to 0.5 or more (see Figure 4.8).

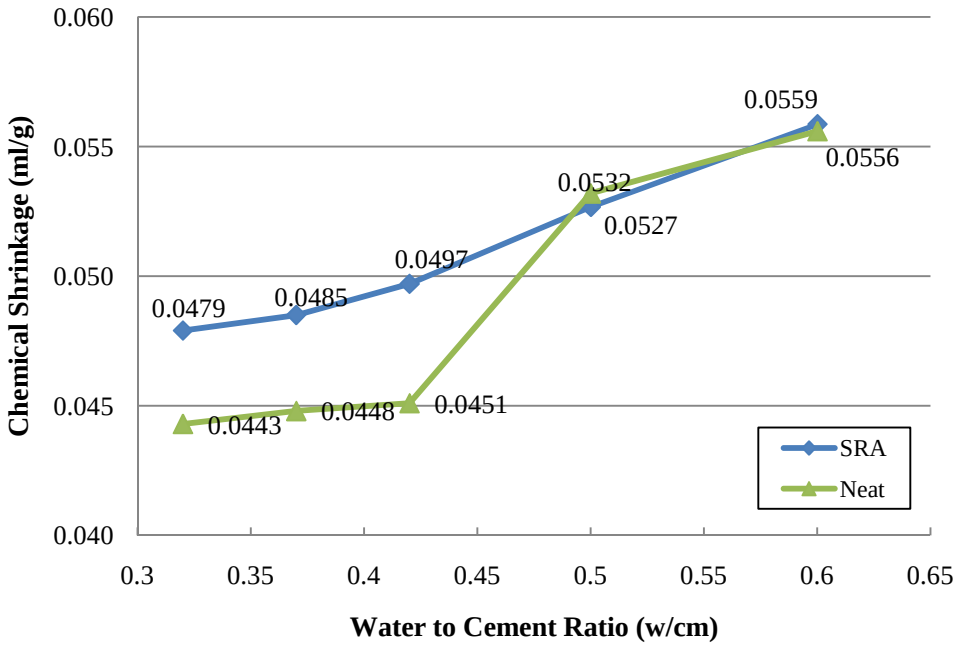

Figure 4.8: Effect of SRA on different w/cm at 14 days, 20 ºC isothermal

It shows that for the paste of 0.5 and 0.6 w/cm, the effect of SRA in terms of chemical shrinkage was eliminated. This might be evidence showing that with an increase of w/cm, much more bigger pores are formed in the paste, which would not close up even without the presence of SRA. Future work is needed on pore distribution study to provide verification.

From Table 4.7 the presence of SRA would also affect the chemical shrinkage development of the paste sample. Mixtures with SRA require much longer time to reach 50% CS_u than same mixtures without SRA, especially for mixtures with fly ash in which case the time is doubled for 0.32 and 0.42 w/cm.

4.1.4 Summary

Section 4.1 presented all the chemical shrinkage OPC system results. A simple experimental model was adopted and verified to predict ultimate chemical shrinkage values regardless of the mixtures (with/without SCMs or SRA) of the pastes. Based on

this prediction model, a modification in simplifying chemical shrinkage estimation for the Bentz Equation was proposed. In addition, effect of different factors on chemical shrinkage, such as w/cm, sample thickness, the addition of SCMs and SRA, were analyzed.

4.2 CAC RESUTLS AND ANALYSIS

Calcium aluminate cements were also investigated as part of this research project for their interest as a rapid repair material for such applications as high performance concrete bridge decks. Figure 4.9 shows a summary of chemical shrinkage test results for CAC systems cured under different temperatures. A typical result of OPC with 0.37 w/cm is also shown in the figure to compare with the CAC results.

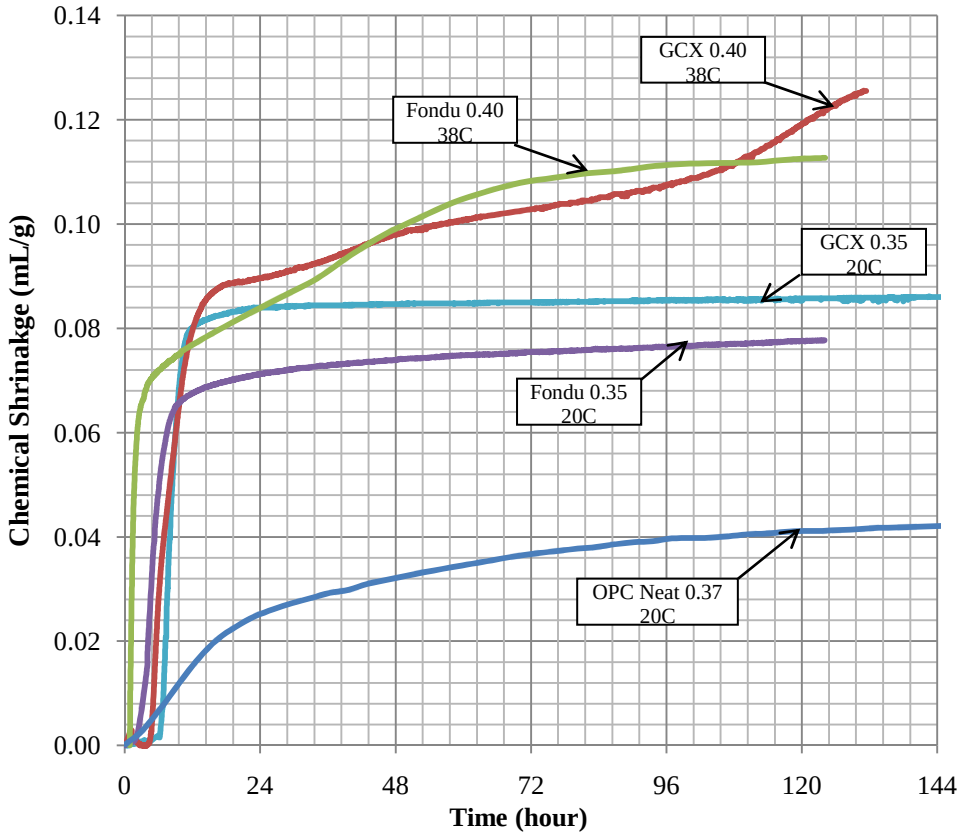

Figure 4.9: Chemical shrinkage development curve, CAC systems

All curves represent the average of at least three samples. It can be seen that in general, chemical shrinkage of CAC systems was 2 to 3 times higher than OPC system. In addition, most of the chemical shrinkage of CAC systems occurred in the first 24 hours after initial contact of cement and water. In other words, CAC is more “mature” at early-age than OPC pastes due to rapid hydration.

Curing temperature had an impact on chemical shrinkage of CAC systems. In a higher temperature (38 °C), significant increases were observed in both Fondu and GCX pastes. Ideker (2008) studied the effect of temperature on GCX binder, showing that if curing temperature reached 30 °C and above, there was about 60% increase in chemical shrinkage. Another interesting finding was that the 20 °C chemical shrinkage curves flattened out after the “initial ascent” while 38 °C chemical shrinkage curves showed a “secondary ascent“ later in the age. Similar findings were discovered in Ideker’s study too. (*Ideker 2008*) It is believed that such impact is related to conversion phenomenon in CAC systems. A detailed discussion on conversion is presented in section 4.2.1. It seems that the chemical shrinkage test can serve as a predictor of the conversion process. To verify this assumption, an X-Ray diffraction (XRD) analysis was performed to study the phase composition in GCX samples. The discussion is presented in 4.2.2.

4.2.1 Conversion in CAC Systems

As mentioned in Chapter 2, the major difference between calcium aluminate cement and portland cement is the chemical make-up of the cement which leads to very different hydration products. In ordinary portland cement, the principle reactants are silicates (C_3S and C_2S). And the major hydration products are amorphous calcium silicate hydrate (C-S-H) and calcium hydroxide (CH). The C-S-H is a stable phase and responsible for the majority of strength in concrete and other key properties such as chemical resistance and permeability. (Mehta and Monteiro 2006) In contrast, in calcium aluminate cement, with very little silica and high alumina content (Table 3.1), the major reactive phase is

monocalciumaluminate (CA) which reacts with water to give calcium aluminate hydrates, CAH_{10} (metastable), C_2AH_8 (metastable) and C_3AH_6 (Stable). (Scrivener et al. 1999)

Unlike the calcium silicate hydrates which will form broadly similar with time and temperatures up to about 100 ºC, the hydration of calcium aluminate cement is highly dependent on temperature. (*Scrivener and Capmas 1998*) Figure 4.10 shows the temperature dependent nature of the calcium aluminate hydrates.

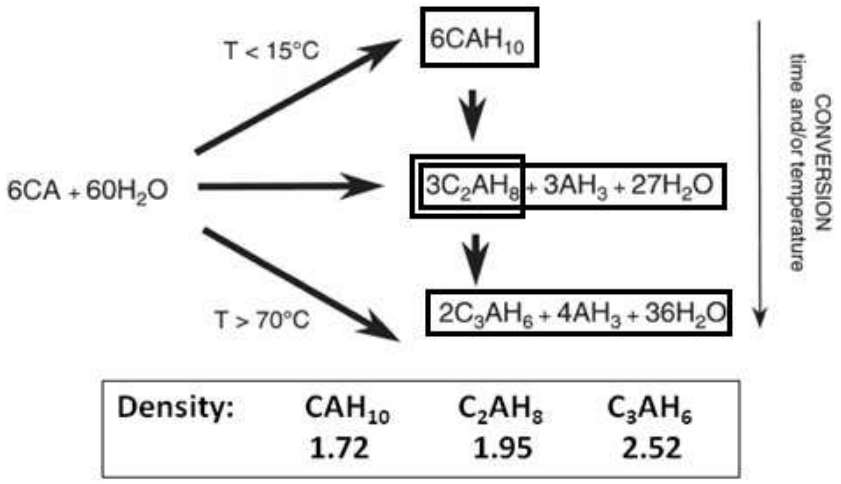

Figure 4.10: Hydration reactions of monocalciumaluminate.(*Scrivener et al. 1999*)

As shown, at the lower temperature (less than 15°C), CAH_{10} is the first and dominant hydrate formed and continues to form up to about 27ºC. Between 15°C and 27°C, CAH_{10} and C_2AH_8 are formed together. When temperature goes above 50 °C, C_3AH_6 rapidly becomes the only and stable hydrate present, and most C_2AH_8 (in the small box, Figure 4.10) begins to transform to this stable hydrate phase. (*Scrivener and Capmas 1998*) The duration spent at elevated temperatures also plays a profound impact on the extent of conversion to stable hydrates. At ambient temperature the metastable hydrates may exist for many years. However, the change from metastable phase to stable phase is an inevitable thermodynamic transformation, which means given time all hydrates will eventually turn to C_3AH_6 regardless of the environmental temperature. This change is

usually referred as conversion. A more detailed description can be found in Chapter 13 of *Lea's Chemistry of Cement and Concrete. (Scrivener and Capmas 1998)* Figure 4.11 shows a schematic of the effect of conversion on strength development on CAC concrete.

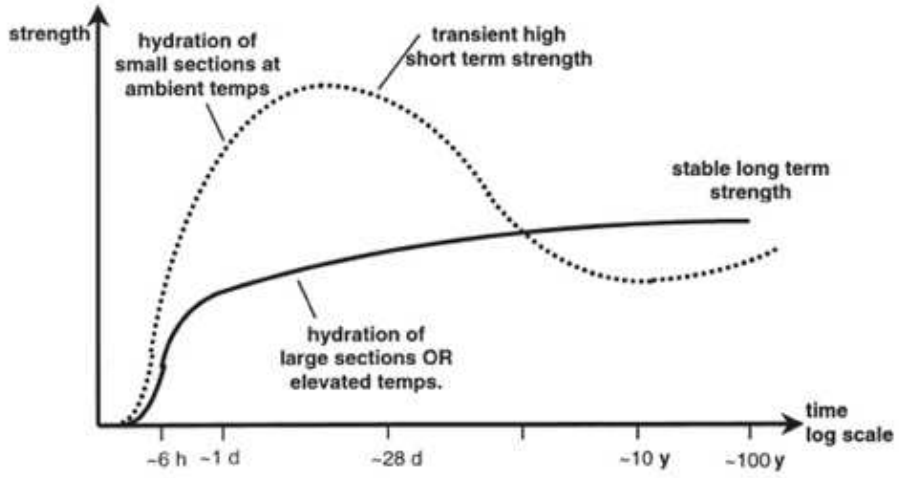

Figure 4.11: Schematic strength development of CAC of 0.40 w/cm.(*Scrivener et al. 1999*)

Small sections cured in ambient temperature will show a very high initial strength which corresponds to the dominate formation of CAH_{10}. During the conversion process, in which the hydration products densify and leave voids behind, a slow decline in strength will happen and eventually drop to a minimum before further increases. A scanning electron microscope images in Figure 4.12 show a very porous CAC microstructure.

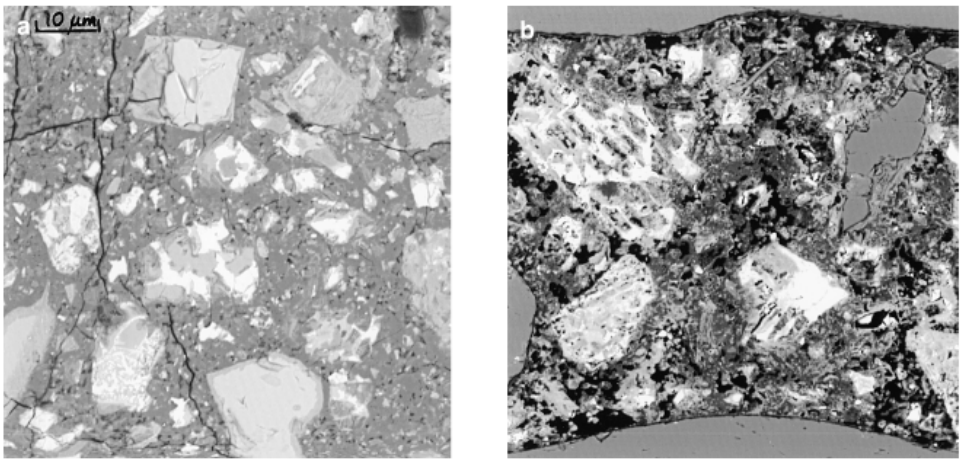

Figure 4.12: Microstructures of CAC concrete with 0.70 w/cm cured at 20°C(left a and the right one cured at 70 ºC) (*Scrivener et al. 1999*)

To understand conversion in CAC system is very important. From 1930s to 1970s, the inproper use of CAC (usually with a high w/cm above 0.6) resulted several failures related to conversion. (*Concrete Society Technical Report 1997, Scrivener and Capmas 1998*) Over 60 years of practical and laboratory experience has resutlted a consent which suggests that to ensure good long-term durability requres a w/cm at or below 0.40. To obtain satifactory workablity under 0.40 w/cm without superplasticizer will require a minimum of 400 kg/m^3 cement content.(*Scrivener et al. 1999*) However, further research is needed to enhace the understanding of hydration of CAC systems in order to utilize them with avoidance of or proper charaterization of conversion.

4.2.2 Chemical Shrinkage and XRD Analysis on GCX

While conversion process may take many years in the field, it can be accelerated in the laboratory by curing at 38°C isothermal condition immediately after casting. In this way, the major hydrates formed are stable phase therefore a minimum in strength (also known as usable strength) can be realized typically within 5 days. (*Concrete Society Technical Report 1997*) If given a closer look at the chemical shrinkage development curve of GCX curing at 38 ºC isothermal condition, a slope change roughly around 5 days(see Figure 4.13) is noticed representing the change of reaction rate is slowing down. This might be interpreted as the completion of the conversion process. To verify this assumption, X-ray diffraction (XRD) analysis was performed on several GCX samples cured at 38°C isothermal condition at different age.

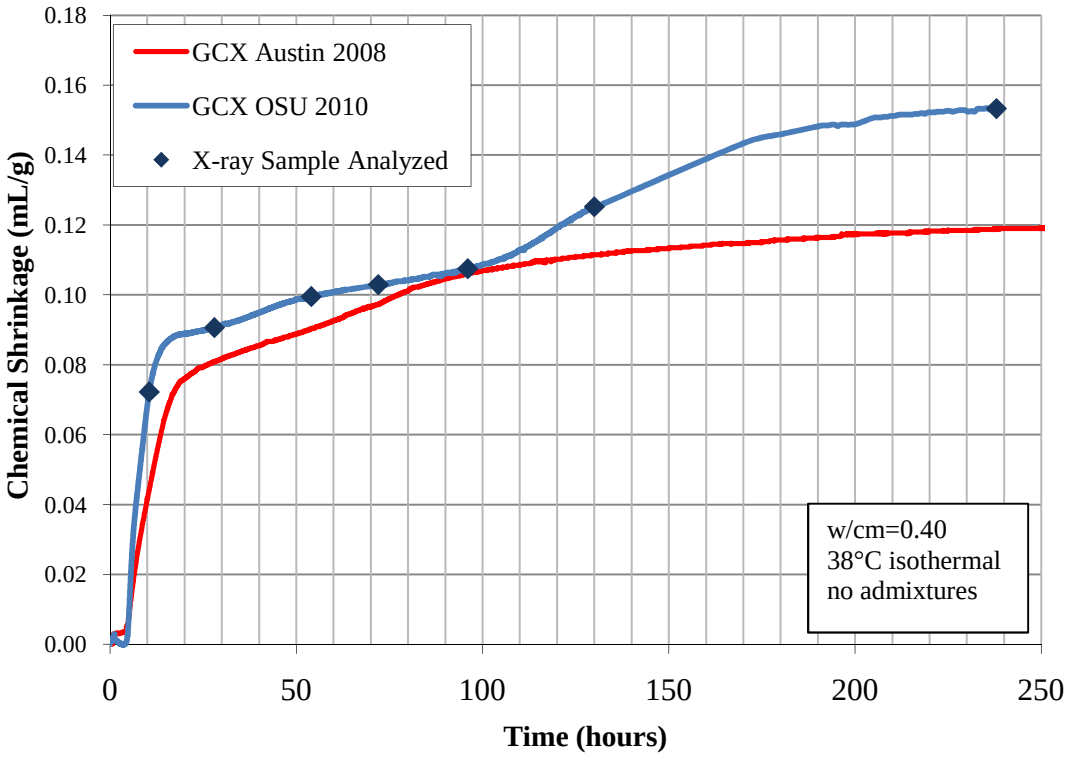

Figure 4.13: Chemical shrinkage GCX, 0.40 w/cm at 38 ºC isothermal

As shown above, the slope of chemical shrinkage development curve changes around 4 to 5 days which represents the change of reaction rate. In a few initial first trails, the glass sample holder described in ASTM C1608 was used but found cracked later indicating a severe expansion. This also happened after 3 days of the test to the brittle vials used for OPC system in this research (Figure 4.14a). The lower line represents the result from the University of Texas, Austin by Ideker using soft plastic sample holder shown in Figure 4.14b. (*Ideker 2008*) The upper line represents a duplicate test at Oregon State University using a different sample holder (Figure 4.14c). Other than the different sample holders, the two testing procedures were identical inclusive of procedures and cementitious materials. It is quite obvious the slope changes are different in these two tests, in which the UT test the reaction rate appears to be slowing down while OSU test was speeding up. One possible explanation would be the sample holder used in Austin test did a better job to accommodate the expansion from the GCX sample without deformation or rupture.

While in the OSU test, the expansion of the sample itself induced geometric change in the sample holder. This enabled the upper part (above cement sample) to accommodate more water. In another words, more water was registered as chemical shrinkage value while in fact it may not have been consumed by cement sample. To eliminate the complication of volume change for expansive systems, a better testing system is needed and discussed in section 4.2.3.

a) OSU, OPC

b) Austin, GCX(*Ideker 2008*)

c) OSU, GCX

Figure 4.14: Different sample holders

As the chemical shrinkage test progressed samples from the same batch cured at the same condition were prepared for XRD analysis. First, the sample was pre-crushed to pieces with a diameter less than 10mm, and then submerged in acetone for at least 2 days to completely stop the hydration process (chemical drying). Then, the samples were stored under vacuum for another 2 days before full grinding to pass through a No. 200 sieve. To better interpret the XRD results, an internal standard component titanium dioxide (TiO_2) was mixed with the fine sample powder in a ratio of 1:9 with pure ethanol, then fully dried in the desiccator. The set-up of the vacuum desiccator is shown in Figure 4.15.

Figure 4.15: Vacuum desiccator to dry and store samples for XRD analysis

Samples taken from ages of 10.5 hour, 28 hour, 54 hour, 3 day, 4 day, 5 day10 hour and 10 day were analyzed by XRD. A summary of the results is shown in Figure 4.16.

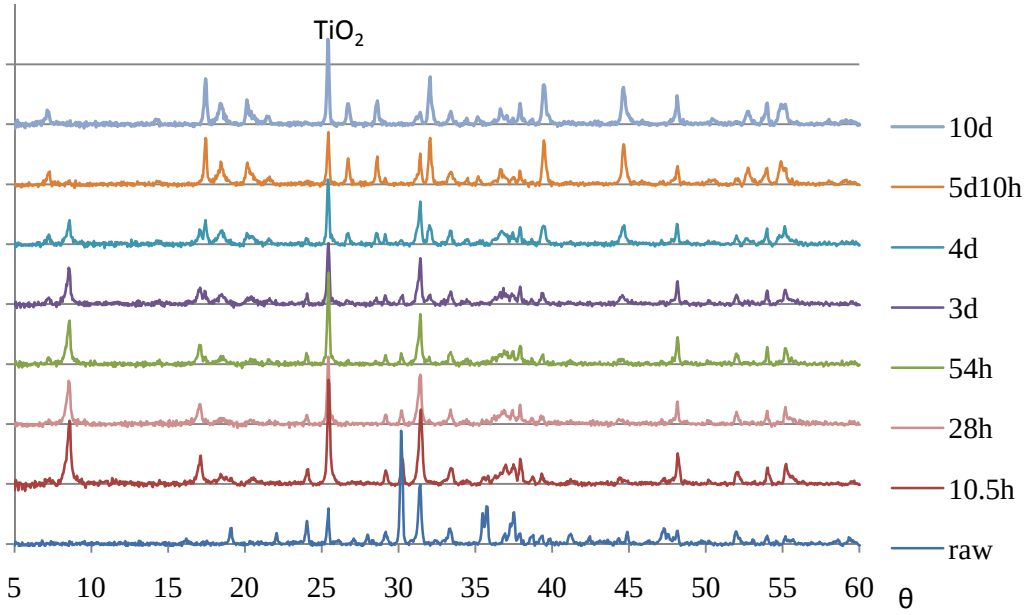

Figure 4.16: XRD analysis on GCX sample, 0.40 w/cm at 38 ºC isothermal

From Figure 4.16, it is very clear there is no formation of CAH_{10} due to curing at higher temperature (38ºC), since there is no peak shown around 12.4°, in any of the samples

tested which represents CAH_{10}. To focus on the components interested, selected results are shown in Figure 4.17. Peaks are labeled for ease of identification.

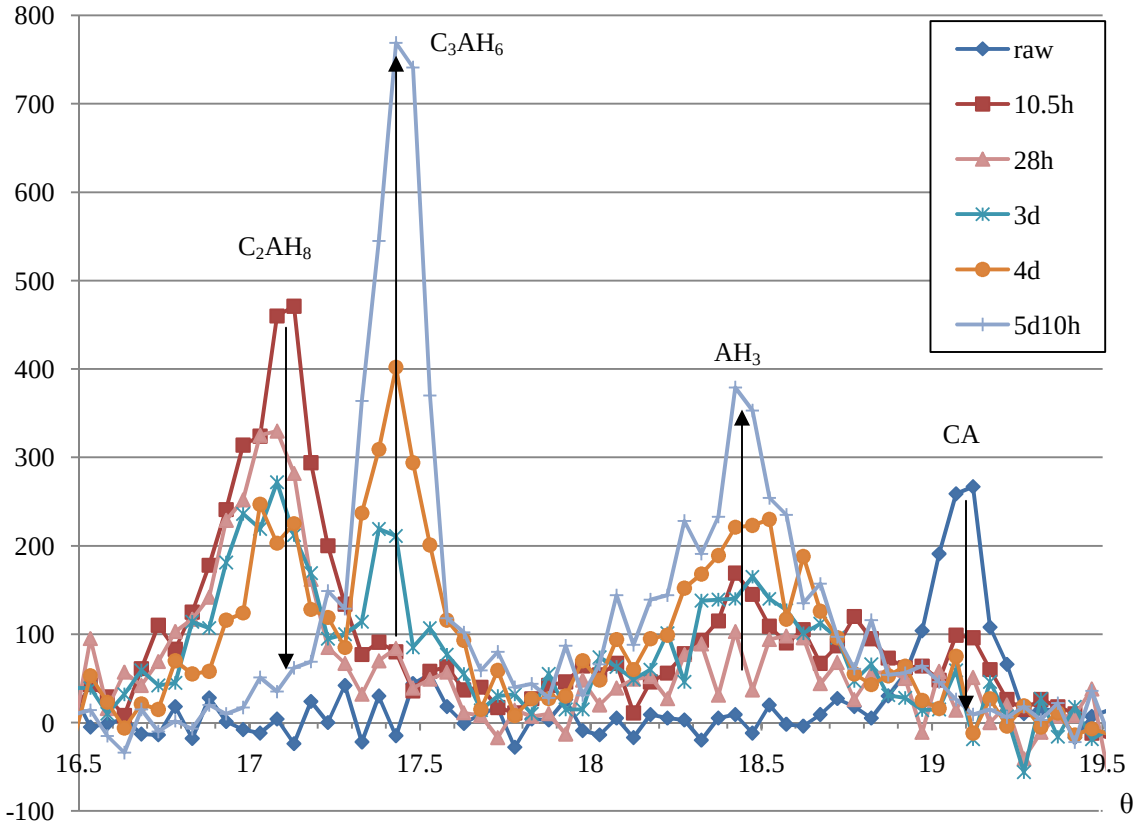

Figure 4.17: XRD analysis on GCX sample, 0.40 w/cm at 38 ºC isothermal, details on C_2AH_8 and C_3AH_6

Figure 4.17 shows several trends of the phase transformation in GCX sample:

- Unreacted CA depleted very quickly and was almost undetectable after 28 hours;
- As CA was depleted, the C_2AH_8 dominated the hydration products at 10.5 hours and no C_3AH_6 was observed in the sample. At the same time, AH_3 was forming along with C_2AH_8, and;
- After 3 days, C_3AH_6 increased rapidly along with the depletion of C_2AH_8 and continued growth of AH_3 up to 5 days. This clearly demonstrates the conversion.

The depletion of C_2AH_8 happened during 4 and 5 days corresponding to the slope change in chemical shrinkage development curve shown in Figure 4.13. Therefore, chemical

shrinkage test can be used as a predictor of conversion process in isothermal conditions. Such testing may be beneficial for field applications where a time and temperature history can be used in small-scale laboratory testing to predict conversion. This information may also be useful for modeling the prediction of conversion. XRD analysis is a useful tool to confirm conversion of metastable to stable hydrate phases. Previous research has been shown that at higher temperature (45°C and 55º C), the slope change in chemical shrinkage development change happened significantly earlier in the hydration process. (*Ideker 2008*) Further work might be done to confirm conversion under different isothermal conditions. The ultimate purpose would be to generate a conversion time prediction model for given CAC sample if given the temperature history. This would greatly benefit the field application in term of prediction of minimum strength.

4.2.3 Chemical Shrinkage on Expansive Cementitious Systems

As discussed previously, the volume change in sample holder or sample itself complicates the dilatometry method to test chemical shrinkage. If given a closer look at ASTM C1608, a rigid glass sample holder is recommended indicating the chemical shrinkage test set-up should be able to accommodate the volume change of sample itself while the volume change of sample holder is not allowed. This is true for gravimetry method described in section 2.2.2. But it is not always true for dilatometry method. Figure 4.18 shows examples of how sample holders are affected by the expansive behavior of cement sample inside.

Figure 4.18: Cracked vial due to expansion of GCX inside, at 38 °C.

The disadvantage of gravimetry method is that it requires one scale for every individual chemical shrinkage sample while no scale is require and multiple samples can be tested simultaneously for dilatometry method. Therefore, based on the same set-up developed in OSU material lab, a modification which enables the test to take account of volume change of sample holder is proposed for further verification (see Figure 4.19).

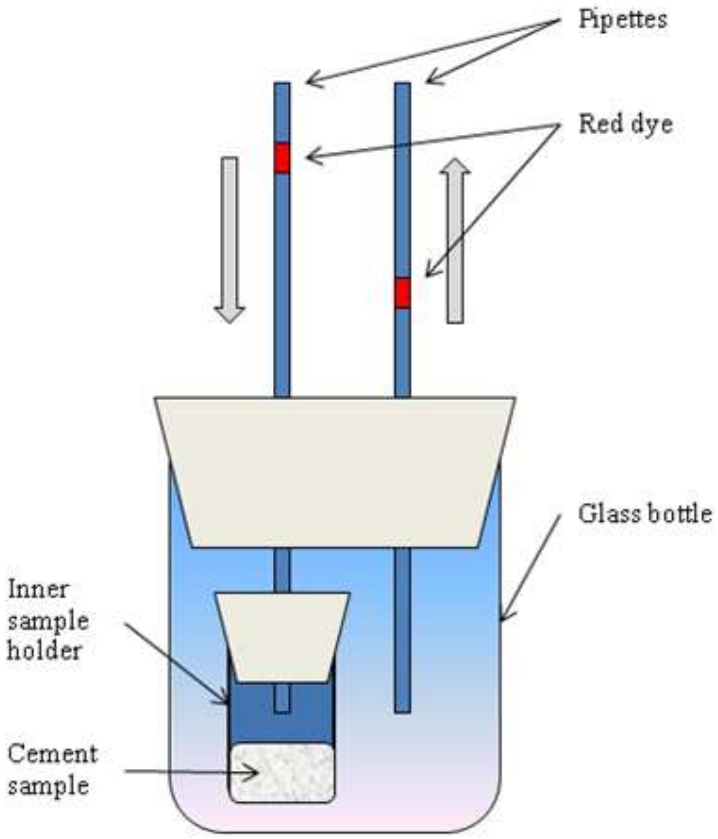

Figure 4.19: Modified dilatometry method for expansive cementitious systems.

The basic concept behind this modified method is to measure chemical shrinkage and volume change of sample holder at the same time. As shown in Figure 4.19, the outer sample holder is made of glass to remain unchanged in volume. And the inner sample holder is made of soft plastic which can easily accommodate the expansion of the cement sample inside. As the test progresses, the red dye in the left pipette would go down representing the water consumption of the sample. At the same time, the red dye in the right pipette would go up representing the expansion of the inner sample holder. All the

movement of the red dye in each pipette would be registered by a webcam, then analyzed by the software. Then, an adjusted chemical shrinkage development curve and more accurate chemical shrinkage value represents true water consumption can be obtained.

The advantage of the modified method is that it can accommodate volume changes of the sample holder therefore yield more accurate chemical shrinkage value for expansive cementitious systems. And it can be applied to existing testing system with multiple sample capacities. Future work is needed to verify this modified method on OPC system and expansive cementitious systems.

4.3 CONCLUSIONS

Chemical shrinkage results and analysis were presented in this chapter, and several important conclusions were drawn:

- Based on the series of observed data, a simplified procedure was proposed to estimate ultimate chemical shrinkage value for OPC systems;
- The water to cement ratio has an insignificant impact on chemical shrinkage in the range of 0.32 to 0.42 for the cementitious systems tested in this research;
- The SCMs (class F fly ash and silica fume) would decrease observed chemical shrinkage values, but would insignificantly affect long term chemical shrinkage values. The presence of SCMs also delayed the chemical shrinkage development;
- SRA was shown to increase chemical shrinkage for mixtures with w/cm in the range of 0.32 to 0.42, but this effect was eliminated when w/cm increased up to 0.5 and higher. The presence of SRA also delayed the development of chemical shrinkage;
- Chemical shrinkage for CAC pastes was significantly greater than that of OPC systems, and it was affected by curing temperature;
- Chemical shrinkage can be used as a predictor of conversion process for CAC system in an isothermal condition, and;
- A modified chemical shrinkage test was proposed and future work is needed to verify the validity of this method.

5 AUTOGENOUS DEFORMATION

Quantifying autogenous deformation (especially autogenous shrinkage as defined in Chapter 2) of concrete systems is of utmost importance at early-ages. For HPC in concrete bridge decks with low w/cm, the risk of early-age cracking increases due to autogenous shrinkage in a restrained element. Although various methods have been proposed to capture or to assess the effectiveness of shrinkage mitigation strategies, there are still challenges in measurement due to the requirement of sealed curing conditions, difficulty in obtaining measurements at early-age due to the transition of cement-based systems from fresh to hardened state, temperature variation and friction between the specimen and the surrounding testing apparatus.

Measurement methods for autogenous deformation were identified in Chapter 2, among which the most frequently applied methods are the membrane method and corrugated tube method. The corrugated tube method was adopted as ASTM C1698. However, due to numerous disadvantages this was not selected as the measurement method for this research. One disadvantage is the temperature control. Due to the size of the specimen (approximately 600g is needed for a paste sample), adequate temperature control is required to exclude the confounding factor of temperature variation due to heat of hydration. This is especially critical for rapid hardening materials such as CAC paste systems due to the shorter duration over which heat is evolved. To perform temperature control for a 600g paste specimen, at a minimum a static water bath is usually required. For systems which evolve heat more rapidly active temperature control water baths may be necessary. The ASTM C 1698 standard specifies: “Do not store specimens in a water bath due to possible water transport trough the corrugated molds” (*ASTM C1698 2009*), which means it is quite challenging to achieve satisfactory sealed curing conditions for the specimen. However, researchers have been able to achieve sealed conditions through careful experimental procedures. (*Lura and Jensen 2005, Sant et al. 2006*) Since sealed

curing conditions and temperature control are vital for measurement of autogenous deformation, the membrane method was selected in this research.

If proper experimental procedures are followed during testing, an adequately sealed specimen will have less than less than 0.02% mass change during the 3 day testing period could be achieved. With a much smaller sample size (about 100g), temperature control by a static water bath is efficient, and a ± 1.0 ºC temperature variation from desired isothermal condition is easily achieved (for OPC systems). In addition, the membrane method is a volumetric measurement rather than a linear measurement, which means it excludes the confounding factor of sample size and dimensions. In addition, it excludes the confounding factor of friction in certain directions since it is in a buoyant, close to frictionless media.

5.1 OPC RESUTLS AND ANALYSIS

Seven OPC mixtures were tested in this research to determine the effect of w/cm, presence of SCMs and SRA. Detailed testing procedure is described in section 3.2.3. For each mixture, two samples were tested to ensure repeatability and the results shown below are the average of two test results. Vicat setting time according to ASTM C191 was also performed in an attempt to provide the proper zero starting strain point to better interpret the results.

5.1.1 Setting Time

Figure 5.1 shows a summary of OPC systems setting time test result using Vicat needle apparatus. The tests were performed on cement pastes of specific w/cm for alignment with the chemical shrinkage and autogenous deformation test.

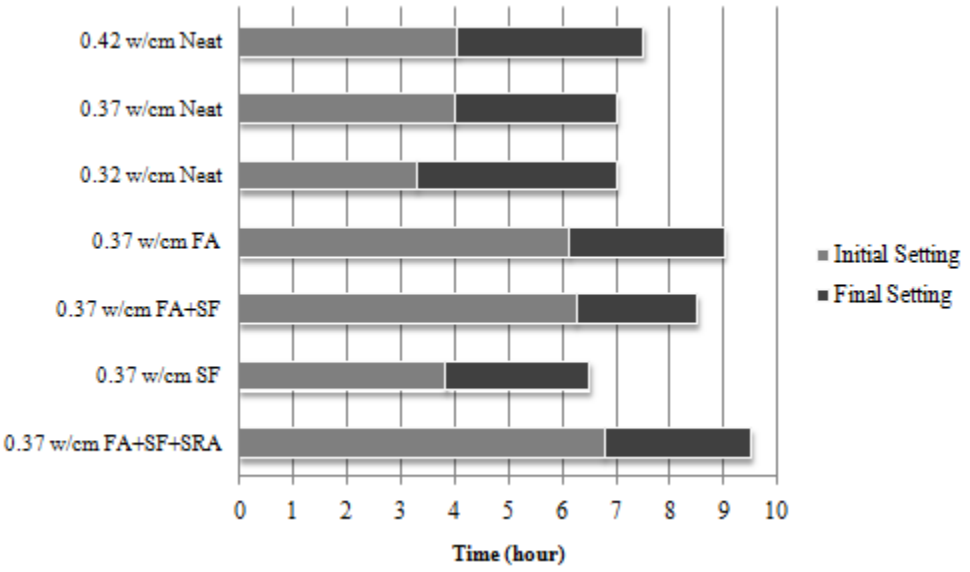

Figure 5.1: Vicat setting time results for OPC systems (20°C)

Generally, the finally setting time is between 7 to 9 hours. It is noted that the presence of fly ash and SRA prolonged the setting process. This was also reflected in autogenous deformation testing and chemical shrinkage testing. Silica fume shortened the setting process although not significantly.

Time of setting, especially for final setting time, plays an important role in interpreting the autogenous deformation results. Most researchers agree on setting the zero strain at final setting time (*Lura and Jensen 2007, Sant et al. 2006*), because it is believed that from this point the stress in the specimen starts to build up. (*Jensen and Hansen 2001*) The final set point as determined by the Vicat test should also be similar to the point that the chemical shrinkage and autogenous shrinkage begins to diverge. (*Sant et al. 2006*) However, the setting time measured in this research does not correlate to the setting time happened in the autogenous deformation specimen, especially in the specimens with addition of fly ash and SRA. Several reasons are believed to cause this disagreement:

- The determination of final set depends on the judgment of an individual operator for “when the needle does not sink visibly into the paste”;
- During the Vicat test, moisture loss during testing is inevitable and drying at the surface of the setting time sample might reduce the setting time, and;
- As a destructive test method, the Vicat test measures setting time by intruding the needle into the paste repeatedly. This might cause a difference from the pastes in autogenous sample which remain unspoiled. A non-destructive Vicat test was proposed recently. (*Sleiman et al. 2010*) Discussion on this test is beyond the scope of this research.

To better interpret and compare results, the zero strain for all autogenous deformation curves were set to be the point where they diverge from the chemical shrinkage curves. all tests for OPC systems were performed under 20 °C isothermal condition. Table 5.1 gives a summary of autogenous deformation testing results at the age of 50 hour for OPC systems cured at 20 °C isothermal condition. The majority of pastes were tested at a w/c=0.37.

Table 5.1: Autogenous stains of OPC systems (μm/m) at 50 hour

20 ºC Isothermal	Neat	FA	SF	FA+SF	FA+ SF+ SRA
w/cm=0.32	-631	-	-	-	-
w/cm=0.37	-205	142	-629	-168	526
w/cm=0.42	-148	-	-	-	-

The negative values represent shrinkage and positive values represent expansion. Only FA and FA+SF+SRA mixtures showed autogenous expansion. And the most severe shrinkage recorded were neat pastes with low w/cm of 0.32 and 0.37 w/cm pastes with silica fume. More detailed discussion of the results is presented in the following sections.

5.1.2 Effect of Water to Cement Ratio

As discussed in the literature review, cement hydration will result in a reduction of the relative humidity within the paste, which is also known as self-desiccation. And this is the major driving force of autogenous shrinkage. With HPC with a low w/cm, the low

permeability inhibited the water transfer from outside the paste which results in more reduction in relative humidity. Therefore, autogenous shrinkage increases with a decrease of w/cm. Figure 5.2 shows the results of autogenous deformation of neat pastes with water to cement of 0.32, 0.37 and 0.42.

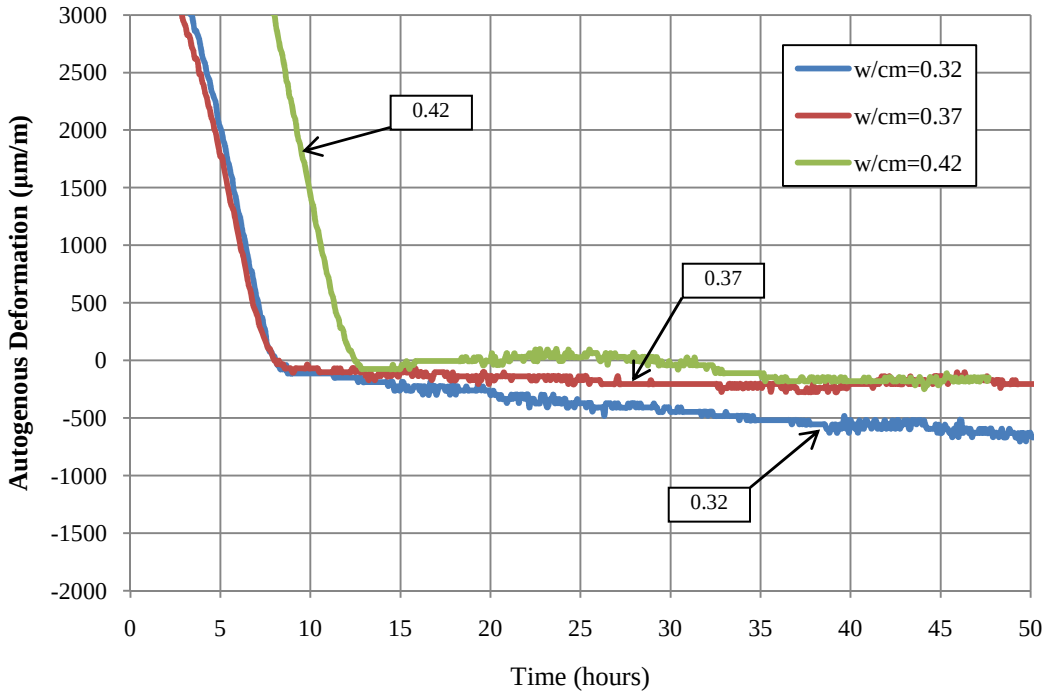

Figure 5.2: Effect of w/cm on autogenous deformation (Neat paste at 20°C)

From the figure above, the trend of autogenous shrinkage between different w/cm neat pastes is noticeable. The 0.32 w/cm neat paste sample showed the highest shrinkage of 630 μm/m, and 0.42 w/cm neat pastes showed 148 μm/m. As discussed previously, the autogenous deformation is closed related to relative humidity change. With a lower w/cm, the pore structure in the paste becomes denser and more isolated, resulting in a more severe relative humidity drop during hydration. Therefore, samples with 0.32 w/cm in this test showed the highest shrinkage values.

The 0.42 w/cm sample shows the least amount of autogenous shrinkage and actually exhibits a minor amount of expansion right after the final set. The expansion within the

first day for cement paste with a 0.40 w/cm or higher were also observed by other researchers. (*Bjøntegaard 1999, Lura 2003, Wei 2009*) One possible explanation for this early age expansion is the reabsorption of bleeding water in samples with a higher w/cm. (*Lura et al. 2001*) It has been observed the by removing the bleeding water, the initial expansion was reduced yet not completely eliminated. (*Bjøntegaard 1999*) Some other researchers attributed the initial expansion to ettringite formation. (*Bentz et al. 2001, Wei 2009*) The initial expansion might be a result of the competition between expansive mechanisms which cause early-age expansion and shrinkage caused by self-desiccation. It is also noticeable that the autogenous deformation was delayed in the 0.42 w/cm neat paste sample. It can be explained that water supply remains sufficient in samples with higher w/cm, the reduction of relative humidity happens later than in low w/cm samples.

5.1.3 Effect of SCMs

In this research, two SCMs, class F fly and silica fume, were replaced for OPC at ratios of 30% and 4% respectively. Figure 5.3 shows the results of samples of different SCMs incorporation with 0.37 w/cm at 20 °C isothermal curing.

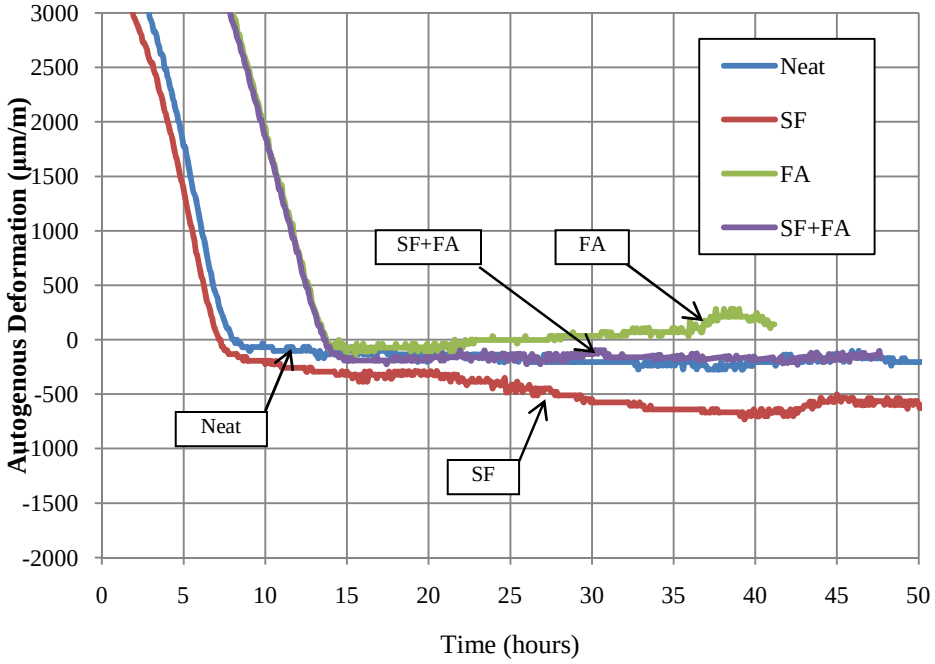

Figure 5.3: Effect of SCMs on autogenous deformation (0.37 w/cm at 20°C)

It was observed that the autogenous shrinkage increased significantly with the presence of silica fume. In general, silica fume increases the water demand in a concrete mixture and contributes to a stiffened and sticky consistency of the concrete mixture. (*PCA 2002*) This is because the surface area of silica fume particles is 50 times larger than cement particles. This also causes an increased capillary tension in the paste matrix. The silica fume particles are also much finer (Φ<0.1μm) than cement and other SCMs, therefore much smaller pores are created in mixtures with silica fume. As discussed in section 2.3.1 (Figure 2.6), pores with radius less than 50 nm can collapse as pore solution leaves these pores during hydration to hydrate adjacent cement grains. Therefore, more autogenous shrinkage was observed. This was also reported by several other researchers. (*Jensen and Hansen 1996, Lura and Jensen 2005, Slatnick et al. 2011*)

Figure 5.3 also shows that the presence of fly ash decreases the autogenous shrinkage, by showing a slight expansion in 2 days. In general, due to its spherical particle shape and glassy texture, the addition of fly ash reduces the water demand for a given concrete consistency. (*Mehta and Monteiro 2006*) This effect is similar to the effect of mixtures with higher w/cm. The expansion is likely due to that the weak solid paste skeleton cannot hold the formation of ettringite needled inside. Some other reported that the expansion is due to the expansive agent (MgO) in the fly ash. (*Liu and Fang 2006*) However, according to *ACI Report on Early-Age Cracking (ACI Committee 231 2010)*, in previous research, fly ash has been found have a variable influence on autogenous deformation. An investigation (*Setter and Roy 1978*) showed that fly ash has no significant effects on the autogenous shrinkage. Another research showed that the influence of fly ash depends on the fineness and replacement ratio of fly ash. Larger autogenous shrinkage was found when the fly ash with finer average particles was incorporated. Furthermore, a lower replacement ratio (25%) resulted in a much higher autogenous shrinkage than control mix, while a higher replacement ratio (50%) resulted in smaller shrinkage than control mix. (*Termkhajornkit et al. 2005*)

It is also quite interesting to find out that, in the current research, based on the materials tested herein, the increase of autogenous shrinkage induced by 4% replacement of silica fume was completely offset by 30% replacement of class F fly ash.

5.1.4 Effect of SRA

Generally, the application of a shrinkage reducing admixture reduces strain related to shrinkage in concrete, thereby reducing the risk for early-age cracking. SRA's work by reducing the surface tension of free water in pores results in the reduction of the capillary pressure, which is believed the most influencing mechanism of SRAs. Therefore, autogenous shrinkage is mitigated due to fewer pores are closed by lowered capillary pressure. Figure 5.4 shows that with the addition of 2% SRA expansion was registered up to 50 hours.

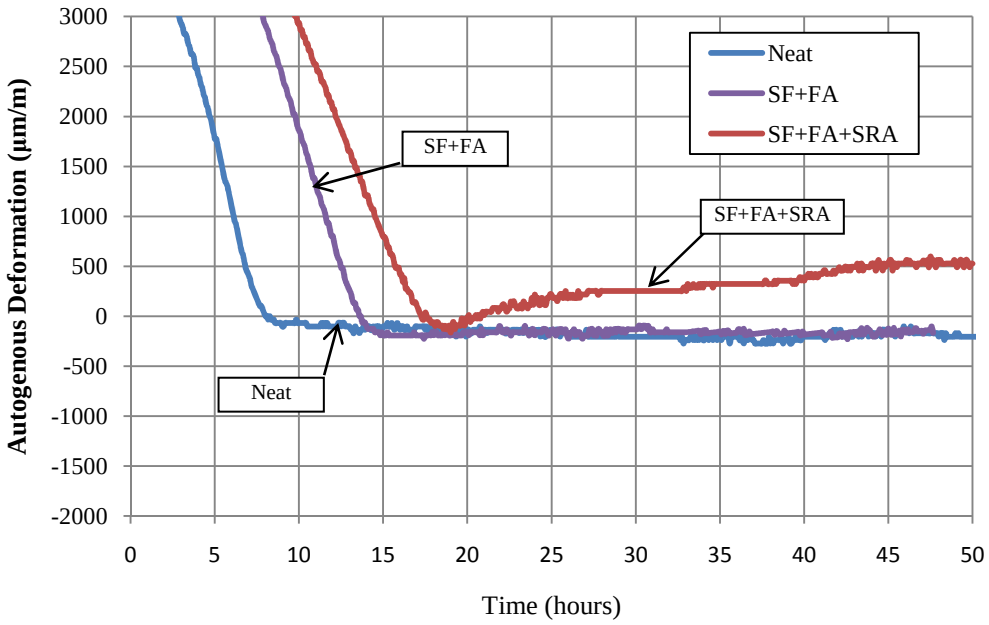

Figure 5.4: Effect of SRAs on autogenous deformation (0.37 w/cm at 20°C)

Other researchers also demonstrated that HPC containing an SRA showed reduction in autogenous shrinkage. (*Bentz et al. 2001, Rongbing and Jian 2005, Slatnick et al. 2011, Weiss 1999*) In addition, it is noticed that, the combination of fly ash and SRA delayed the autogenous shrinkage even further than fly ash alone. However, in the further

research of assessing SRA as a shrinkage cracking mitigation strategy, those effects should also be taken account.

5.2 CAC RESUTLS AND ANALYSIS

5.2.1 Setting Time

Figure 5.5 shows a summary of the setting time of CAC systems using the Vicat needle apparatus.

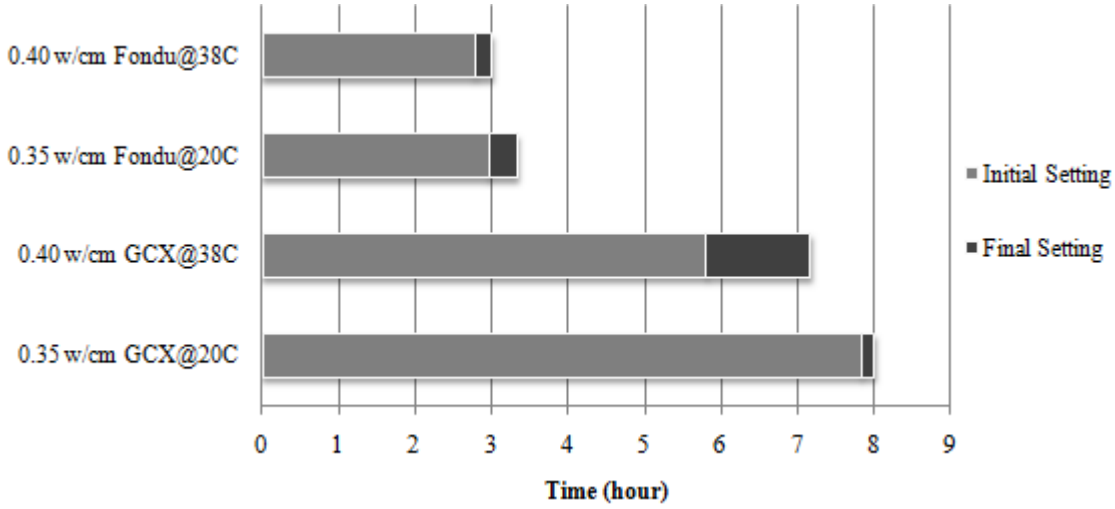

Figure 5.5: Vicat setting time results for CAC systems

The time period from initial set to final set of CAC is only 10 to 20 minutes, much less compared to the OPC systems studied. Also a significant amount of heat was generated (characteristic of CACs) during the testing. As a result ice was added to the water bath to better control the sample temperature within ±1°C of the desired isothermal temperature. While the GCX sample cured at 38°C seemed to have a longer period of setting which was about 1.3 hours. The GCX sample needs much longer time to set than Fondu sample. This is because the CA phase in these two types of CAC is not the same. In the GCX sample, nucleation is difficult in the absence of nucleation sites such as edges of sand or rock grains or chemical admixtures. (*Banfill 1995*) In the field, he setting time of CAC

concrete can be very well controlled by accelerator and retarder. In addition, the presence of aggregates provides nucleation sites to reduce the setting time.

5.2.2 Results and Analysis

Figure 5.6 shows the autogenous deformation testing results for CAC systems cured under difference temperatures. The zero strain for all autogenous deformation curves was set to be the point where they diverge from the chemical shrinkage curve.

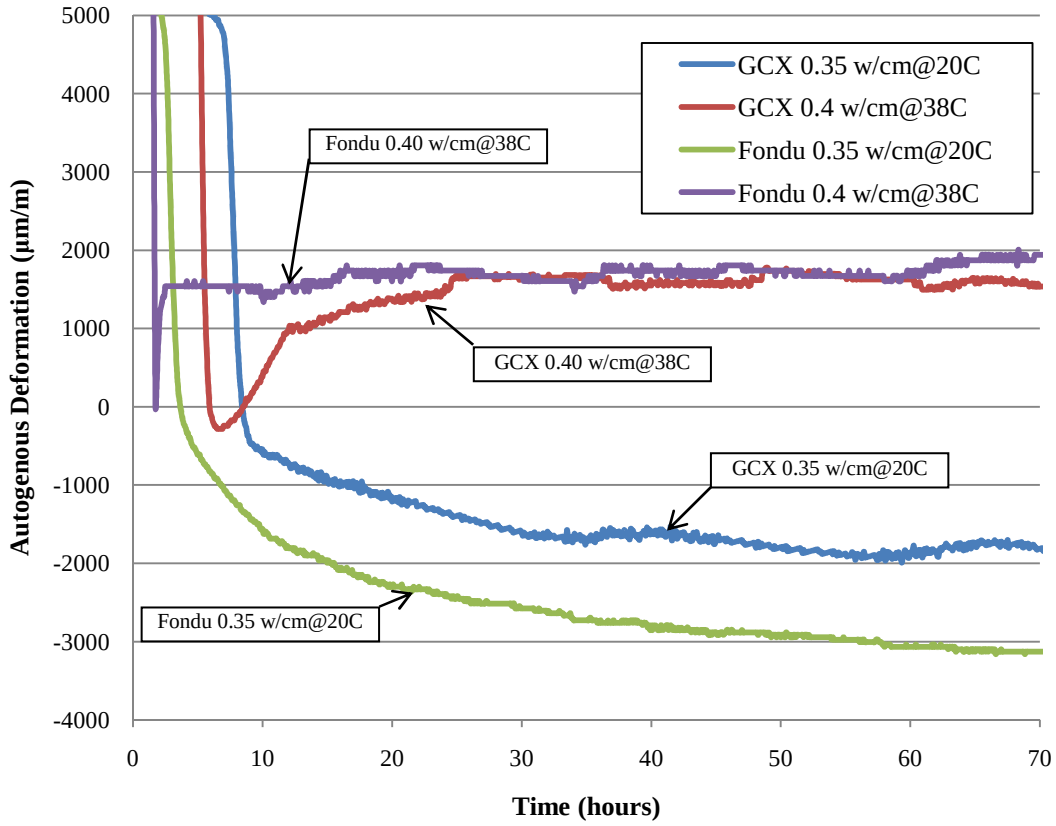

Figure 5.6: Autogenous deformation, GCX and Fondu

It is quite interesting to observe that under different isothermal temperatures, the autogenous deformation of CAC systems is very different. At lower temperatures (20°C), shrinkage was recorded throughout the entire experiment, while expansion was observed at higher isothermal temperature (38°C). Although exact knowledge behind this phenomenon is still unknown, it is believed that the expansion is related to the

conversion. Similar results were observed by Ideker (2008) using a free deformation frame described in section 2.3.2.3. Other similar findings were also reported when CAC were used as dental materials in Europe. (*Kraft et al. 2004*)

Compared to OPC systems, autogenous deformation of CAC systems are significantly greater under isothermal conditions. However, in the field, the CAC concrete shows no particular problem in cracking. One possible reason is that in the field isothermal conditions do not exist and the material goes through a realistic time-temperature history where a mixture of different hydrates is formed. The bulk CAC concrete may be achieved higher than ambient temperatures due to rapid heat liberation in the early–age (e.g. first 24 hours). A field study showed that CAC concrete slabs exhibited expansive strain commensurate with temperature generation and during the timer period investigated the slabs stayed in a state of positive strain therefore not reaching a point of shrinkage. (*Ideker 2008*) In addition, with a rapid strength gain in the early-age, CAC concrete may be more crack resistant than comparable OPC concrete which gains strength much more slowly. Clearly more investigation is needed to characterize the dimensional stability of CAC systems under both isothermal and realistic time-temperature histories.

5.3 CONCLUSIONS

Autogenous deformation results and analysis were presented in this chapter, and several important conclusions were drawn:

- In OPC systems, autogenous shrinkage increased with a decrease of w/cm. Neat paste samples with a w/cm greater than 0.40 exhibit expansion during the first 24 hours after casting;
- For the particular ODOT standard HPC mixture design with 30% class F fly ash and 4% silica fume, the increase of autogenous shrinkage induced by silica fume was completely offset by replacement of class F fly ash. The overall shrinkage of this particular ternary blend paste was similar to neat paste;

- In OPC systems, the presence of fly ash and SRA postponed the development of autogenous shrinkage, and prolonged the setting time;
- The addition of SRA in OPC systems induced expansion in autogenous deformation testing;
- In CAC systems, at lower temperature (20°C), shrinkage was observed, The recorded deformations were generally 5 to 10 times larger than OPC system. Expansion was recorded if cured at higher temperature (38°C).

6 CONCLUSIONS

6.1 SUMMARY

Significant studies in the laboratory and in field applications have demonstrated that internal curing by LFWA is an effective way to mitigate early-age cracking in high performance concrete bridge decks. The major task of this research effort was to characterize the chemical shrinkage value as one important factor in determining the optimum replacement ratio of LWFA in the mixture. Autogenous deformation of paste systems was also investigated.

Early-age volume change, specifically chemical shrinkage and autogenous deformation, of high performance cementitious systems (OPC and CAC systems) was investigated. A standard ASTM C1608 was applied to perform chemical shrinkage testing, and a membrane method was adopted to perform autogenous deformation testing. The investigation included the effect of SCMs (class F fly ash and silica fume) and the effect SRA. The autogenous deformation and setting time of OPC systems as well as CAC systems was also evaluated.

In addition, X-ray diffraction analysis was performed along with chemical shrinkage tests on calcium aluminate cement (GCX binder) to verify the potential application of chemical shrinkage as a predictive tool for conversion.

6.2 CONCLUSIONS

The primary findings from this research provided a contribution to existing literature on autogenous deformation and chemical shrinkage on ternary OPC systems as well as CAC systems. Also, most information on chemical shrinkage will be used to further the goal of finding the optimum replacement of LWFA for internal curing in the project. These findings are summarized in the following page:

- Based on series of observed data, a model was adopted and verified to estimate ultimate chemical shrinkage value for OPC system. The adopted model was capable of predicting ultimate chemical shrinkage value for OPC systems with SCMs and/or SRA;

- SCMs generally decreased chemical shrinkage values although the impact observed was not significant. The presence of SCMs also delayed the chemical shrinkage development;

- Including SRA in the OPC system increased chemical shrinkage for mixtures with w/cm in the range of 0.32 to 0.42, but this effect was eliminated when w/cm increases up to 0.5 and more. The presence of SRA also delayed the development of chemical shrinkage;

- Chemical shrinkage for CAC pastes was 2 to 3 times greater than that of OPC systems due to the complete different hydration mechanism;

- XRD was a useful tool to verify conversion in CAC systems, and chemical shrinkage can be used as a predictor of the conversion process for CAC systems cured under isothermal condition;

- For autogenous deformation testing, the Vicat setting time was not an accurate test to determine the zero strain point. The point when the autogenous deformation curve diverged from chemical shrinkage curve was a better reference as a “zero” point;

- For the particular ODOT standard HPC mixture design with 30% class F fly ash and 4% silica fume, the increase of autogenous shrinkage induced by silica fume was completely offset by replacement of class F fly ash. The addition of SRA was also shown to induce expansion in the autogenous deformation test, and;

- In CAC systems cured at lower temperature (20°C), shrinkage was observed, while expansion was observed at higher temperature (38°C). The recorded deformation was significantly higher than OPC systems.

6.3 FUTURE WORK

The following are recommendations for future work related to chemical and autogenous shrinkage testing in high performance cementitious systems:

- Use ultimate chemical shrinkage values predicted by the adopted model in the Bentz equation. Verify the effectiveness in determining the optimum LWFA replacement ratio through laboratory testing on concrete and field verification;
- Develop and verify the proposed chemical shrinkage testing system for expansive cementitious systems;
- Extend the autogenous deformation test to OPC mortars/concrete with or without LWFA. Compare and verify the effectiveness of internal curing provided by LWFA, and;
- Further verify the chemical shrinkage used as a predictor of conversion process for CAC systems, by testing Ciment Fondu and GCX cured under higher temperatures (55°C and 65°C). The ultimate goal would be to develop a tool/model to predict conversion and strength parameters using the curing temperature history.

BIBLIOGRAPHY

ACI Committee 116, Cement and Concrete Terminology. Farmington Hills, Mich.: American Concrete Institute, 2000.

ACI Committee 231, Report on Early-Age Cracking: Causes, Measurement, and Mitigation. Farmington Hills, Mich.: American Concrete Institute, 2010.

P.-C. Aitcin, "Autogenous Shrinkage Measurement," *Proc., Autoshrink '98: International Workshop on Autogenous Shrinkage of Concrete,* Hiroshima, Japan, 1988, pp. 245 - 256.

A. Al-Manaseer and S. Ristanovic, "Predicting Drying Shrinkage of Concrete," *Concrete International,* vol. 26, pp. 79-83, 2004.

ASTM C157: Standard Test Method for Length Change of Hardened Hydraulic-Cement Mortar and Concrete, ASTM International, 2006.

ASTM C305: Standard Practice for Mechanical Mixing of Hydraulic Cement Pastes and Mortars of Plastic Consistency, ASTM International ASTM C 305, 2006.

ASTM C618: Standard Specification for Coal Fly Ash and Raw or Calcined Natural Pozzolan for Use in Concrete, ASTM International, 2009.

ASTM C1579: Standard Test Method for Evaluating Plastic Shrinkage Cracking of Restrained Fiber Reinforced Concrete (Using a Steel Form Insert), ASTM International, 2006.

ASTM C1581: Standard Test Method for Determining Age at Cracking and Induced Tensile Stress Characteristics of Mortar and Concrete under Restrained Shrinkage, ASTM International, 2004.

ASTM C1608: Standard Test Method for Chemical Shrinkage of Hydraulic Cement Paste, ASTM International, 2005.

ASTM C1698: Standard Test Method of Autogenous Deformation, ASTM International, 2009.

C. D. Atiş, "High-Volume Fly Ash Concrete with High Strength and Low Drying Shrinkage," *Journal of Materials in Civil Engineering,* pp. 153-156, 2003.

K. Babaei and A. M. Fouladgar, "Solutions to Concrete Bridge Deck Cracking," *Concrete International,* vol. 19, pp. 34-37, 1997.

P. F. G. Banfill, "Superplasticizers for Ciment Fondu. Part 2: Effects of temeprature on the hydration reactions," *Advances in Cement Research,* vol. 7, pp. 151-157, October 1995.

A. Bentur, "Early age Cracking in Cementitious Systems," RILEM Committee 181 EAS, 2003.

D. Bentz, O. Hansen, K. Jensen, J. Olesen, H. Stang, and C. Haecker, "Influence of Cement Particle-Size Distribution on Early Age Autogenous Strains and Stresses in Cement-Based Materials," *Journal of the American Ceramic Society,* vol. 84, pp. 129-135, 2001.

D. Bentz, "Curing with Shrinkage-Reducing Admixtures," *Concrete International,* vol. 27, pp. 55-60, 2005.

D. Bentz, H. Kim, D. Mokarem, F. Rodriguez, P. Lura, and J. Weiss, "ACI 2009 Spring Convention-Early-Age Test Methods," March 17, 20092009.

D. P. Bentz and K. A. Snyder, "Protected Paste Volume in Concrete: Extension to Internal Curing Using Saturated Lightweight Fine Aggregate," *Cement and Concrete Research,* vol. 29, pp. 1863-1867, 1999.

D. P. Bentz, M. R. Geiker, and K. K. Hansen, "Shrinkage-Reducing Admixtures and Early-Age Desiccation in Cement Pastes and Mortars," *Cement and Concrete Research,* vol. 31, pp. 1075-1085, 2001.

D. P. Bentz, P. Lura, and J. W. Roberts, "Mixture Proportioning for Internal Curing," *Concrete International,* vol. 27, pp. 35-40, 2005.

D. P. Bentz, "Influence of Shrinkage-Reducing Admixtures on Early-Age Properties of Cement Pastes," *Journal of Advanced Concrete Technology,* vol. 4, pp. 423-429, 2006.

D. P. Bentz, "Internal Curing of High-Performance Bended Cement Mortar," *ACI Materials Journal,* vol. 104, pp. 408-414, 2007.

D. P. Bentz, "Curing Concrete from Inside Out," ESCSI Special Workshop, May 7, 2008.

D. P. Bentz and S. Remond, "Incorporation of Fly Ash into a #-D Cement Hydration Microstructure Model," *NISTIR 6050, U.S. Department of Commerce,* p. 48pp, Aug. 1997.

S. Bishnoi, "Automated Chemical Shrinkage Test and Shrinkage Suite Software," ed, 2009.

B. Bissonnette, P. Pierre, and M. Pigeon, "Influence of Key Parameters on Drying Shrinkage of Cementitious Materials," *Cement and Concrete Research,* vol. 29, pp. 1655-1662, 1999.

O. Bjøntegaard, "Thermal Dilation and Autogenous Deformation as Driving Forces to Self-Induced Stresses in High Performance Concrete," Division of Structural Engineering, The Norwegian University of Science and Technology, 1999.

S. Boivin, P. Acker, S. Rigaud, and B. Clavaud, "Experimental Assessment of Cemical Shrinkage of Hydrating Cement Paste," *Autoshrink '98 Proceedings of the International Workshop on Autogenous Shrinkage of Concrete*, 1998, pp. 77-88.

M. Bouasker, P. Mounanga, P. Turcry, A. Loukili, and A. Khelidj, "Chemical Shrinkage of Cement Pastes and Mortars at Very Early Age: Effect of Limestone Filler and Granular Inclusions," *Cement and Concrete Composites*, vol. 30, pp. 13-22, 2008.

M. D. Brown, C. A. Smith, J. G. Sellers, K. J. Folliard, and J. E. Breen, "Use of Alternative Materials to Reduce Shrinkage Cracking in Bridge Decks," *ACI Materials Journal*, vol. 104, pp. 629-637, November 1, 2007.

J. Castro, De la Varga, I., Golias, M., and Weiss, W. J. , "Extending Internal Curing Concepts to Mixtures Containing High Volumes of Fly Ash," *International Bridge Conference*, 2010.

P.-W. Chen and D. D. L. Chung, "Low-Drying-Shrinkage Concrete Containing Carbon Fibers," *Composites Part B: Engineering*, vol. 27, pp. 269-274, 1996.

Concrete Q&A, "Estimating Evaporation Rates to Prevent Plastic Shrinkage Cracking," *Concrete International*, vol. 29, pp. 80-82, 2007.

Concrete Society Technical Report, "Calcium Aluminate Cements in Construction: A Reassessment," ed: Concrete Society, 1997, p. 63.

M. Costoya, "Effect of Particle Size on the Hydration Kinetics and Microstructural Development of Tricalcium Silicate," Doctoral Thesis, Thesis No 4102, EPFL, Lausanne, Switzerland, 2008.

D. Cusson, "Effect of Blended Cements on Effectiveness of Internal Curing of HPC," *ACI*, vol. SP-256, pp. 105-120, 2008.

D. Cusson and T. Hoogeveen, "Internal Curing of High-Performance Concrete with Pre-soaked Fine Lightweight Aggregate for Prevention of Autogenous Shrinkage Cracking," *Cement and Concrete Research*, vol. 38, pp. 757-765, 2008.

H. E. Davis, "Autogenous Volume Change of Concrete," *Proceedings of the 43rd Annual American Society for Testing Materials, Atlantic City, NJ, June*, 1940, pp. 1103-1112.

A. Durán-Herrera, P.-C. Aïtcin, and N. Petrov, "Effect of Saturated Lightweight Sand Substitution on Shrinkage in 0.35 w/b Concrete," *ACI Materials Journal*, vol. 104, pp. 48-52, 2007.

A. Durán-Herrera, N. Petrov, O. Bonneau, K. Khayat, and P.-C. Aïtcin, "Autogenous Control of Autogenous Shrinkage," *ACI*, vol. SP-256, pp. 1-12, 2008.

X. Feng, D. P. Bentz, and P. E. Stutzman, "Experimental Studies of Portland Cement/Slag Hydration," *Presentation at the 102nd Annual Meeting of the American Ceramic Society, St. Louis, Mo.*, 2000.

K. J. Folliard and N. S. Berke, "Properties of High-Performance Concrete Containing Shrinkage-Reducing Admixture," *Cement and Concrete Research*, vol. 27, pp. 1357-1364, 1997.

T. Friggle and D. Reeves, "Internal Curing of Concrete Paving: Laboratory and Field Experience," *ACI*, vol. SP-256, pp. 71-80, 2008.

Z. Grasley and D. Lange, "Thermal Dilation and Internal Relative Humidity of Hardened Cement Paste," *Materials and Structures*, vol. 40, pp. 311-317, 2007.

P. W. Gruner and G. A. Plain, "Type K Shrinkage-Compensating Cement in Bridge Deck Concrete," *Concrete International*, vol. 15, pp. 44-47, 1993.

T. A. Hammer, "High Strength LWFA Concrete with Silica Fume – Effect of Water Content in the LWFA on Mechanical Properties," *Supplementary Papers of the 4th CANMET/ACI International Conference on Fly Ash, Silica Fume, Slag and Natural Pozzolans in Concrete*, Istanbul, Turkey, , 1992, pp. 314-330.

R. Henkensiefken, P. Briatka, D. Bentz, T. Nantung, and J. Weiss, "Plastic Shrinkage Cracking in Internally Cured Mixtures Made with Pre-wetted Lightweight Aggregate," *Accepted by Concrete International*, 2009.

R. Henkensiefken, J. Castro, H. Kim, D. Bentz, and J. Weiss, "Internal Curing Improves Concrete Performance throughout its Life," *Concrete InFocus*, vol. 8, pp. 22-30, 2009.

P. C. Hewlett, Lea's Chemistry of Cement and Concrete, Fourth ed. Oxford, UK: Elsevier, Ltd., 1998.

X. Huo and L. U. Wong, "Early-Age Shrinkage of HPC Decks under Different Curing Methods," Philadelphia, Pennsylvania, USA, 2000, pp. 168-168.

J. H. Ideker, "Early-Age Behavior of Calcium Aluminate Cement Systems," Thesis(PhD), University of Texas, Austin, 2008.

O. Jensen, "Dilatometer-Further Development," Building Materials Laboratory, The Technical University of Denmark Lyngby, Denmark, 1996.

O. M. Jensen and P. F. Hansen, "Autogenous Deformation and Change of Relative Humidity in Silica Fume Modified Cement Paste," *ACI Materials Journal*, vol. 28, pp. 539-543, Nov.-Dec., 1996 1996.

O. M. Jensen and P. F. Hansen, "Autogenous Deformation and RH-Change in Perspective," *Cement and Concrete Research*, vol. 31, pp. 1859-1865, 2001.

H. Justnes, E. J. Sellevold, B. Reyniers, D. V. Loo, A. V. Gemert, F. Verboven, and D. V. Gemert, "The Influence of Cement Characteristics on Chemical Shrinkage,"

Autoshrink '98 Proceedings of the International Workshop on Autogenous Shrinkage of Concrete, 1998, pp. 71-80.

H. Justnes, F. Clemmens, P. Depuydt, D. Van Gemert, and E. J. Sellevold, "Correlating the Deviation Point Between Extrenal and Total Chemical Shrinakge with Setting Time and Other Characteristics of Cement Pastes," *Shrinkage 2000 - International RILEM Workshop on Shrinkage of Concrete*, Paris, France, 2000, pp. 57-73.

M. I. Khan, C. J. Lynsdale, and P. Waldron, "Porosity and strength of PFA/SF/OPC ternary blended paste," *Cement and Concrete Research*, vol. 30, pp. 1225-1229, 2000.

S. H. Kosmatka, B. Kerkhoff, and W. C. Panarese, Design and Control of Concrete Mixtures, 14th edition ed. Skokie, Illinois: Portland Cement Association, 2002.

K. Kovler and O. M. Jensen, "Novel Techniques for Concrete Curing," *Concrete International*, vol. 27, pp. 39-42, 2005.

L. Kraft, H. Engqvist, and L. Hermansson, "Early-Age Deformation, Drying Shrinkage and Thermal Dilation in A New Type of Dental Restorative Material Based on Calcium Aluminate Cement," *Cement and Concrete Research*, vol. 34, pp. 439-446, 2004.

B. Kumar, G. K. Tike, and P. K. Nanda, "Evaluation of Properties of High-Volume Fly-Ash Concrete for Pavements," *Journal of Materials in Civil Engineering*, vol. 19, pp. 906-911, 2007.

H. La Chatelier, "Sur les Changements de Volume qui Accompagent le durcissement des Ciments," *Bulletin Societe de l'Encouragement pour l'Industrie Nationale*, vol. Seme Serie, 1900.

S.-T. Lin and R. Huang, "Effect of Viscosity Modifying Agent on Plastic Shrinkage Cracking of Cementitious Composites," *Materials and Structures*, vol. 43, pp. 651-664, 2010.

S. Liu and K. Fang, "Study on Autogenous Deformation of Concrete Incorporating MgO as Expansive Agent," *Key Engineering Materials*, vol. 302-303, pp. 155-161, Jan, 2006.

P. Lura, K. van Breugel, and I. Maruyama, "Effect of Curing Temperature and Type of Cement on Early-Age Shrinkage of High-Performance Concrete," *Cement and Concrete Research*, vol. 31, pp. 1867-1872, 2001.

P. Lura, Autogenous Deformation and Internal Curing of Concrete. Delft: DUP Science, 2003.

P. Lura and O. M. Jensen, "Volumetric Measurement in Water Bath - An Inappropriate Method to Measure Autogenous Strain of Cement Paste," PCA R&D Serial No. 29252005.

P. Lura and O. Jensen, "Measuring Techniques for Autogenous Strain of Cement Paste," *Materials and Structures,* vol. 40, pp. 431-440, 2007.

P. Lura, B. Pease, G. B. Mazzotta, F. Rajabipour, and J. Weiss, "Influence of Shrinkage-Reducing Admixtures on Development of Plastic Shrinkage Cracks," *ACI Materials Journal,* vol. 104, pp. 187-194, 2007.

P. Lura, J. Couch, O. M. Jensen, and J. Weiss, "Early-age Acoustic Emission Measurements in Hydrating Cement Paste: Evidence for Cavitation During Solidification due to Self-Desiccation," *Cement and Concrete Research,* vol. 39, pp. 861-867, 2009.

P. K. Mehta and P. J. M. Monteiro, Concrete: Microstructure, Properties, and Materials, 3 ed. New York: McGraw-Hill, 2006.

J. Mora-Ruacho, R. Gettu, and A. Aguado, "Influence of Shrinkage-Reducing Admixtures on the Reduction of Plastic Shrinkage Cracking in Concrete," *Cement and Concrete Research,* vol. 39, pp. 141-146, 2009.

P. Mounanga, A. Khelidj, A. Loukili, and V. Baroghel-Bouny, "Predicting Ca(OH)2 Content and Chemical Shrinkage of Hydrating Cement Pastes Using Analytical Approach," *Cement and Concrete Research,* vol. 34, pp. 255-265, 2004.

M. Newlands, A. Paine, A. Vemuri, and K. Dhir, "A Linear Test Method for Determining Early-Age Shrinkage of Concrete," *Magazine of Concrete Research,* vol. 60, pp. 747-757, 2008.

A. H. Nilson, D. Darwin, and C. W. Dolan, Design of Concrete Structures 13th Edition. New York: McGraw Hill, 2004.

P. Paulini, "A Weighing Method for Cement Hydration," presented at the 9th International Congress on the Chemistry of Cement New Delhi, India, 1992.

PCA, "Supplementary Cementing Materials for Use in Concrete," P. C. Association, Ed., ed. Skokie, Illinoise, 2002.

S. Peethamparan, E. Weissinger, J. Vocaturo, J. Zhang, and G. Scherer, "Monitoring Chemical Shrinkage Using Pressure Sensors," in *Special Publication* vol. 270, ed: ACI, 2010, pp. 77-88.

T. C. Powers, "Absorption of Water by Portland Cement Paste During the Hardening Process," *Industrial and Engineering Chemistry,* vol. 27, pp. 790-794, 1935.

C. Qi, J. Weiss, and J. Olek, "Characterization of Plastic Shrinkage Cracking in Fiber Reinforced Concrete Using Image Analysis and A Modified Weibull Function," *Materials and Structures,* vol. 36, pp. 386-395, 2003.

A. Radlinska, F. Rajabipour, B. Bucher, R. Henkensiefken, G. Sant, and J. Weiss, "Shrinkage Mitigation Strategies in Cementitious Systems: A Closer Look at Differences in Sealed and Unsealed Behavior," *Transportation Research Record: Journal of the Transportation Research Board,* vol. 2070, pp. 59-67, 2008.

A. Ramniceanu, R. E. Weyers, D. W. Mokarem, and M. M. Sprinkel, "Bridge Deck Concrete Volume Change," Virginia Transportation Research Council, Charlottesville, VA.2010.

K. A. Riding, J. L. Poole, A. K. Schindler, M. C. G. Juenger, and K. J. Folliard, "Quantification of Effects of Fly Ash Type on Concrete Early-Age Cracking," *ACI Materials Journal,* vol. 105, pp. 149-155, 2008.

RILEM Committee 119, Prevention of Thermal Cracking in Concrete at Early Ages. London and New York: E & FN Spon, 1998.

J. W. Roberts, "Internal Curing in Pavements, Bridge Decks and Parking Structures, Using Absorptive Aggregates to Provide Water to Hydrate Cement not Hydrated by Mixing Water," *Proceedings of the 83rd Annual Meeting of the Transportation Research Board,* Washington, D.C., 2004.

B. Rongbing and S. Jian, "Synthesis and Evaluation of Shrinkage-Reducing Admixture for Cementitious Materials," *Cement and Concrete Research,* vol. 35, pp. 445-448, 2005.

E. Sakai, S. Miyahara, S. Ohsawa, S.-H. Lee, and M. Daimon, "Hydration of Fly Ash Cement," *Cement and Concrete Research,* vol. 35, pp. 1135-1140, 2005.

J. Saliba, E. Rozière, F. Grondin, and A. Loukili, "Influence of Shrinkage-Reducing Admixtures on Plastic and Long-Term Shrinkage," *Cement and Concrete Composites,* vol. 33, pp. 209-217, 2011.

G. Sant, P. Lura, and J. Weiss, "Measurements of Volume Change in Cementitious Materials at Early Ages: Review of Testing Protocols and Interpretation of Results," *Transportation Research Record: Journal of the Transportation Research Board,* pp. 21-29, 2006.

K. L. Scrivener and A. Capmas, "Lea's Chemistry of Cement and Concrete," in *Calcium Aluminate Cements,* P. C. Hewlett, Ed., Fourth ed New York and Toronto: Arnold, 1998, p. 69.

K. L. Scrivener, J.-L. Cabiron, and R. Letourneux, "High-Performance Concretes from Calcium Aluminate Cements," *Cement and Concrete Research,* vol. 29, pp. 1215-1223, 1999.

N. Setter and D. M. Roy, "Mechanical Features of Chemical Shrinkage of Cement Paste," *Cement and Concrete Research,* vol. 8, pp. 623-634, 1978.

S. Slatnick, K. A. Riding, K. J. Folliard, M. C. G. Juenger, and A. K. Schindler, "Evaluation of Autogenous Deformation of Concrete at Early Ages," *ACI Materials Journal,* vol. 108, pp. 21-28, January 1, 2011 2011.

H. Sleiman, A. Perrot, and S. Amziane, "A New Look at the Measurement of Cementitious Paste Setting by Vicat Test," *Cement and Concrete Research,* vol. 40, pp. 681-686, 2010.

L. Snell and A. Munir. (2009, 2/1/2011). *Evaluating Concrete Curing Conditions*. Available: http://construction.asu.edu/cim/curing/curingfirstpage.htm

R. Springenschmid, Prevention of Thermal Cracking in Concrete at Early Ages: State-of-the-Art Report Prepared by RILEM Technical Committee 119, Avoidance of Thermal Cracking in Concrete at Early Ages vol. 15. London: E & FN Spon, 1998.

E. Tazawa, Autogenous Shrinkage of Concrete : Proceedings of the International Workshop, Organized by JCI (Japan Concrete Institute), Hiroshima, June 13-14, 1998. New York: Routledge, 1999.

P. Termkhajornkit, T. Nawa, M. Nakai, and T. Saito, "Effect of Fly Ash on Autogenous Shrinkage," *Cement and Concrete Research*, vol. 35, pp. 473-482, 2005.

M. D. A. Thomas, M. H. Shehata, S. G. Shashiprakash, D. S. Hopkins, and K. Cail, "Use of ternary cementitious systems containing silica fume and fly ash in concrete," *Cement and Concrete Research*, vol. 29, pp. 1207-1214, 1999.

G. E. Troxell and H. E. Davis, Composition and Properties of Concrete. New York: MacGraw-Hill Book Co., 1956.

V. H. Villarreal, "Internal Curing - Real Word Ready Mix Production and Applications: A Practical Approach to Lightweight Modified Concrete," *ACI* vol. SP-256, pp. 45-56, 2008.

Y. Wei and W. Hansen, "Pre-soaked Lightweight Fine Aggregates as Additives for Internal Curing in Concrerte," *ACI*, vol. SP-256, pp. 35-44, 2008.

Y. Wei, "Modeling of Autogenous Deformation in Cementitious Materials, Restraining Effect from Aggregate, and Moisture Warping in Slabs on Grade," Doctor of Philosophy (Civil Engineering), Civil Engineering, University of Michigan, Ann Anbor, 2009.

W. J. Weiss, "Prediction of Early-Age Shrinkage Cracking in Concrete Elements," PhD Dissertation, Department of Civil and Environmental Engineering, Northwestern University, Evanston, IL, 1999.

K. T. Xiao, H. Q. Yang, and Y. Dong, "Study on the Influence of Admixture on Chemical Shrinkage of Cement Based Materials," *Key Engineering Materials*, vol. 405-406, pp. 226-233, 2009.

J. Yajun and J. Cahyadi, "Simulation of Silica Fume Blended Cement Hydration," *Materials and Structures*, vol. 37, pp. 397-404, 2004.

J. C. Yates, "Effect of Calcium Chloride Onreadings of A Volumeter Inclosing Portland Cement Pastes and on Linear Changes of Concrete," *Highway Research Board Proc.21*, pp. 294-304, 1941.

M.-H. Zhang, L. Li, and P. Paramasivam, "Shrinkage of High-Strength Lightweight Aggregate Concrete Exposed to Dry Environment," *ACI Materials Journal*, pp. 86-92, 2005.

APPENDIX A: MATERIAL CERTIFICATES

WYOMING ANALYTICAL LABORATORIES, INC.

14335 W. 44th Avenue
Golden, CO 80403

www.wal-lab.com
Email: walxray@aol.com

(303) 278-2446
Fax: (303) 278-2439

September 8, 2010

Kelsea Schwing
Oregon State University
220 Owen Hall
Corvallis, OR 97331

WAL #100898-2
Sample ID: Lafarge Type I/II Cement

CHEMICAL ANALYSIS
Wt%, as Rec'd Basis

Silicon Dioxide	SiO_2	20.51	
Aluminum Oxide	Al_2O_3	4.72	
Iron Oxide	Fe_2O_3	3.23	
Calcium Oxide	CaO	64.21	
Magnesium Oxide	MgO	0.80	
Sodium Oxide	Na_2O	0.30	
Potassium Oxide	K_2O	0.29	
Total Alkalies as Na_2O			0.49
Titanium Dioxide	TiO_2	0.23	
Manganic Oxide	Mn_2O_3	0.08	
Phosphorus Pentoxide	P_2O_5	0.07	
Strontium Oxide	SrO	0.17	
Barium Oxide	BaO	0.07	
Sulfur Trioxide	SO_3	2.70	
Loss on Ignition		2.62	
Insoluble Residue		0.21	
Tricalcium Silicate	C_3S	61.51	
Tricalcium Aluminate	C_3A	7.03	
Dicalcium Silicate	C_2S	12.40	
Tetracalcium Aluminoferrite	C_4AF	9.84	

*TiO_2 and P_2O_5 not included in Al_2O_3

Analysis per ASTM C 114

Charles R. Wilson,
Division Manager

MEMBER
ACIL

WYOMING ANALYTICAL LABORATORIES, INC.
14335 W. 44th Avenue
Golden, CO 80403
www.wal-lab.com
Email: walxray@aol.com
(303) 278-2446
Fax: (303) 278-2439

September 8, 2010

Kelsea Schwing
Oregon State University
220 Owen Hall
Corvallis, OR 973310

Denver Div. # 100898-1
Sample ID: Centralia Lafarge Class F Fly Ash

CHEMICAL ANALYSIS
WT%, DRY BASIS

Silicon Dioxide, SiO2	55.24	
Aluminum Oxide, Al2O3	15.77	
Iron Oxide, Fe2O3	6.27	
Total (SiO2 + Al2O3 + Fe2O3)		77.28
Calcium Oxide, CaO	10.20	
Magnesium Oxide, MgO	3.64	
Sodium Oxide, Na2O	3.64	
Potassium Oxide, K2O	2.08	
Titanium Dioxide, TiO2	0.94	
Manganese Dioxide, MnO2	0.12	
Phosphorus Pentoxide, P2O5	0.23	
Strontium Oxide, SrO	0.32	
Barium Oxide, BaO	0.62	
Sulfur Trioxide, SO3	0.70	
Loss on Ignition	0.23	
Moisture, as Received	0.05	

Analysis per ASTM C 311

Charles R. Wilson
Division Manager

MEMBER
ACIL

WYOMING ANALYTICAL LABORATORIES, INC.

14335 W. 44th Avenue
Golden, CO 80403

www.wal-lab.com
Email: walxray@aol.com

(303) 278-2446
Fax: (303) 278-2439

November 30, 2010

Tengfei Fu
Oregon State University
220 Owen Hall
Corvallis, OR 973310

Denver Div. # 101196-1
Sample ID: GCX CAC Nov 2

CHEMICAL ANALYSIS
WT%, DRY BASIS

Silicon Dioxide, SiO2	5.24	
Aluminum Oxide, Al2O3	52.61	
Iron Oxide, Fe2O3	2.10	
Total (SiO2 + Al2O3 + Fe2O3)		59.94
Calcium Oxide, CaO	35.99	
Magnesium Oxide, MgO	0.45	
Sodium Oxide, Na2O	0.06	
Potassium Oxide, K2O	0.38	
Titanium Dioxide, TiO2	2.18	
Manganese Dioxide, MnO2	0.05	
Phosphorus Pentoxide, P2O5	0.16	
Strontium Oxide, SrO	0.06	
Barium Oxide, BaO	0.04	
Sulfur Trioxide, SO3	0.04	
Loss on Ignition	0.66	
Moisture, as Received	0.00	

Analysis per ASTM C 311

Charles R. Wilson
Division Manager

MEMBER
ACIL

WYOMING ANALYTICAL LABORATORIES, INC.
14335 W. 44th Avenue
Golden, CO 80403
www.wal-lab.com
Email: wabray@aol.com
(303) 278-2446
Fax: (303) 278-2439

November 30, 2010

Tengfei Fu
Oregon State University
220 Owen Hall
Corvallis, OR 973310

Denver Div. # 101196-2
Sample ID: Fondu CAC Nov 2

CHEMICAL ANALYSIS
WT%, DRY BASIS

Silicon Dioxide, SiO_2	4.62	
Aluminum Oxide, Al_2O_3	40.25	
Iron Oxide, Fe_2O_3	15.15	
Total (SiO_2 + Al_2O_3 + Fe_2O_3)		60.02
Calcium Oxide, CaO	35.54	
Magnesium Oxide, MgO	0.76	
Sodium Oxide, Na_2O	0.14	
Potassium Oxide, K_2O	0.14	
Titanium Dioxide, TiO_2	1.71	
Manganese Dioxide, MnO_2	0.31	
Phosphorus Pentoxide, P_2O_5	0.15	
Strontium Oxide, SrO	0.03	
Barium Oxide, BaO	0.01	
Sulfur Trioxide, SO_3	0.16	
Loss on Ignition	1.03	
Moisture, as Received	0.00	

Analysis per ASTM C 311

Charles R. Wilson
Division Manager

MEMBER
ACIL

APPENDIX B: CHEMICAL SHRINKAGE TEST RESULTS

B.1 OPC CS TEST RESULTS

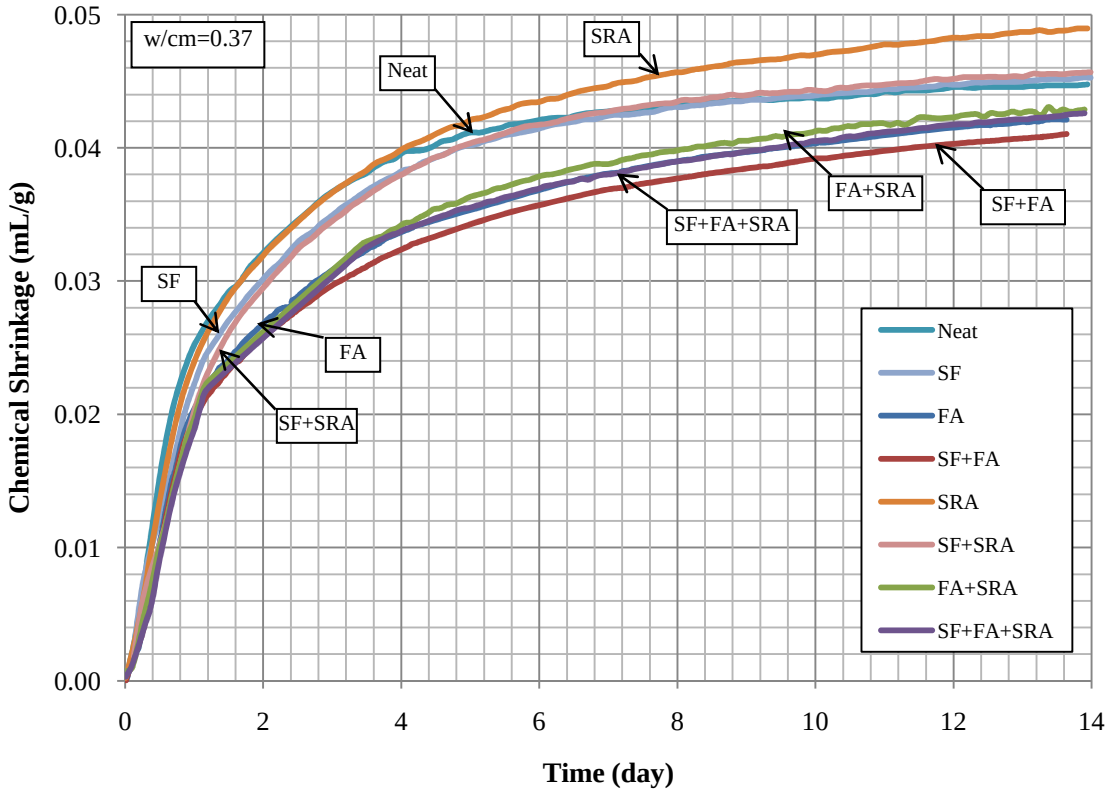

Figure B.1: Chemical shrinkage development curve, OPC w/cm=0.37 at 20 ºC isothermal

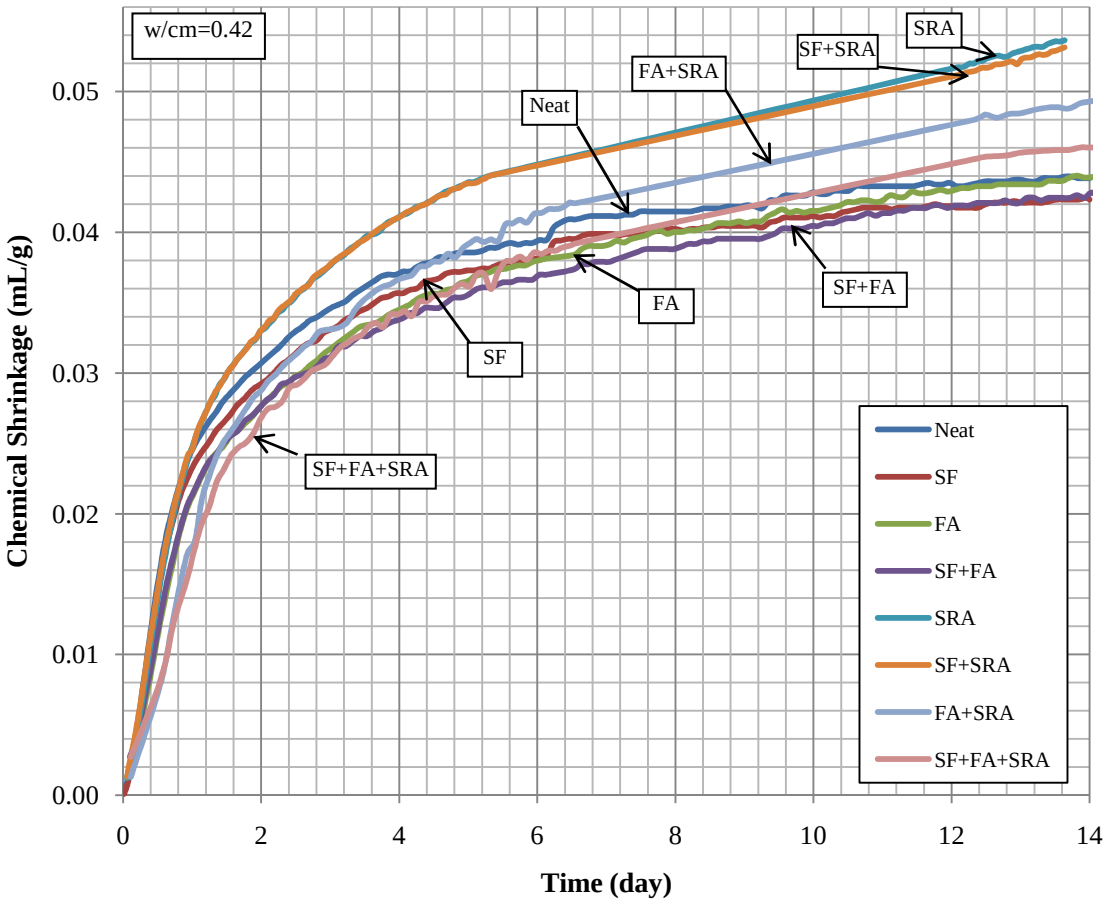

Figure B.2: Chemical shrinkage development curve, OPC w/cm=0.42 at 20 ºC isothermal

B.2 OPC 14 DAY CS DATA SHEETS

Table B.1: Chemical Shrinkage 14-Day Results, w/cm=0.32

w/cm=	0.32		Data:	08/06/10									
	#	empty	with paste	Initial (hand)	Final(hand)	CS(hand)	Ave	SD	Initial(Pro)	Final(Pro)	CS(Pro)	Ave	SD
Neat	1	-	-	-	-	-	0.0446	0.00102	-	-	-	0.0443	0.00069
	2	6.7	21.0	0.925	0.450	0.0438			0.9276422	0.452846	0.0438		
	3	7.0	20.7	0.930	0.460	0.0453			0.9260162	0.460976	0.0448		
SF	4	6.8	20.8	0.880	0.405	0.0448	0.0441	0.00062	0.8774194	0.41129	0.0439	0.0435	0.00036
	5	6.7	21.7	0.915	0.420	0.0436			0.9129032	0.420968	0.0433		
	6	6.5	21.8	0.920	0.410	0.0440			0.9176706	0.414859	0.0434		
FA	7	7.0	21.4	0.945	0.485	0.0422	0.0420	0.00026	0.9384615	0.490769	0.0410	0.0411	0.00033
	8	6.8	20.9	0.920	0.475	0.0417			0.9184048	0.482822	0.0408		
	9	7.0	21.6	0.920	0.455	0.0420			0.9201238	0.46192	0.0414		
Fa+SF	10	7.0	20.9	0.915	0.480	0.0413	0.0410	0.00044	0.9170808	0.488509	0.0407	0.0407	0.00002
	11	7.0	21.6	0.920	0.470	0.0407			0.9203762	0.470533	0.0407		
	12	7.0	21.8	-	-	-			-	-	-		
w/cm=	0.32		Data:	08/20/10									
	#	empty	with paste	Initial (hand)	Final(hand)	CS(hand)			Initial(Pro)	Final(Pro)	CS(Pro)		
SRA	1	6.9	19.4	0.940	0.480	0.0486	0.0486	0.00057	0.939867	0.483057	0.0482	0.0479	0.00086
	2	6.6	19.2	0.940	0.470	0.0492			0.9373376	0.474675	0.0485		
	3	6.9	19.8	0.950	0.480	0.0481			0.9434084	0.485209	0.0469		
SF+SRA	4	6.8	18.9	0.960	0.550	0.0447	0.0455	0.00085	0.9528846	0.549038	0.0441	0.0448	0.00065
	5	7.0	19.8	0.940	0.490	0.0464			0.9318471	0.492357	0.0453		
	6	6.7	19.5	0.910	0.470	0.0454			0.9111821	0.47508	0.0450		
FA+SRA	7	-	-	-	-	-	0.0439	0.00038	-	-	-	0.0434	0.00037
	8	6.6	18.7	0.930	0.525	0.0442			0.929595	0.529283	0.0437		
	9	6.9	19.3	0.940	0.530	0.0436			0.9372671	0.531988	0.0431		
FA+SF+SRA	10	6.8	19.6	0.935	0.535	0.0413	0.0418	0.00054	0.937037	0.534259	0.0415	0.0414	0.00014
	11	6.8	19.4	0.950	0.550	0.0419			0.9417956	0.545511	0.0415		
	12	6.7	19.8	0.925	0.505	0.0423			0.9233644	0.513707	0.0413		

Table B.2: Chemical Shrinkage 14-Day Results, w/cm=0.37

w/cm=	0.37		Data:	07/02/10									
	#	empty	with paste	Initial (hand)	Final(hand)	CS(hand)	Ave	SD	Initial(Pro)	Final(Pro)	CS(Pro)	Ave	SD
Neat	1	-	-	-	-	-	0.0448	0.00001	-	-	-	0.0448	0.00008
	2	6.9	20.8	0.905	0.450	0.0448			0.9061360	0.4510779	0.0449		
	3	6.7	20.3	0.895	0.450	0.0448			0.8962109	0.4520593	0.0447		
SF	4	6.8	21.0	0.840	0.380	0.0444	0.0452	0.00114	0.8414724	0.3831902	0.0442	0.0451	0.00124
	5	6.9	20.9	0.920	0.450	0.0460			0.9220048	0.4522005	0.0460		
	6	6.9	20.1	-	-	-			-	-	-		
FA	7	-	-	-	-	-	0.0423	0.00080	-	-	-	0.0426	0.00044
	8	6.5	23.9	0.890	0.360	0.0417			0.8995984	0.3624161	0.0423		
	9	6.8	23.1	0.930	0.420	0.0429			0.9234828	0.4129288	0.0429		
FA+SF	10	6.9	23.9	0.905	0.400	0.0407	0.0412	0.00047	0.9052632	0.4013158	0.0406	0.0413	0.00060
	11	6.8	24.1	0.900	0.380	0.0412			0.9018325	0.3743455	0.0418		
	12	6.8	24.4	0.885	0.350	0.0416			0.8841146	0.3515625	0.0415		
w/cm=	0.37		Data:	06/18/10									
	#	empty	with paste	Initial (hand)	Final(hand)	CS(hand)			Initial(Pro)	Final(Pro)	CS(Pro)		
SRA	1	6.9	20.2	0.900	0.430	0.0484	0.0487	0.00026	0.9009837	0.4301639	0.0485	0.0485	0.00005
	2	6.8	20.1	0.880	0.405	0.0489			0.8796085	0.4084829	0.0485		
	3	6.9	20.7	0.930	0.440	0.0486			0.9313821	0.4435773	0.0484		
SF+SRA	4	6.8	20.6	0.915	0.460	0.0452	0.0455	0.00149	0.9121472	0.4626994	0.0446	0.0449	0.00110
	5	6.6	20.4	0.930	0.455	0.0472			0.9244142	0.4594328	0.0462		
	6	6.9	21.3	0.910	0.445	0.0442			0.9100371	0.4472119	0.0440		
FA+SRA	7	6.9	23.0	0.850	0.340	0.0434	0.0431	0.00037	0.8532009	0.3465838	0.0431	0.0429	0.00027
	8	7.0	23.7	0.900	0.380	0.0427			0.9098901	0.3857143	0.0430		
	9	6.6	25.5	0.875	0.280	0.0431			0.8798236	0.2921771	0.0426		
FA+SF+SRA	10	6.5	25.6	0.930	0.320	0.0438	0.0425	0.00112	0.9284141	0.3268712	0.0431	0.0424	0.00115
	11	6.6	24.9	0.925	0.370	0.0415			0.9282580	0.3800490	0.0410		
	12	6.6	24.1	0.880	0.340	0.0423			0.8858693	0.3379141	0.0429		

Table B.3: Chemical Shrinkage 14-Day Results, w/cm=0.42

w/cm=	0.42		Data:	09/14/10									
	#	empty	with paste	Initial (hand)	Final(hand)	CS(hand)			Initial(Pro)	Final(Pro)	CS(Pro)	Ave	SD
Neat	1	7.0	18.6	1.220	0.840	0.0465	0.0460	0.00058	1.2170212	0.8493369	0.0450	0.0451	0.00057
	2	6.8	17.6	1.095	0.750	0.0454			1.0894180	0.7507937	0.0445		
	3	6.7	17.8	1.370	1.010	0.0461			1.3686170	1.0117648	0.0457		
SF	4	6.8	18.5	0.980	0.620	0.0437	0.0445	0.00071	0.9821138	0.6243243	0.0434	0.0444	0.00083
	5	7.0	17.1	1.500	1.180	0.0450			1.4989071	1.1796703	0.0449		
	6	6.8	18.2	1.300	0.940	0.0448			1.2969697	0.9370166	0.0448		
FA	7	6.8	18.6	1.140	0.780	0.0433	0.0444	0.00098	1.1368821	0.7922814	0.0415	0.0444	0.00258
	8	6.8	18.8	1.280	0.900	0.0450			1.2766917	0.8947368	0.0452		
	9	6.8	17.2	1.550	1.220	0.0451			1.5538461	1.2139194	0.0464		
FA+SF	10	6.7	17.7	1.330	1.000	0.0426	0.0429	0.00031	1.3217391	1.0000000	0.0415	0.0426	0.00101
	11	7.0	18.5	1.320	0.970	0.0432			1.3240143	0.9713262	0.0435		
	12	6.6	17.5	1.600	1.270	0.0430			1.5964663	1.2685512	0.0427		
w/cm=	0.42		Data:	09/08/10									
	#	empty	with paste	Initial (hand)	Final(hand)	CS(hand)	Ave	SD	Initial(Pro)	Final(Pro)	CS(Pro)	Ave	SD
SRA	1	7.0	18.4	0.920	0.500	0.0523	0.0536	0.00180	0.9244897	0.5065306	0.0521	0.0534	0.00187
	2	6.6	19.8	0.930	0.420	0.0549			0.9291498	0.4206478	0.0547		
	3	6.6	18.9	-	-	-			-	-	-		
SF+SRA	4	6.8	20.4	0.910	0.420	0.0512	0.0525	0.00200	0.9096000	0.4216000	0.0510	0.0522	0.00194
	5	6.6	18.9	0.915	0.440	0.0548			0.9111553	0.4394423	0.0545		
	6	6.8	18.9	0.910	0.470	0.0516			0.9128000	0.4760000	0.0513		
FA+SRA	7	6.8	22.1	0.900	0.375	0.0487	0.0491	0.00130	0.9064935	0.3810390	0.0488	0.0487	0.00057
	8	6.7	20.6	0.900	0.430	0.0480			0.9062176	0.4352332	0.0481		
	9	6.8	18.6	0.920	0.500	0.0505			0.9186046	0.5093023	0.0493		
FA+SF+SRA	10	6.8	18.2	0.915	0.540	0.0467	0.0469	0.00378	0.9123711	0.5381444	0.0466	0.0464	0.00353
	11	6.7	19.2	0.925	0.545	0.0432			0.9262211	0.5491260	0.0428		
	12	7.0	19.6	0.920	0.470	0.0507			0.9185090	0.4758355	0.0499		

B.3 OPC CS TEST RESULTS (FITTED)

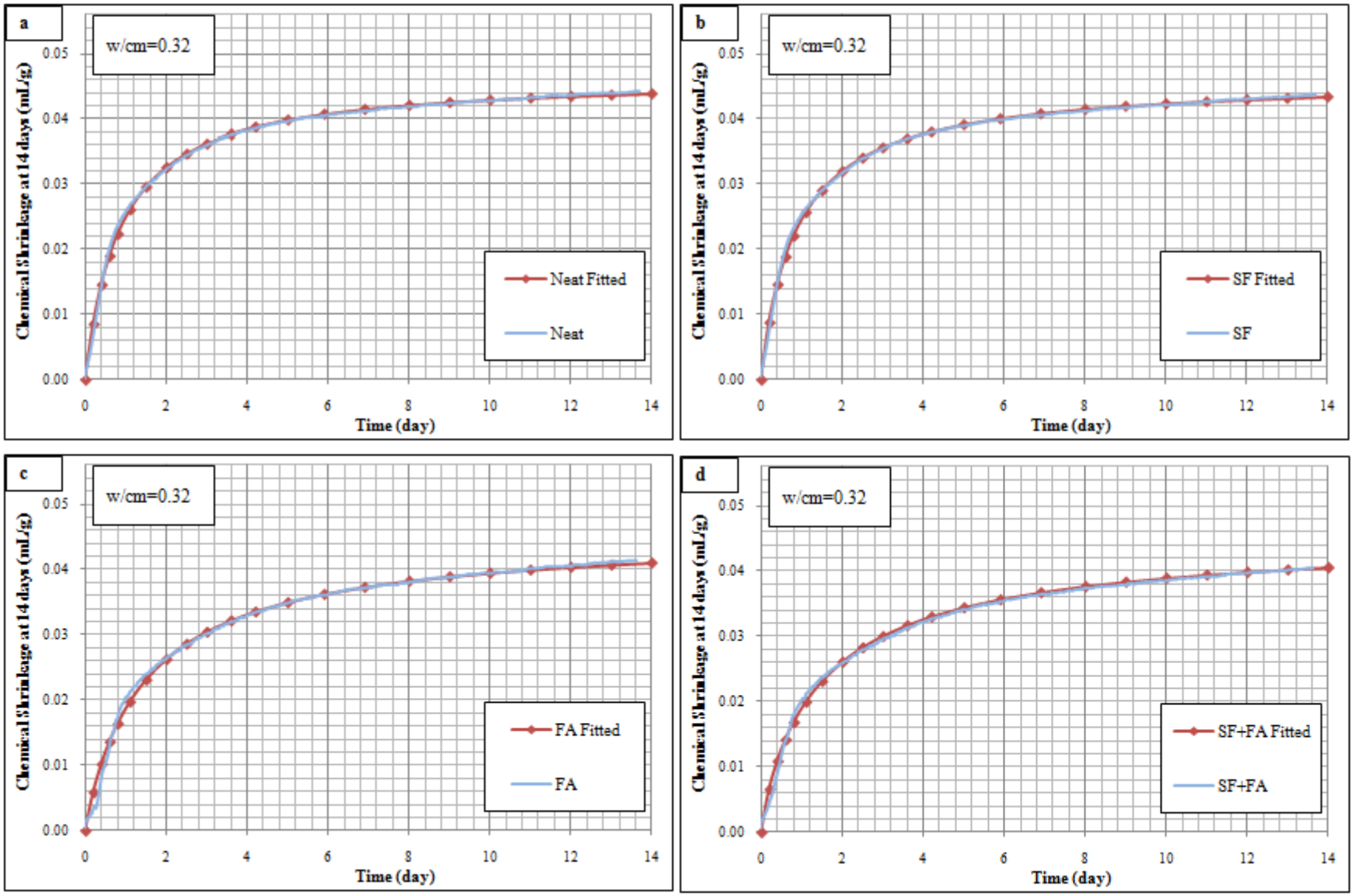

Figure B.3: Fitted and measured CS curves for OPC (0.32 w/cm without SRA)

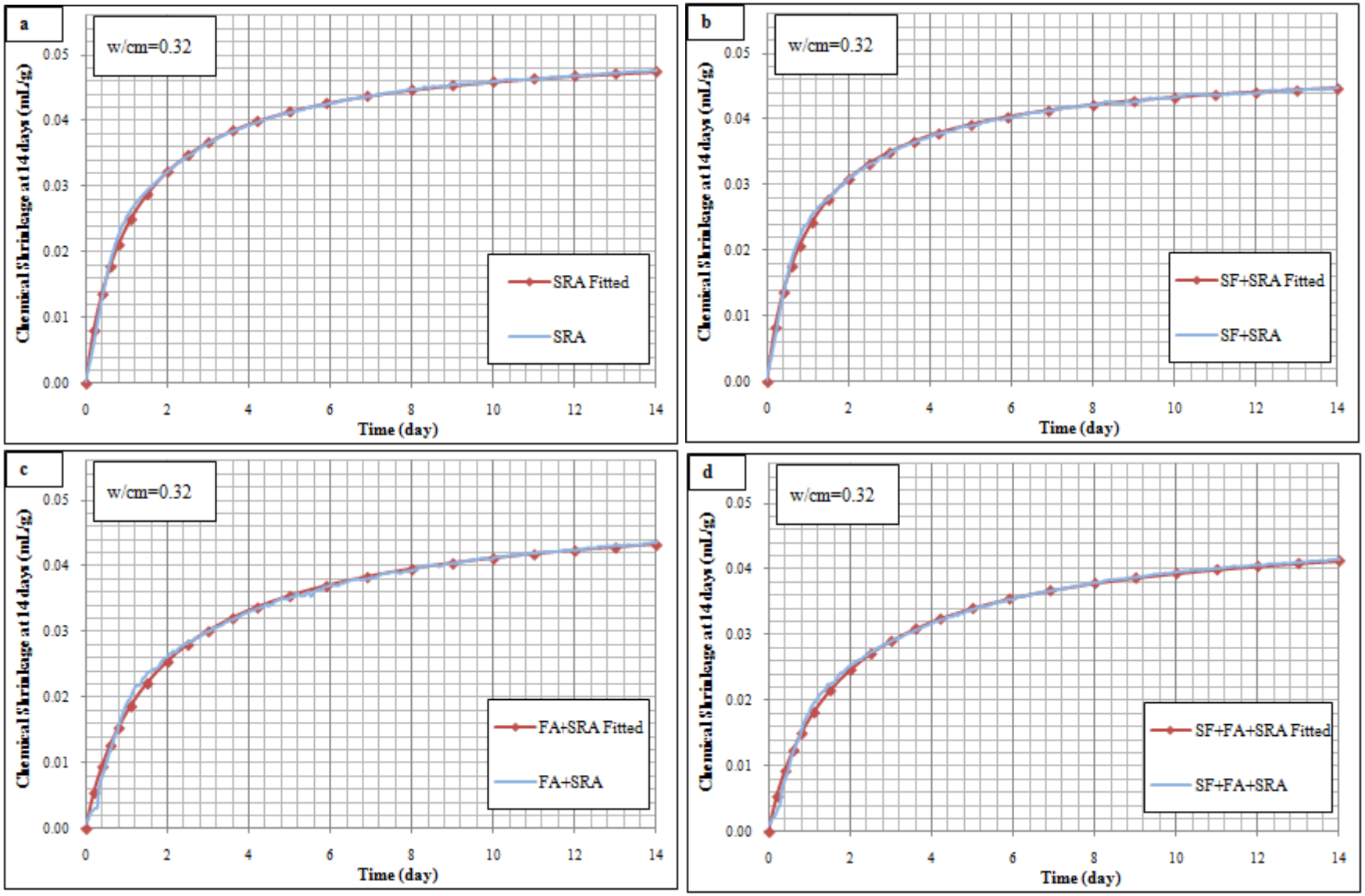

Figure B.4: Fitted and measured CS curves for OPC (0.32 w/cm with SRA)

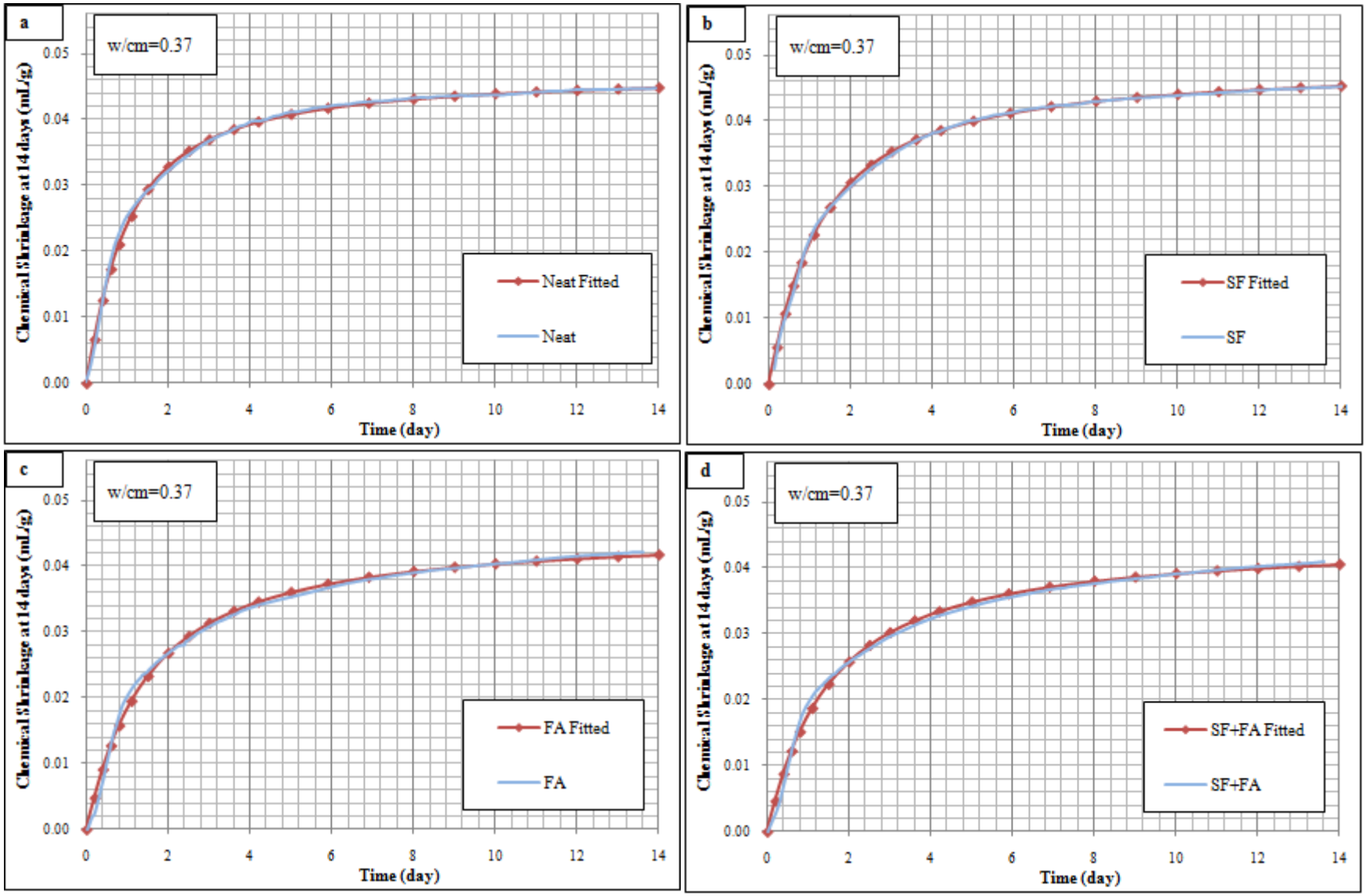

Figure B.5: Fitted and measured CS curves for OPC (0.37 w/cm without SRA)

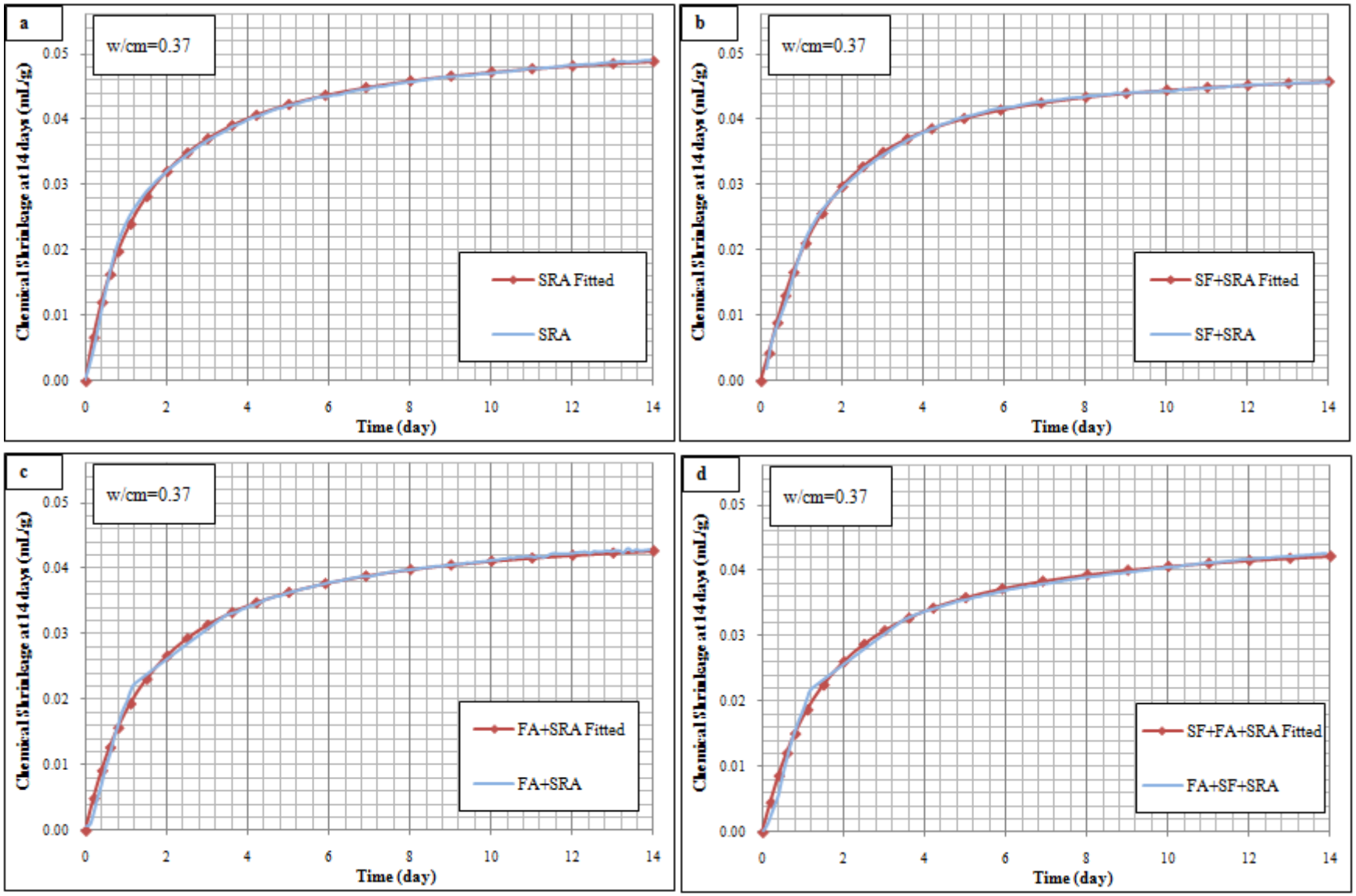

Figure B.6: Fitted and measured CS curves for OPC (0.37 w/cm with SRA)

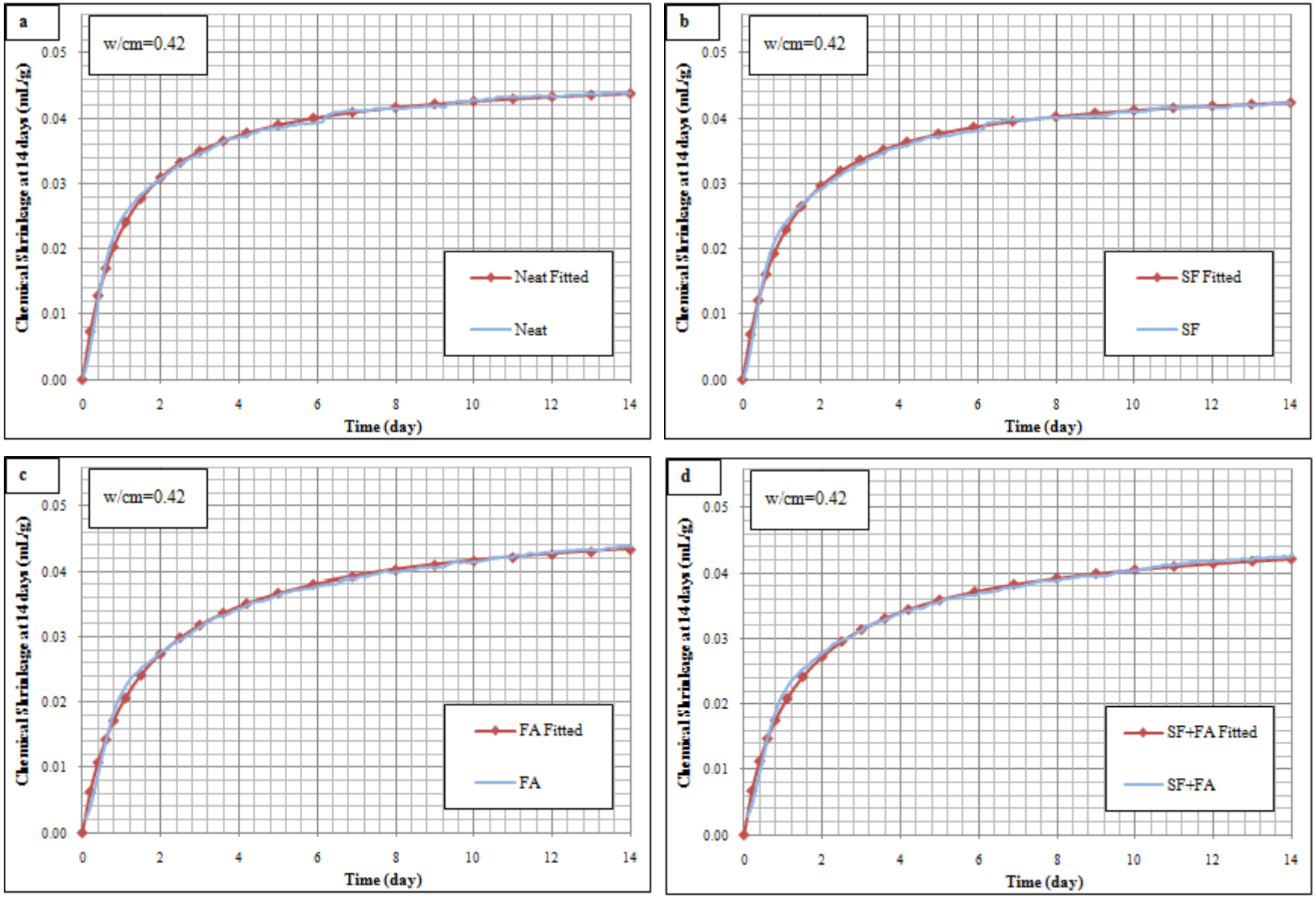

Figure B.7: Fitted and measured CS curves for OPC (0.42 w/cm without SRA)

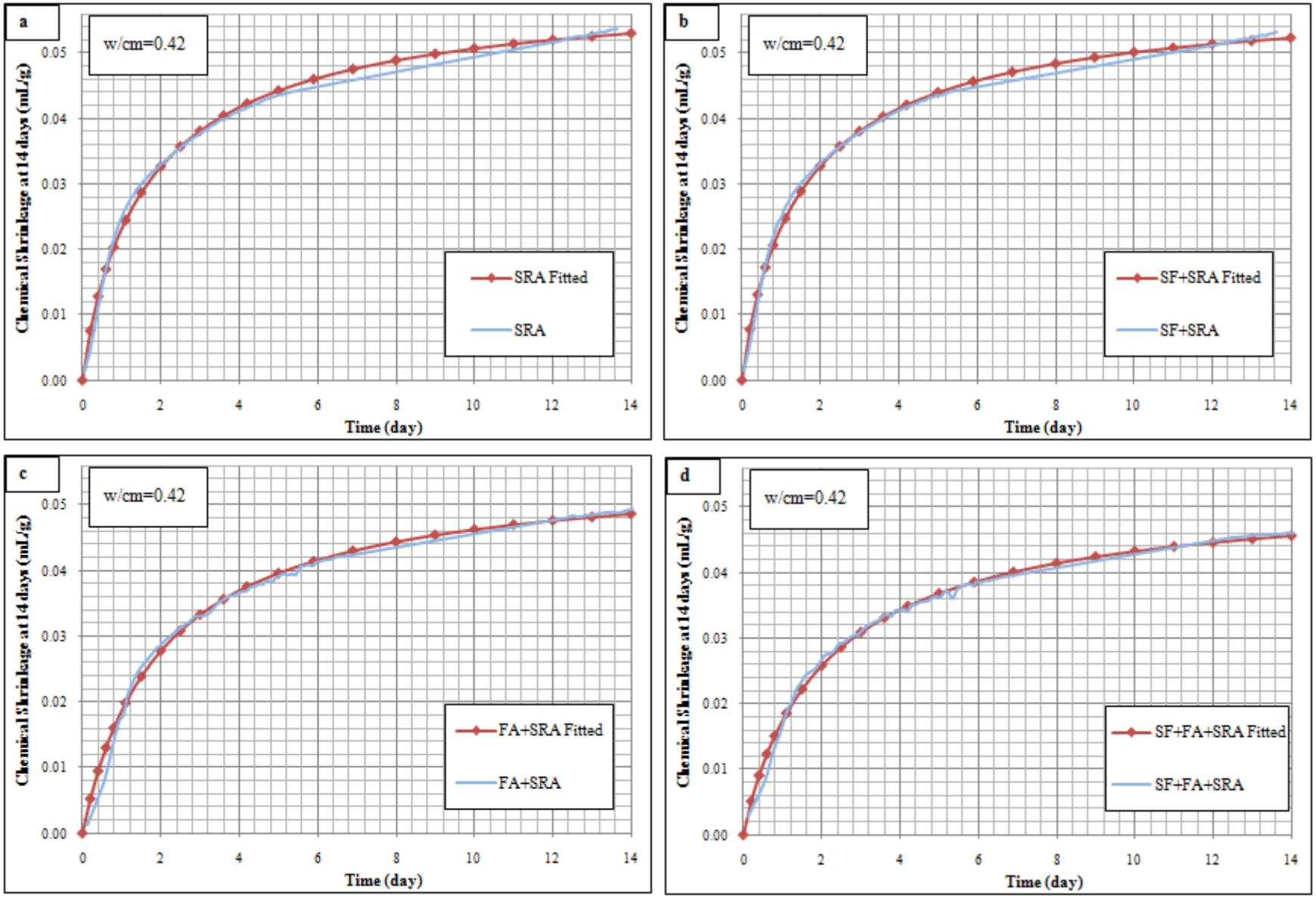

Figure B.8: Fitted and measured CS curves for OPC (0.42 w/cm with SRA)